

Cellular pathogenic mechanisms linked to TBK-1 and optineurin in amyotrophic lateral sclerosis

Faculty of Medicine and Health Sciences

Biomedical Department

Reka P.Toth

Macquarie University

2016

Supervisor: Associate Professor Julie D. Atkin

Content

Declaration.....	vii
Acknowledgments	ix
Publication arising from this candidature	xi
Abstract.....	xiii
List of Tables	xv
List of Figures.....	xvii
Abbreviations	xix
1-Introduction	1
1.1-Introduction to Amyotrophic Lateral Sclerosis (ALS)/Motor Neuron Disease (MND)	2
1.2-Diagnosis of ALS	3
1.3-Subtypes and clinical symptoms of ALS.....	4
1.4-Frontotemporal dementia and its relation to ALS.....	7
1.5-Genes associated with ALS.....	8
1.5.1-Superoxide dismutase 1.....	8
1.5.2-TAR DNA binding protein 43 kDa.....	8
1.5.3-Fused in sarcoma.....	9
1.5.4-C9ORF72.....	9
1.6-Underlying pathological mechanisms of ALS.....	10
1.6.1-Protein aggregates.....	10
1.6.2-Axonal dysfunction.....	11
1.6.3-Mitochondrial dysfunction.....	14
1.6.4-Non-cell autonomous mechanisms.....	14
1.6.5-Endoplasmic reticulum stress and unfolded protein response.....	14
1.6.6-Autophagy.....	17
1.6.7-Intersection of ER-stress and autophagy.....	20
1.7-Optineurin.....	20
1.8-TBK-1.....	24

2-Thesis topic	27
3-Materials and Methods	29
3.1-Materials and Solutions.....	30
3.2 –Methods	33
3.2.1-General cell maintenance.....	33
3.2.1.1-Cell plating.....	33
3.2.1.2-Transient transfection.....	34
3.2.1.3-Autophagy induction.....	35
3.2.2-Immunoblotting and immunoprecipitation.....	35
3.2.2.1-Cell lysis.....	35
3.2.2.2-Protein quantification.....	35
3.2.2.3-Protein sample preparation for SDS-gel separation.....	35
3.2.2.4-SDS-gel.....	36
3.2.2.5-Antibody incubation	36
3.2.2.6-Protein immunoprecipitations.....	37
3.2.3-Immunocytochemistry and microscopy.....	38
3.2.3.1. Microscopy.....	38
3.2.4-Mutagenesis, Bacteria transformation and plasmid purification.....	39
3.2.4.1-Mutagenesis.....	39
3.2.4.2-Bacteria transformation with plasmid DNA.....	40
3.2.4.3-Plasmid DNA amplification.....	41
3.2.4.4-Sequencing.....	41
3.2.5-Statistical analysis.....	41
4-Results	43
4.1-Intracellular levels and localization of TBK-1 in the presence of ALS-mutant optineurin	44
4.2-TBK-1 and its role in autophagy.....	53
4.3-Site-directed mutagenesis of TBK-1.....	54
4.3.1-Design of TBK-1 mutations.....	54
4.3.2-Generation of TBK-1 mutations.....	55

4.4-TBK-1 overexpression in mammalian cell lines	59
4.4.1-TBK-1 detection using the FLAG-tag	59
4.4.2-TBK-1 overexpression in neuronal NSC34 and SH-SY5Y cells.....	62
4.4.3-TBK-1 overexpression in HEK293 cells.....	65
4.4-Characterisation of expression of WT and mutant TBK-1 in HEK293 cells by immunoblotting and immunofluorescence.....	67
4.6-Optimisation of conditions to induce autophagy in HEK293 cells	74
4.7-ALS-associated TBK-1 mutants dysregulate autophagy in HEK293 cells.....	77
4.8-Kinase deficient mutant TBK-1 affects CHOP-expression.....	86
5-Discussion	89
5.1-Recruitment of TBK-1 to autophagosomes is inhibited in cells expressing ALS-associated mutant optineurin	90
5.2-TBK-1 is an ALS gene.....	91
5.3-ALS-mutant TBK-1 may dysregulate autophagy.....	95
5.4-Kinase deficient TBK-1 mutants inhibit CHOP expression	96
Future directions	100
Concluding remarks.....	102
References	103

Declaration

I wish to acknowledge the following assistance in the research outlined in this project;

- TBK-1-FLAG overexpressing constructs (WT/D50A/G159A) were a kind gift of a Professor Casanova, Rockefeller University, New York
- The following overexpression constructs, OPTN-E478G, OPTN-Q398X, OPTN-E50K were previously designed and generated by Dr Vinod Sundaramoorthy. The EGFP-WT-OPTN overexpressing construct was a kind gift of Dr Ghanshyam Swarup, Centre for Cellular and Molecular Biology, Hyderabad, India
- The LC-3-dsRed construct was a kind gift of Dr Yung-Feng Liao, Institute of Cellular and Organismic, Academia Sinica, Taiwan.
- Plasmid DNA sequencing of vectors were outsourced to AGRF (Australian Genomic Research Facility)

All other data presented in this thesis is my own work.

Acknowledgments

First of all, I wish to thank to my supervisor, Julie Atkin, for the great opportunity to work on this project and for guiding and inspiring me through the entire project.

I also wish to thank Vinod Sundaramoorthy, who was a great mentor throughout these 10 months. You always had an answer and a solution for everything.

I would like to thank Adam Walker, Damian Spencer and Audrey Raganin for their help, comments and suggestions for this thesis.

I wish to thank all the member of JDA lab; Sonam, Jess, Emma, Cyril, Anna and Hamideh for their support, especially during the stressful moments, for being patient with me and giving up your booking time if I needed it a bit more.

Last, but not least I wish to thank Marta Vidal, who was the greatest support of all. You were a friend rather than a colleague to me.

Publication arising from this candidature

“Rab1-dependent ER–Golgi transport dysfunction is a common pathogenic mechanism in SOD1, TDP-43 and FUS-associated ALS”

Kai Y. Soo, Mark Halloran, Vinod Sundaramoorthy, Sonam Parakh, **Reka P. Toth**, Katherine A. Southam, Catriona A. McLean, Peter Lock, Anna King, Manal A. Farg, Julie D. Atkin

Acta Neuropathologica November 2015, Volume 130, Issue 5, pp 679-697

Abstract

Amyotrophic lateral sclerosis (ALS) is a fatal neurodegenerative disease associated with the loss of both upper and lower motor neurons in the motor cortex, brain stem and spinal cord. The pathogenic mechanisms underlying ALS remain largely unknown. The pathological hallmark of ALS is the presence of cytoplasmic inclusions containing misfolded proteins in degenerating motor neurons. These inclusions are present regardless of the site of symptom onset, age or gender of the patient. Moreover, these inclusions are present in both sporadic and familial forms of ALS. Misfolded protein accumulation triggers stress in the endoplasmic reticulum (ER), inducing the unfolded protein response (UPR), and ER stress is now a well described feature of ALS. The UPR aims to restore proteostasis, but if unresolved triggers apoptosis. The UPR is also linked to autophagy, a self-degradative process that could clear protein aggregates. However, the presence of protein inclusions suggests that both UPR and autophagy could be dysfunctional in ALS. One of the genes most recently identified in ALS encoded, TBK-1, a kinase involved in different forms of selective autophagy including mitophagy and xenophagy. Interestingly, TBK-1 phosphorylates optineurin an autophagy adaptor protein that is also linked genetically to ALS. In this project the effect of ALS-causing mutations in TBK1 on ER-stress, autophagy and the association between optineurin and TBK-1 autophagy were examined. Using site directed mutagenesis kinase and substrate binding deficient ALS-mutant TBK-1 overexpressing constructs were generated and the effect of expression of the mutants was examined. Preliminary results showed that expression of kinase deficient mutants decreased expression of CHOP, a pro-apoptotic transcription factor, normally induced during ER-stress. This suggests that the kinase activity of TBK-1 is associated with CHOP, independent of ALS. Furthermore, a slight but significantly decrease in LC3-II levels was detected upon ALS-mutant TBK-1 overexpression, suggesting ALS-mutants inhibit autophagy. Additionally, ALS-mutant optineurin failed to recruit endogenous TBK-1 to autophagosomes in NSC-34 cells. This thesis therefore provides novel insight into cellular pathways perturbed in ALS-associated mutants of TBK-1.

List of Tables

1.1	Comparison between lower and upper motor neurons.	2
1.2	List of genes implied in ALS and the proteins they encode.	6
1.3	ALS and FTD associated mutations in TBK-1.	24
3.1	Standard operating protocol (SOP) for Lipofectamine transfection.....	34
3.2	Preparation of SDS-polyacrylamide gels.....	36
3.3	Antibody concentrations used in this study.....	37
3.4	Primer sequences designed to introduce mutations in <i>TBK-1</i> gene.....	38
3.5	PCR reaction used for site-directed mutagenesis.....	39
3.6	PCR cycles used for site-directed mutagenesis.....	40
3.7	Protocol for KLD-reaction.....	40
3.8	Sequencing primers designed for <i>TBK-1</i>	41
4.1	The TBK-1 mutations used in this study, illustrating both the altered nucleotide and amino acid sequences.	55

List of Figures

1.1	Location of the motor cortex in the human brain from lateral and medial view.	3
1.2	Involvement of different genes in ALS, ALS-FTD, and FTD.	7
1.3	Composition of the pathological inclusions in ALS and FTD.	11
1.4	Mechanisms involved in ALS pathology.	13
1.5	The three pathways of the unfolded-protein response.	16
1.6	Pathways involved in autophagy cascade.	18
1.7	Schematic overview of selective and non-selective autophagy in mammalian cells.	19
1.8	Location of binding sites and ALS-associated mutations in optineurin.	22
1.9	Domain organization of TBK-1.	23
3.1	Diagram of pcDNA3.1 vector from Invitrogen.	32
3.2	Diagram of EGFP-C3 vector from Addgene.	32
3.3	Diagram of pDsRed-monmer-C1 vector from Clontech.	33
4.1	Optneurin and TBK-1 expression in NSC-34 cells upon optineurin transient transfection.	45
4.2	Colocalization of optineurin and TBK-1 in NCS-34 cells.	47
4.3	Colocalization of optineurin and TBK-1 with LC-3 in NSC-34 cells.	50
4.4	Coimmunoprecipitation of optineurin and TBK-1 in NSC-34 cells.	52
4.5	Location of the mutations in TBK-1 protein selected in this study.	55
4.6	Sequences of R308Q, R357Q, E643X, and E696K mutations.	58
4.7	Detection of the FLAG-tag at the protein and DNA levels.	61
4.8	Overexpression of TBK-1 in NSC-34 and SH-S5Y5 cell lines and using Lipofectamine and calcium-phosphate transfection methods.	64
4.9	TBK-1 overexpression in HEK293 cells, and separation of exogenous and endogenous TBK-1 using SDS-PAGE.	67
4.10	Total and p-TBK-1(Ser172) detection in WT and mutant TBK-1 overexpressing HEK293 cells.	70

4.11 Separation of endogenous and overexpressed TBK-1-FLAG by SDS-polyacrylamide gels.....	71
4.12 Detection of overexpressed TBK-1 via immunocytochemistry in HEK293 cells.	72
4.13 Autophagy induction in HEK293 cells.....	76
4.14 Immunoblotting analysis of TBK-1 transfected HEK293 cells.	78
4.15 Immunoblotting analysis of TBK-1 transfected and serum starved HEK293 cells.	79
4.16 Immunoblotting analysis of TBK-1 transfected, serum-starved, and bafilomycin treated HEK293 cells.	81
4.17 Colocalization of LC-3 and TBK-1 in transfected HEK293 cells.	84
4.18 Decreased CHOP expression in cells expressing kinase-deficient TBK-1 mutants.	88

Abbreviations

ALS: amyotrophic lateral sclerosis

ALS2: alsin

AMPK: AMP activated protein kinase

ANG: angiogenin

ATF4: activating-transcription factor 4

ATF6: activating-transcription factor 6

ATG: autophagy-related genes

ATP: adenine triphosphate

BIP: binding immunoglobulin protein

bvFTD: behavioral variant frontotemporal dementia

C9ORF72: C9 open reading frame 72

CCD: coiled-coil domain

CHOP: CCAAT-enhancer-binding protein homologous protein

CNS: central nervous system

DNA: deoxyribonucleic acid

ER: endoplasmic reticulum

ERAD: endoplasmic-reticulum protein degradation

FTD: frontotemporal dementia

FTLD: frontotemporal lobar degeneration

FUS: fused in osteosarcoma

GWAS: genome wide association study

IKK: I κ B kinase

IRE-1: inositol-requiring kinase 1

IRF3: interleukin factor 3

KD: kinase domain

KLD: kinase-ligase-Dpnl

LC3: microtubule associated 1 light chain 3 β

LIR: LC3 interacting motif

LMN: lower motor neuron

MTOR: mammalian target of rapamycin

MW: molecular weight

NDP52: nuclear domain 10 protein 52

NEMO: NF-kappa B essential modulator

NLS: nuclear localization signal

NAP1: NAK-associated protein 1

NT: non-transfected

PAS: phagophore assembly site

PCR: polymerase chain reaction

PERK: PKR-like endoplasmic reticulum kinase

PNFA: progressive non-fluent aphasia

RNA: ribonucleic acid

ROS: reactive oxygen species

SC: spinal cord

SD: semantic dementia

SETX: senataxin

SOD1: superoxide dismutase 1

TANK: TRAF family member-associated NF-kappa-B activator

TBK-1: TANK binding kinase 1

TDP-43: Tar-DNA binding protein 43kDa

ULD: ubiquitin like domain

ULK: Unc51 like autophagy activating kinase

UMN: upper motor neuron

UPR: unfolded protein response

VEGF: vascular epithelial growth factor

WT: wild type

XBP1: x-box binding protein 1

1

Introduction

1.1. Introduction to Amyotrophic Lateral Sclerosis (ALS)/MN Disease (MND)

Neurodegenerative diseases are characterized by the malfunction and consequent death of neurons in the brain and/or in the spinal cord. Neurodegenerative diseases are also known as ‘Protein Misfolding Disorders’ because the characteristic pathological hallmark of these conditions is the presence of misfolded protein inclusions in affected tissues. These disorders can be divided into several groups based on their primary symptoms. Cognitive disorders are associated with the impairment of cognitive functions, and they include dementias, such as frontotemporal dementia (FTD) and Alzheimer’s disease. Another group consists of diseases that result in disorders in movement, including Parkinson’s disease and Huntington’s disease. The final group are diseases affecting motor neurons (MN), and they include amyotrophic lateral sclerosis (ALS), progressive lateral sclerosis, and spinal muscular atrophy. MN diseases are associated with the loss of MNs in the motor cortex, brainstem, and/or in the ventral horn regions of the spinal cord¹. MNs are neuronal cells located in the central nervous system (CNS) that control a variety of downstream targets². There are two different types of MNs; upper MNs (UMNs), have their cell bodies in the cerebral cortex and brainstem, and lower MNs (LMNs), with cell bodies in the brainstem and spinal cord². The UMNs and LMNs also differ in a number of other properties, as outlined in *Table 1.1*.

Table 1.1: Comparison between lower and upper MNs. Adapted from Stifani et al.³ (CNS- central nervous system, SC-Spinal cord).

	UMN	LMN
LOCATION	Cortex+ Brainstem	Brainstem and SC
NEUROTRANSMITTER	Glutamate	Acetylcholine
TARGETING	Within the CNS	Outside of CNS
SYMPTOMS	Spasticity	Paralysis

The motor cortex is the main part of the cerebral cortex where UMN cell bodies originate and it is composed of the primary motor cortex, lateral and medial premotor cortex (*Figure 1.1*). They initiate and organize movement and also transmit information to LMNs either directly or indirectly via connections with interneurons.

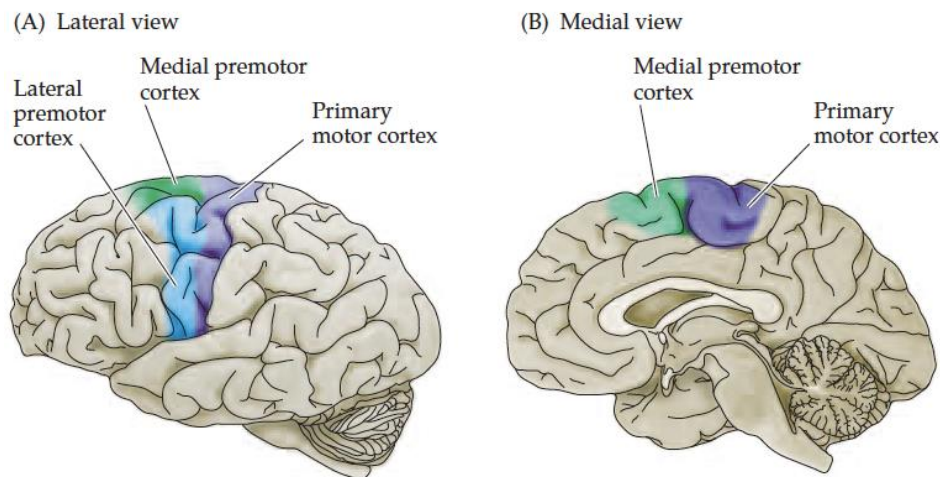


Figure 1.1: Location of the motor cortex in the human brain from lateral (A) and medial (B) view. Adapted from Purves et al.²

The cell bodies of LMNs are located in specific nuclei in the brainstem, the cranial nerve nuclei, and the ventral horn regions of the spinal cord². Their axonal extensions and connections are outside of the CNS. LMNs receive inputs from UMNs, sensory neurons and interneurons², and they are responsible for movement because they innervate muscle fibers².

1.2 Diagnosis of ALS

MN diseases are associated with the death of either UMNs or LMNs, but ALS is characterized by the death of both types of MNs. The El Escorial criteria for the diagnosis of ALS were established in 1994⁴, and were subsequently revised in 2000⁵. The diagnosis of ALS requires evidence for both LMN and UMN degeneration by clinical, electrophysiological or neuropathological examination, as well as the progressive

spread of symptoms or signs⁵. In addition, patients must not present electrophysiological or pathological evidence of other diseases that may explain the symptoms⁵.

1.3. Subtypes and clinical symptoms of ALS

Based on the site of symptom onset, ALS can be divided into three groups; spinal-onset ALS, bulbar-onset ALS, and respiratory-onset ALS. Spinal-onset ALS manifests in asymmetric weakness in the limbs and occurs in approximately 80% of all ALS patients⁶. It is associated with atrophy and weakness of muscles, fasciculation, hyper-reflexia (over-responsive reflexes) and hypertonia (abnormal increase in muscle tension), and these patients usually survive 3-5 years from symptom onset⁷. Bulbar-onset ALS occurs in approximately 20% of patients, and the first symptoms are dysarthria (unclear articulation), dysphagia (difficulties in swallowing) and tongue fasciculation⁶. Bulbar-onset patients have a worse prognosis⁸, and their mean survival time is only 2 years from symptom onset⁸. Approximately 3-5% of patients first show symptoms in the respiratory system, manifesting in orthopnea (shortness of breath), dyspnea (sensation of uncomfortable breathing) and mild/absent spinal or bulbar signs^{6,8}. The prognosis of these patients is poor; the mean survival period after symptom onset averages only 1.4 years^{1,9}. The first symptoms of neurodegeneration in 60% of ALS patients appear between 50 and 70 years¹⁰. In contrast, there are rare cases of juvenile, slow-progressing ALS which affect young adults below 25 years of age¹⁰⁻¹³. The median survival is approximately 3 years from diagnosis, and only 10% of patients live longer than 10 years¹². Longer periods of survival are more frequent in juvenile ALS, and UMN dominant forms^{12,14}.

Genome-wide sequencing of families presenting with more than one affected member, also called 'familial ALS' (fALS), has identified multiple genetic mutations associated with the disease. Most of these are still rare and only cause ALS in a small

group of patients, hence, non-familial or sporadic ALS represents 90% of all cases (sALS), with no previous family history. Numerous genes have also been implicated in both fALS and sALS¹⁵. However, despite the enormous progress made in genetic research over the last 7-8 years, the etiology of sALS is largely unknown. Regardless of the different etiology, both fALS and sALS are very similar in the rate of progression and symptoms, although specific fALS cases are associated with faster progression, such as the A4V mutation in the *SOD1* gene¹⁶. So far, over twenty genes have been identified as likely sites for ALS-linked mutations (*Table 1.2* gives a complete list).

The characteristic pathological hallmark of ALS is the presence of misfolded protein inclusions within MNs. In fALS, the inclusions contain misfolded mutant proteins, and despite the fact that mutations represent a small portion of all ALS, in sALS, wildtype versions of some of the same proteins misfold and form inclusions. The most recent gene linked to ALS is *CCNF*, which encodes G2/mitotic-specific cyclin-F¹⁷. The subject of this thesis is TANK-binding kinase 1 (TBK-1), encoded by the *TBK-1* gene, and mutations in *TBK-1* were first linked to ALS in 2015. Interestingly, TBK-1 is a binding partner of optineurin, and mutations within the *OPTN* gene are also associated with ALS.

Table 1.2: List of genes mutated in ALS and the proteins they encode. Adapted from Boylan et al.¹⁸

Gene	Protein	Reference	Year of discovery
ALS2	Alsin	19	2001
ANG	Angiogenin	20,21	2011
ATXN2	Ataxin-2	22,23	2010
CCNF	G2/mitotic-specific cyclin-F	17	2016
CHCHD10	Coiled-coil-helix-coiled-coil-helix domain containing 10	24,25	2014
CHMP2B	Chromatin modifying protein 2B	26	2006
C9ORF72	Chromosome 9 open reading frame 72	27-30	2011
DAO	d-Amino acid oxidase	31	2010
DCTN1	Dynactin	32-34	2004
FIG4	SAC1 lipid phosphatase domain containing (S cerevisiae)	35	2009
FUS	Fused in sarcoma	36 37	2009
HNRNPA1	Heterogenous nuclear ribonucleoprotein A1	38	2013
HNRNPA2B1	Heterogenous nuclear ribonucleoprotein A2B1	38	2013
MATR3	Matrin 3	39	2014
OPTN	Optineurin	40	2010
PDIA1/3	Protein disulphide isomerase1/3	41	2016
PFN1	Profilin 1	42	2012
SETX	Senataxin	43	2004
SIGMAR1	Sigma nonopioid intracellular receptor 1	44 45,46	2011
SOD1	Superoxide dismutase 1	47	1993
SPG11	Spataccin	48	2012
SQSTM1	Sequestosome 1	49	2011
TARDBP	TAR DNA binding protein 43	50	2006
TBK1	TANK-binding kinase 1	51	2015
TUBA4A	Tubulin α 1	52	2014
UBQLN2	Ubiquilin 2	53	2011
VAPB	Vesicle-associated membrane associated-protein B	54	2004
VCP	Valosin-containing protein	55	2010

1.4. Frontotemporal dementia and its relation to ALS

In some instances, the same genes associated with ALS are also mutated in frontotemporal dementia (FTD), and it is becoming increasingly recognized that FTD and ALS represent the two ends of a continuum of a broad range of neurodegenerative disorders⁵⁶ (Figure 1.2). FTD represents heterogeneous syndrome caused by degeneration of the frontal and temporal lobes, while the posterior cortical regions are spared.

Approximately 40% of FTD patients show signs of MN involvement, and up to 15% of FTD patients meet ALS criteria⁵⁷. Similarly, ALS can be accompanied by cognitive behavioral impairment, and 15% of ALS patients show FTD symptoms^{50,57-59}. Genes that are linked to both ALS and/or FTD are now scattered across the ALS-FTD continuum (Figure 1.2). Some genes are so-called 'pure FTD' or 'pure ALS' genes, as they associate with only one of these diseases (Figure 1.2). The underlying pathological mechanisms linking these mutations with either or both diseases remain unclear.

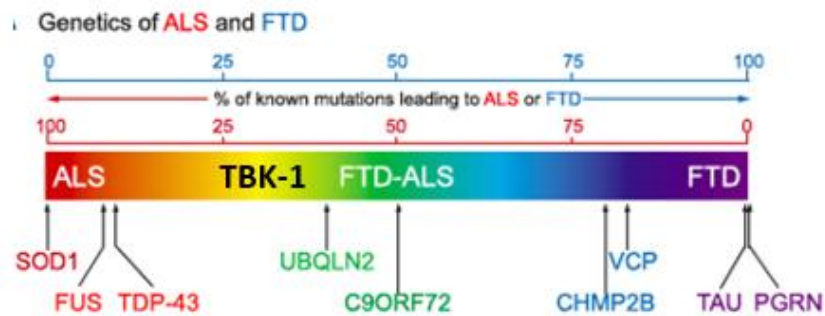


Figure 1.2: Involvement of different genes in ALS, ALS-FTD, and FTD. ALS and FTD represent opposite ends of a disease spectrum. Several genes, including *UBQLN2* and *C9ORF72* are associated with both ALS and FTD. However, *SOD1* mutations have been only identified in pure ALS patients, and *TAU* or *PGRN* mutations have not been previously identified in ALS patients. *TBK-1* is the subject of this thesis and it is mutated in both FTD and ALS. Adapted from Ling et al.⁵⁶

1.5. Genes associated with ALS

The genes that are associated with the greatest proportion of fALS cases are *SOD1*, *TARDBP*, *FUS* and *C9ORF72*, and these genes will be discussed below *OPTN* and *TBK1* and are discussed in sections 1.7 and 1.8 below respectively.

1.5.1 Superoxide dismutase 1

Superoxide dismutase-1 (SOD1) was the first gene identified in fALS, in 1993⁴⁷. *SOD1* uniquely found in ALS patients, and causative *SOD1* mutations are not present in ALS-FTD or FTD patients. *SOD1* mutations are responsible for 20% of fALS and to date, 170 different *SOD1* mutations have been reported in fALS⁶⁰. SOD1 is a 153 amino acid metalloprotein predominantly expressed in the cytosol, and mice lacking SOD1 suffer extensive oxidative damage, as early as 3 months of age⁶¹. Misfolded mutant SOD1 is found as oligomers and intracellular inclusions in MNs from human patient and animal disease models, and in cells expressing mutant SOD1. Misfolded mutant SOD1 mediates its effect through a gain of toxic function mechanism, rather than a loss of function mechanism, because several ALS-associated mutations have enhanced enzyme activity compared to wildtype SOD1⁶². Evidence from transgenic mice expressing human mutant SOD1 proteins, which are the most widely studied animal disease model, support this notion⁶³. Similarly, knockout mice in which the SOD1 gene is deleted do not develop MN disease⁶⁴.

1.5.2 TAR DNA binding protein 43 kDa

TDP-43 was first associated with ALS in 2006, when it was identified as a major misfolded protein component of inclusions in sALS⁵⁰. Mutations in *TARDBP*, the gene encoding TDP-43, were subsequently identified in both fALS and sALS in 2008^{65,66}. Whilst mutations in *TARDBP* are responsible for only 5% of fALS and 2% of sALS cases

overall, TDP-43-positive cytoplasmic inclusions are present in almost all (97%) of ALS patients⁶⁷, illustrating the importance of TDP-43 in ALS. TDP-43 is a 414 amino acid RNA binding protein involved in many aspect of RNA-metabolism, including splicing, microRNA biogenesis, RNA transport, and stress granule formation⁶⁸⁻⁷⁰. TDP-43 normally shuttles between the cytosol and nucleus, but the natively folded protein is located predominately in the nucleus^{71,72}. Pathological inclusions of TDP-43 can be found in the cytosol of both neurons and glia, where it is abnormally phosphorylated, ubiquitinated and fragmented to form several C terminal fragments (termed 'TDP-43 pathology')⁵⁰. More than 40 TDP-43 mutations have now been identified in sALS/fALS patients, or in FTD⁵⁶. Both loss of nuclear TDP-43 function and a gain of toxic function in the cytoplasm are implicated as pathogenic mechanisms^{73,74}, although the level of expression of TDP-43 also determines disease severity⁷⁵⁻⁷⁸.

1.5.3 Fused in sarcoma

Mutations in the *FUS* (fused in sarcoma) gene are responsible for 5% of fALS and also rare cases of FTD^{36,37} and were first identified in 2009. *FUS* is present within MN inclusions in less than 1% of ALS patients and 9% of FTD patients. *FUS* bears striking structural and functional similarities to TDP-43, with similar functions in RNA metabolism, mediating transcription and RNA splicing⁷⁹. Similar to TDP-43, *FUS* normally shuttles between the nucleus and the cytosol⁸⁰, but it is found predominantly in the cytoplasm in ALS MNs⁸¹. To date more than 50 mutations have been identified in the *FUS* gene in ALS patients⁸².

1.5.4. C9ORF72

The discovery of mutations in *C9ORF72* in both fALS and sALS patients in 2011 was a major discovery in the field, because these mutations cause the greatest

proportion of fALS and FTD cases, and they provided the first molecular link between ALS and FTD⁵⁶. The *C9ORF72* mutation is an intronic hexanucleotide repeat expansion (GGGGCC) in a non-coding region of the gene, which accounts for up to 80% of fALS-FTD, 20-50% of fALS, 35-20% of sALS, and 10-30% of FTD⁸³⁻⁸⁹. In normal individuals less than 30 GGGGCC intronic repeats within the *C9ORF72* gene are present, but in ALS/FTD patients, this region is greatly expanded, up to several thousand repeats. *C9ORF72* was previously an uncharacterized protein. However, bioinformatics studies first predicted that *C9ORF72* encodes a Rab GEF (guanine nucleotide exchange factor), and studies from our laboratory demonstrated that *C9ORF72* regulates Rab-dependent endosomal trafficking and autophagy⁹⁰. The *C9ORF72* repeat expansion is associated with a higher incidence of bulbar-onset ALS, and also with cognitive impairment and earlier disease onset, with accelerated progression^{84,91-93}.

1.6. Underlying pathological mechanisms of ALS

1.6.1. Protein aggregates

Protein aggregation results from the misfolding of proteins through changes in their conformation⁹⁴. Normally, the exterior of a protein is hydrophilic, whereas the interior is hydrophobic, but in misfolded proteins, hydrophobic portions become exposed, which interact with each other and lead to aggregation. Large inclusions and smaller aggregates containing misfolded proteins are present in degenerating MNs and surrounding glial cells in ALS. Pathological inclusions may consist of multiple misfolded proteins in ALS/FTD (*Figure 1.3*). In ALS, misfolded TDP-43 makes up the largest protein constituent of the inclusions (97%), whereas in FTD Tau and TDP-43 make up similar proportions, (45%). Interestingly, inclusions containing mutant or wildtype TDP-43- are present in fALS and sALS respectively⁵⁶.

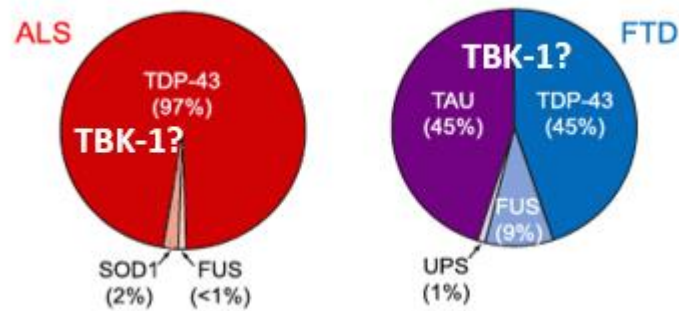


Figure 1.3: Composition of the pathological inclusions in ALS and FTD. In ALS 97% of inclusions are positive for TDP-43 whereas TDP-43-negative inclusions contain SOD1 or FUS. In contrast, in FTD only 45% of patients bear TDP-43-positive inclusions, and Tau is also present in another 45% of inclusions. Tau positive inclusions are not detected in ALS. The inclusions contain many other protein constituents', but it remains unknown if TBK-1 is present. Adapted from Ling et al. ⁵⁶

Several pathogenic mechanisms that lead to pathology are implicated in ALS, as discussed in more detail in the sections below and illustrated in *Figure 1.4*.

1.6.2. Axonal dysfunction

The axon represents approximately 99% of a neuron's cell volume⁹⁵, but protein and lipid synthesis occurs primarily in the cell body. Hence well-functioning axonal transport mechanisms are crucial for neuronal function and viability. This is particularly true for MNs, which have very long axons, up to 1 meter in length in an adult human⁹⁶. Active axonal transport processes are required to remove damaged proteins, organelles and autophagosomes from the synapse towards the cell body for degradation, and to supply the axon and synapse with newly synthesized materials and neurotrophic factors⁹⁷⁻⁹⁹.

The presence of the abnormal accumulation of neurofilaments, damaged mitochondria, and autophagosomes within axons of MNs in sALS patients¹⁰⁰⁻¹⁰³ implies that axonal transport defects are present in ALS. Further evidence for this was

demonstrated by the presence of axonal trafficking defects in *Drosophila* MNs expressing ALS mutations TDP-43^{M337V} and TDP-43^{A315T} ¹⁰⁴ Similarly, axonal transport defects are present in transgenic mutant SOD1 mice, where they are early events in pathogenesis^{105,106}.

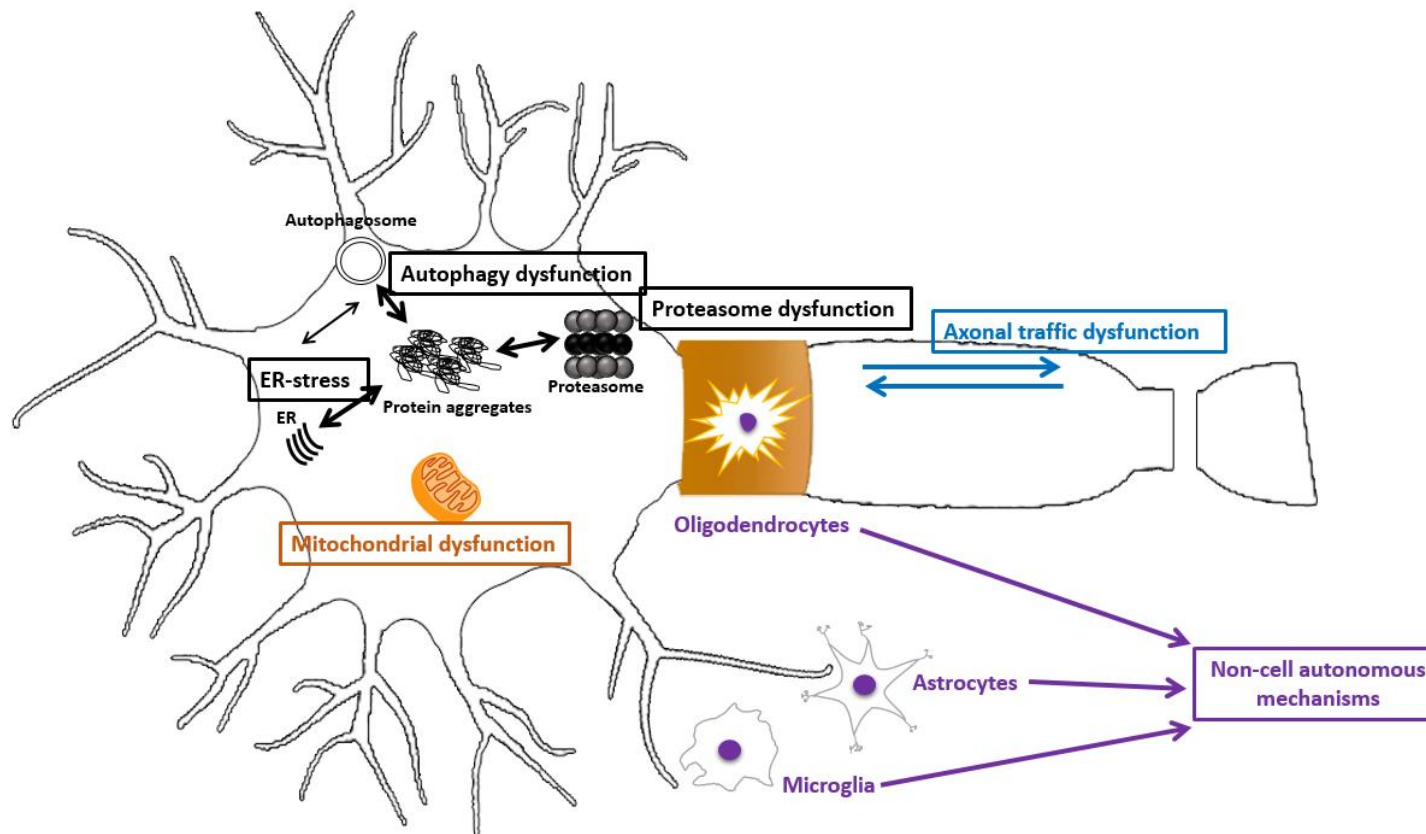


Figure 1.4: Mechanisms involved in ALS pathology. The hallmark of ALS is the presence of intracellular protein aggregates. Axonal transport defects, mitochondrial dysfunction are also important pathologies implicated in ALS. Non-cell autonomous mechanisms are also involved in ALS pathology, including oligodendrocytes, microglia and/or astrocytes that affect disease progression. Presence of cytoplasmic inclusion may be due to the failure of autophagy or the ubiquitin proteasome system. Protein aggregates also lead to ER-stress, which may have further effects on autophagy

1.6.3. Mitochondrial dysfunction

Mitochondria have important cellular roles, including ATP production, calcium homeostasis, and apoptosis. Mitochondrial dysfunction has been long implicated in ALS, because swollen and vacuolated mitochondria can be detected in sALS patient MNs^{101,107}. Similar mitochondrial abnormalities have been described in transgenic mutant SOD1 mice MNs, as well as in skeletal muscle of these animals before symptom onset¹⁰⁸⁻¹¹⁰. In addition, in SOD1 mouse models, dysfunction of mitochondrial respiration, ATP synthesis, anterograde axonal transport of mitochondria, and induction of apoptosis, are also observed (reviewed in ¹¹¹).

1.6.4. Non-cell autonomous mechanisms

ALS is not only a disease of MNs, because other cell types within the central nervous system are also implicated in disease progression, and importantly, expression of mutant SOD1 exclusively in MNs of mice does not cause ALS-like symptoms¹¹². Multiple lines of evidence support a role for other cell types in ALS disease progression, including astrocytes, oligodendrocytes and microglia ¹¹³⁻¹²⁵. For example oligodendrocytes degenerate in mutant SOD1 mice and they are replaced by newly proliferated oligodendrocytes that show abnormal morphology and are not fully differentiated¹¹⁴. These data however imply that although MN death is central to disease, the surrounding cells, also have an important role in disease progression in ALS.

1.6.5. Endoplasmic reticulum stress and unfolded protein response

The endoplasmic reticulum (ER) is the first cellular compartment where secreted and transmembrane proteins are synthesized and folded. The ER is also a major intracellular calcium storage and is important for lipid synthesis¹²⁶. The presence of misfolded proteins within the ER causes ER stress, which engages the unfolded protein

response (UPR): signal transduction pathways that aim to reestablish cellular homeostasis by inhibiting translation and increasing the protein folding capacity of the ER¹²⁷ (*Figure 1.5*). However, whilst initially protective, chronic ER stress leads to apoptosis¹²⁸. Cytoplasmic proteins can also induce ER stress by indirect mechanisms, such as by interfering with ER-Golgi transport^{129,130}.

The presence of misfolded proteins within the ER leads to their binding to BiP (binding immunoglobulin protein). This subsequently initiates dissociation of BiP from three ER-stress sensor proteins, leading to their activation; IRE1 (inositol-requiring kinase 1), PERK (PKR-like endoplasmic reticulum kinase) and ATF-6 (activating-transcription factor 6), which each represent a separate branch of the UPR (*Figure 1.5*)¹²⁶. Activation of IRE1 leads to induction of specific transcription of ER-chaperones and ERAD (endoplasmic-associated protein degradation) associated genes. Activation of PERK inhibits eIF2 α (eukaryotic initiation factor 2), leading to reduction of the entry of newly synthesized proteins to the ER-lumen, thus reducing the load of misfolded proteins in the ER, and reducing ER stress. Similarly, activation of ATF6 leads to its cleavage and translocation to the nucleus, which also induces gene expression of chaperones and ERAD proteins¹³¹. The transition of UPR from pro-survival to pro-apoptosis is mediated by transcription factor CHOP (CCAAT-enhancer-binding protein homologous protein), which is induced by both ATF6 and PERK pathways.

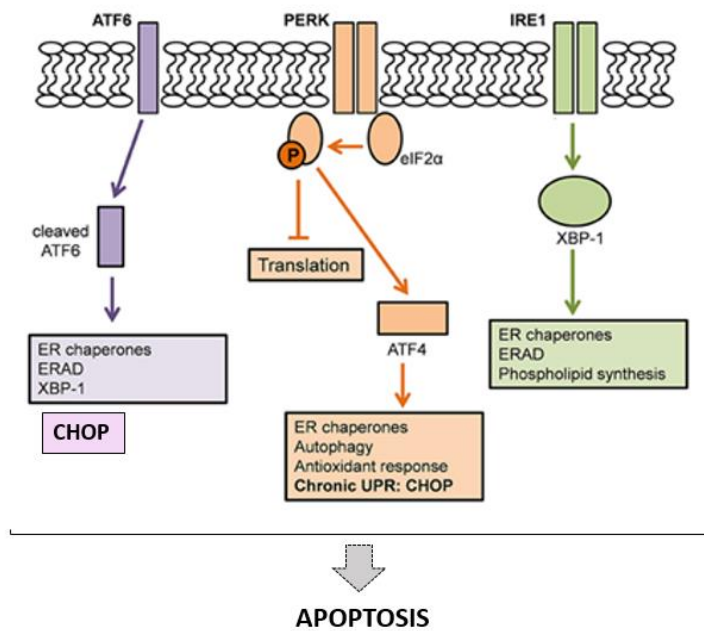


Figure 1.5: The three pathways of the UPR. Activation of UPR leads to expression of ER chaperones and ERAD proteins, and suppression of general protein translation. If unresolved, the UPR triggers apoptosis. Adapted from Perri et al. ¹²⁶.

The role of ER stress in ALS has now been studied extensively by our laboratory and others. Induction of many UPR proteins, including ER stress sensor proteins ATF6, IRE1 and PERK, ER chaperones BiP, Erp57 and PDI, and apoptotic effectors, CHOP, ASK1 and caspase3, has been detected in tissues from sALS patients and animal models¹³². Similarly, the UPR is induced in neuronal cells expressing ALS-associated mutant proteins, including mutant SOD1¹³³, TDP-43¹³⁴, and FUS ¹³⁵. Systematic transcriptional analysis using laser microdissection of MNs that degenerate first in transgenic mutant SOD1 mice (fast fatigue)¹³⁶ demonstrated that those MNs were selectively vulnerable to ER stress compared to those MNs targeted later in disease. This implies that ER stress is an important and early event in pathology in ALS¹³⁶.

Most mutant proteins associated with ALS are located in the cytoplasm rather than the ER. Hence, the mechanisms responsible for ER stress by cytoplasmic proteins in ALS were initially unclear. However, mutant SOD1 was found to interact with ERAD protein Derlin-1 in the cytoplasm, thus triggering ER stress by impairing ERAD¹³².

Furthermore, our laboratory recently demonstrated that several mutant ALS proteins inhibit ER-Golgi transport, leading to an accumulation of secretory and transmembrane proteins within the ER, thus triggering ER stress. This was observed for mutant forms of SOD1¹³⁰, misfolded wildtype SOD1¹³³, mutant TDP-43¹³⁴, and mutant FUS¹²⁹. The author performed immunohistochemistry studies for the latter publication before commencing the studies outlined in this thesis¹²⁹.

1.6.6. Autophagy

Autophagy, literally meaning 'self-eating', describes a catabolic process in which cells deliver their organelles and long-lived proteins for degradation into the lysosome. Three types of autophagy can be distinguished in mammalian cells: (1) microautophagy, a direct engulfment of small volumes of the cytosol by lysosomes¹³⁷; (2) chaperone-mediated autophagy (CMA), a selective receptor-mediated translocation of proteins into the lysosome¹³⁸, and (3) macroautophagy¹³⁹, degradation of proteins or cellular organelles. During macroautophagy, this degradation occurs through compartmentalisation in double membrane structures, called 'autophagosomes' that subsequently fuse with the lysosome.

Macroautophagy involves several distinct stages (*Figure 1.6*). The first step is the nucleation and formation of the phagophore. The phagophore then elongates and forms the autophagosome, which encloses the cargo for degradation inside¹⁴⁰. The ER has been implicated as the source of membranes for the autophagosome¹⁴¹. The autophagosome then fuse with endosomes, forming amphisomes and fusion of autophagosomes with lysosomes results in autolysosomes. Finally, the cytoplasmic contents of the autolysosome are degraded by lysosomal acid hydrolases.

Macroautophagy is a very tightly regulated catabolic process (schematic diagram illustrated in *Figure 1.5*). The presence of cellular stress stimuli inhibits MTOR

(mammalian target of rapamycin), leading to activation of a Unc51-like autophagy activating kinase (ULK) complex¹⁴⁰. The ULK complex initiates vesicle nucleation by translocating Beclin1 to the site of phagophore assembly¹⁴⁰. Vesicle nucleation is followed by elongation of the phagophore membrane. During elongation, microtubule-associated 1 light chain 3 β (LC3) becomes conjugated to phosphatidylethanolamine, to form a modified form of LC3 (LC3-II), which stably binds to the membrane of both phagophores and autophagosomes¹⁴⁰. The sequestered cargo is then degraded when the autophagosome fuses with the autolysosome.

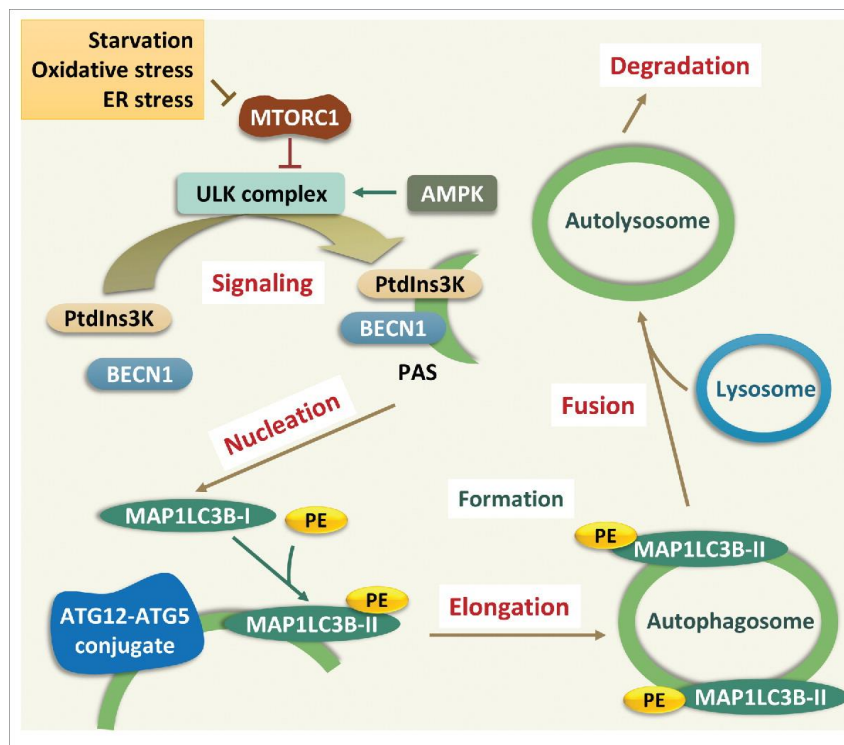


Figure 1.6: Pathways involved in the autophagy cascade. Stress induced activation of the ULK complex leads to translocation of beclin 1 to the phagophore assembly site. During membrane elongation, LC-3 conjugates phosphatidylethanolamine to form LC3-II, and it stably relocates to the membrane on phagophores and autophagosomes. Finally, the autophagosome fuses with the autolysosome and the sequestered cargo becomes degraded. Adapted from Cai et al.¹⁴⁰

Macroautophagy is the term used to describe both the selective and non-selective degradation processes. During selective forms of autophagy, organelles or long-lived proteins are directed to autophagosomes by labelling with ubiquitin. In contrast, during non-selective macroautophagy, which typically occurs during glucose

or amino acid starvation, intracellular organelles or macromolecules are directed towards the autophagosome for degradation. However, once the cargo is engulfed in the autophagosome, no difference can be detected between the selective and non-selective forms of autophagy (Figure 1.7).

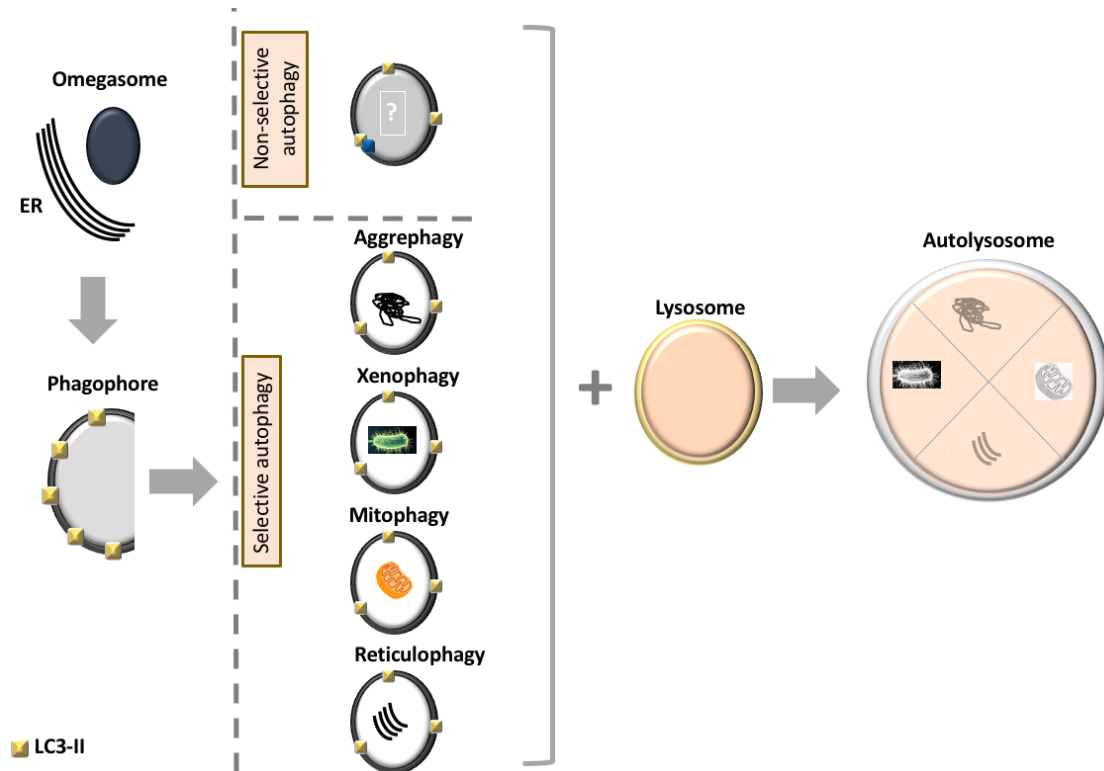


Figure 1.7: Schematic overview of selective and non-selective autophagy in mammalian cells. The response to cellular starvation usually manifests in non-selective autophagy, where cells engulf macromolecules, organelles and proteins that are dispensable. In contrast, during selective autophagy, the removal of specific organelles or protein occurs. Selective degradation of the mitochondria (mitophagy)¹⁴², endoplasmic reticulum (reticulophagy)¹⁴³, microorganisms (xenophagy)¹⁴⁴, and protein aggregates (aggrephagy)¹⁴⁵ can be distinguished as distinct forms of autophagy.

Neurons are highly sensitive cells when it comes to intracellular proteostasis, because of their large size, and unique structural and functional properties. Furthermore, mature neurons are post-mitotic and hence do not divide, hence they cannot dilute their waste burdens to the same extent as other cells. Therefore, autophagy could be a crucial process in neurons compared to other cell types. Previous

studies have indicated that activation of autophagy is protective in ALS^{146,147}, although this has been debated in other studies¹⁴⁸.

As the pathological hallmark of ALS in the presence of protein aggregates in degenerating MNs, mechanisms that clear these aggregates, such as the UPR and autophagy, may have an important role in ALS.

1.6.7 Intersection of ER-stress and autophagy

Emerging studies have demonstrated mechanistic links between ER-stress and autophagy. ATF4, a downstream mediator of the UPR, induces autophagy genes *beclin1*, *ATG5*, or *ATG7* in response to ER-stress¹⁴⁹. Similarly, IRE1 deficiency leads to inhibition of autophagosome formation in neuronal cells¹⁵⁰. Moreover, UPR activation induces autophagy via alteration in MTOR¹⁵¹. In addition, ATF6, can trigger autophagy through up-regulation of death-associated protein kinase 1, under ER-stress¹⁵²⁻¹⁵⁴. Furthermore, there is increasing evidence that the source of the autophagosome membrane is the ER¹⁵⁵. These mechanisms are not fully understood but together indicate a close link between the ER and autophagy.

1.7. Optineurin

Optineurin is a 67 kDa protein with functional roles in autophagy, and mutations in *OPTN*, which encodes optineurin, were identified in ALS patients in 2010^{156,157}. To date, 27 mutations in *OPTN* have been identified in fALS and sALS patients¹⁵⁸. Mutations within *OPTN* are also associated with normal tension glaucoma¹⁵⁹ and FTD¹⁶⁰. Optineurin is an autophagy adaptor that binds to the molecular motor protein myosin VI, which mediates trafficking along actin filaments¹⁶¹. Optineurin is present within the inclusions in sALS¹⁶², suggesting a general involvement for optineurin in sALS. Optineurin

contains a NEMO-like domain, at least one leucine-zipper, multiple coiled-coil motifs, an ubiquitin binding domain, and an LC3 interacting motif, (LIR)¹⁶³. Optineurin is normally located in the cytoplasm in human neurons¹⁶¹ and is ubiquitously expressed in many tissues¹⁶⁴.

Our laboratory previously demonstrated that ALS-linked mutations Q398X and E478G in optineurin disrupt its normal association with myosin VI in MN-like NSC-34 cells, leading to an abnormal diffuse cytoplasmic distribution, inhibition of secretory protein trafficking, ER stress and Golgi fragmentation. Moreover, WT optineurin associated with lysosomes and promoted autophagosome fusion to lysosomes¹⁶¹. We also observed that the interaction between myosin VI and optineurin was disrupted in sALS patients without optineurin mutations, implying that this mechanism may also exist in sALS¹⁶¹.

Optineurin contains a number of binding partners (*Figure 1.8*) including TBK-1, which was identified as an optineurin binding partner using a yeast two-hybrid system¹⁶⁵. The TBK1 binding site in optineurin is located between residues 1 and 127, as illustrated in *Figure 1.8*¹⁶⁵.

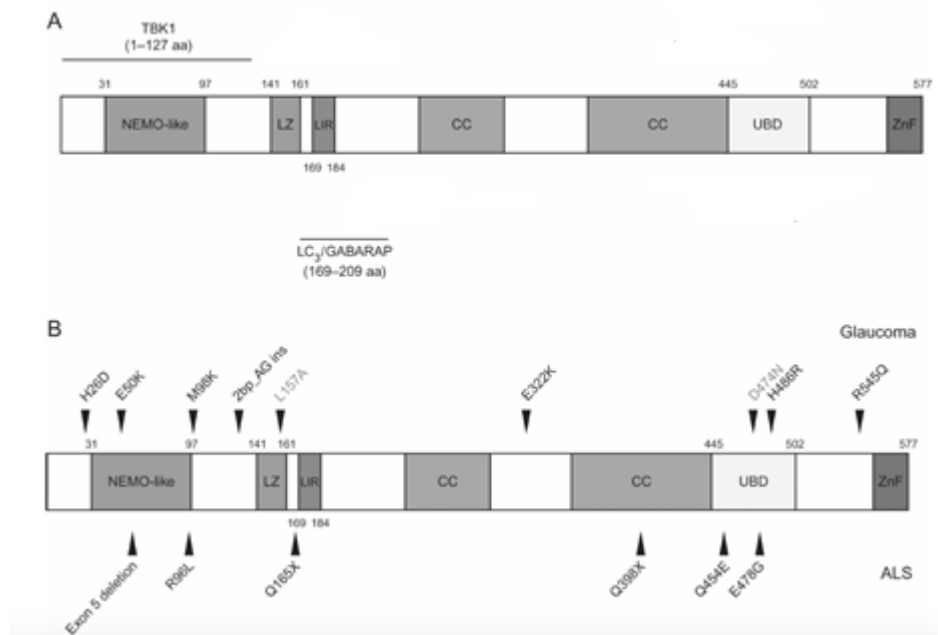


Figure 1.8: The location of binding sites and ALS-associated mutations in optineurin. (A) The binding site of TBK1 and LC-3 are located at the N-terminal end of optineurin. (B) Disease-associated mutations of optineurin. The glaucoma and ALS-linked mutations of optineurin are scattered throughout the protein. The E50K glaucoma mutation, as used in this study, is present at the N-terminus of optineurin, while the Q398X and E478Q mutations, also used in this study, are localized at the ubiquitin-binding domain (UBD). Adapted from Ying et al. ¹⁶⁶

1.8. TBK-1

Exome sequencing of 2896 ALS patients identified *TBK-1* as a novel ALS-causing gene in 2015¹⁶⁷. TBK-1 is important in innate immunity and the NFKB (nuclear factor kappa-light-chain-enhancer of activated B cells) pathway¹⁶⁸. TBK-1 is one of the two non-canonical I κ B kinases (IKKs) that directly regulate the activation of IFN regulatory factor 3 (IRF3)^{169,170}. TBK1 is an 84 kDa, 729 amino acid protein, containing an N-terminal kinase domain (KD), an ubiquitin like domain (ULD), and two coiled-coil domains at the C-terminus (CCD1/2)^{168,171} (Figure 1.9). To date, more than 40 mutations have been identified in ALS and FTD (complete list is given in Table 1.3).



Figure 1.9: Domain organization of TBK1. The kinase domain is located at the N-terminus of the protein, followed by the ubiquitin like domain (UBD). The coiled-coiled domain (CCD) is localized at the C-terminus.

TBK-1 is a serine-threonine protein kinase that transfers phosphate groups from ATP to the side chain of serine or threonine residues that regulates type-1 interferon production. The KD of TBK-1, located at the N-terminus, contains a serine residue at position 172, and phosphorylation at this position is crucial for enzymatic activity. The residue at position 135 is also a catalytic residue, responsible for phosphorylation of Ser172 on a neighboring TBK1 molecule; TBK-1 therefore autophosphorylates itself¹⁷¹. Mutational analysis of TBK1 has revealed that the ULD has a role in the TBK-1 kinase activity, because binding of ULD to KD is necessary for activity¹⁷². The CCD1/2 domains function in substrate binding for three well-known substrates of TBK1; Sintbad, NAP1 (NAK-associated protein 1) and TANK (TRAF family member-associated NF-kappa-B activator)¹⁷³. The optineurin binding site is also located at the CCD¹⁶³.

Table 1.3: ALS and FTD associated mutations in TBK-1. Mutations in TBK-1 have been found in both FTD and f/sALS. NA: non applicable, UN: unknown. +++: levels equals to wild type's protein, -: completely abolished, +: mostly abolished

Mutation: nucleotide sequence	Mutation: resulting amino acid	Affected domain	Kinase activity	Optineurin binding	FTD/ALS	Reference
g.3815C>T	p.Gln2*	KD	UN	NA	UN	Gijssels et al. ¹⁷⁴
c.10A>G	p.Thr4Ala	KD	UN	UN	FTD	Le Ber et al. ¹⁷⁵
c.77G>A	p.Gly26Glu	KD	UN	UN	ALS	Le Ber et al. ¹⁷⁵
c.140G>A	p.Arg47His	KD	-	+++	fALS	Fresichmidt et al. ¹⁶⁷
c.314A>G	p.Tyr105Cys	KD	UN	UN	sALS	Fresichmidt et al. ¹⁶⁷
c.349C>T	p.Arg117X	-	UN	NA	FTLDP-TDP	Pottier et al. ¹⁶⁰
c.358+T>C	p.Thr77TrpfsX4	-	UN	NA	fALS	Fresichmidt et al. ¹⁶⁷
c.427C>T	p.Arg143Cys	KD	UN	UN	ALS	Le Ber et al. ¹⁷⁵
c.467_468delCA	p.Thr156ArgfsX6	-	UN	NA	FTD-ALS	Le Ber et al. ¹⁷⁵
c.555T>A	p.Tyr185X	-	UN	NA	fALS	Fresichmidt et al. ¹⁶⁷
g.14982_14984del	p.Asp167del	KD	UN	UN	UN	Gijssels et al. ¹⁷⁴
g.28063G>T	p.Arg271Leu	KD	UN	UN	UN	Gijssels et al. ¹⁷⁴
g.29963G>T	p.Gly272_Thr331del	KD - ULD	UN	UN	UN	Gijssels et al. ¹⁷⁴
g.29841A>G	p.Lys291Glu	KD	UN	UN	UN	Gijssels et al. ¹⁷⁴
c.914T>C	p.Ile305Thr	ULD	UN	UN	sALS	Fresichmidt et al. ¹⁶⁷
c.916C>A	p.Ley306Ile	ULD	UN	UN	FTLDP-TDP	Pottier et al. ¹⁶⁰
c.923G>A	p.Arg308Gln	ULD	+	+++	sALS	Fresichmidt et al. ¹⁶⁷
c.958_958delA	p.Thr320GlnfsX40	-	UN	NA	fALS	Fresichmidt et al. ¹⁶⁷
c.959C>T	p.Thr320Ile	ULD	UN	UN	ALS	Le Ber et al. ¹⁷⁵
g.29934C>T	p.His322Tyr	ULD	UN	UN	UN	Gijssels et al. ¹⁷⁴
c.1070G>A	p.Arg357Gln	ULD	+	+++	fALS	Fresichmidt et al. ¹⁶⁷

g.33398delT	p.Ser398Profs*11	CCD	UN	UN	UN	Gijssels et al. ¹⁷⁴
c.1197delC	p.L399fs	-	UN	NA	fALS	Williams et al.
c.1201A>G	p.Lys401Glu	CCD	UN	UN	FTLDP-TDP	Pottier et al. ¹⁶⁰
c.1318C>T	p.Arg440X	-	UN	NA	ALS-dementia	Le Ber et al. ¹⁷⁵
c.1340+1G>1	p.Ala417X	-	UN	NA	fALS/3sALS	Fresichmidt et al. ¹⁶⁷
c.1343_1346delAATT	p.Ile450LysfsX15	-	UN	NA	2fALS	Fresichmidt et al. ¹⁶⁷
c.1434_1435delATG	p.Val479GluX4	-	UN	NA	fALS	Fresichmidt et al.
c.1446T>G	p.Tyr482X	-	UN	NA	FTD-ALS	Le Ber et al. ¹⁷⁵
g.43446T>C	p.Ile515Thr	CCD	UN	UN	UN	Gijssels et al. ¹⁷⁴
g.43453_43454insTT	p.Ser518Leufs*32	CCD	UN	UN	UN	Gijssels et al. ¹⁷⁴
g.43505G>A	p.Ala535Thr	CCD	UN	UN	UN	Gijssels et al. ¹⁷⁴
c.1676T>G	p.Met559Arg	CCD	-	-	fALS	Fresichmidt et al. ¹⁶⁷
c.1712C>T	p.Ala571Val	CCD	UN	UN	sALS	Fresichmidt et al. ¹⁶⁷
c.1792A>G	p.Met598Val	CCD	UN	UN	sALS	Fresichmidt et al. ¹⁶⁷
c.1928_1930delAAG	p.Glu643del	CCD	+++	-	2sALS	Fresichmidt et al. ¹⁶⁷
c.1960_2A>G	-	CCD	UN	UN	FTD-ALS	Le Ber et al. ¹⁷⁵
c.1963C>T	p.Gln655X	-	UN	NA	FTD-ALS	Le Ber et al. ¹⁷⁵
c.1985T>C	p.Met662Thr	CCD	UN	UN	FTD-ALS	Le Ber et al. ¹⁷⁵
c.2086G>A	p.Glu696Lys	CCD	+++	-	f/sALS+FTLDP	Fresichmidt et al. ¹⁶⁷
c.2138+2T>C	p.690-713del	-	NA	NA	2fALS	Fresichmidt et al. ¹⁶⁷

The kinase activity of TBK-1 is regulated by phosphorylation of Ser172, within the so-called 'activation loop' of the protein¹⁷⁶. Neighboring TBK-1 molecules interact with each other, which provide the necessary structural elements to achieve the active kinase conformation. TBK-1 forms dimers in such way that autophosphorylation is impossible due to the kinase domains facing away from each other. TBK1 is inactive until it becomes recruited by specific adaptor proteins to signaling complexes, where it becomes auto-phosphorylated, either due to high concentrations¹⁷⁷ or due to activation by other kinases¹⁷⁸. Upon activation, two KDs, within the dimer, interact with each other and Ser172 becomes phosphorylated. Endogenous TBK1 requires an adaptor-binding motif localized in the CCD1/2 domains for activation, while overexpression of TBK-1 can lead to activation in the absence of the AB motif or stimulus¹⁷³.

2

Aims of the thesis

The broad aim of this thesis was to examine possible mechanisms by which autophagy is dysregulated by ALS-mutations in optineurin and TBK-1. The normal cellular function of both optineurin and TBK-1 is associated with autophagy, and our previous studies demonstrated that autophagy is disrupted by the ALS-mutations in optineurin. Based on these results and evidence that autophagy is mechanistically linked to ER-stress in ALS; we aimed to determine whether ALS-mutations in optineurin inhibit autophagy by disrupting its interaction with TBK-1, and also whether the ALS/FTD-mutations in *TBK-1* cause dysfunction of autophagy, leading to ER-stress and induction of the UPR.

Hypothesis

ALS/FTD associated mutations in *TBK-1* lead to dysfunction in autophagy, thus inducing ER-stress and the UPR.

Specific Aims

Hence the specific aims of this study were to;

- Examine the relationship between ALS-mutant optineurin and TBK-1 both in basal conditions and during autophagy,
- Design and generate ALS/FTD-mutant and control TBK-1 overexpressing vectors,
- Overexpress these constructs in neuronal-like cells,
- Examine the intracellular localization of both WT and mutant TBK-1,
- Induce and monitor autophagy *in vitro* in the presence of WT and mutant TBK-1,
- Examine the effect of WT and mutant TBK-1 during ER-stress.

3

Materials and Methods

3.1 Materials and Solutions

The following solutions have been used during the study.

Tris-buffered saline (TBS) contains 50 mM Tris and 150 mM NaCl in miliQ water and pH is set at 7.6 with HCl. If required 10 ml of Tween was dissolved in 1 L of TBS resulting TBS-T.

Cell lysis buffer contains 500 mM Tris, 150 mM NaCl, 0.1% NP40, 0.1% SDS in miliQ water and pH is set to 7.6. Solution is kept at 4°C.

GFP-trap buffer contains 10 mM Tris, 150 mM NaCl, 0.5 mM EDTA in miliQ water and pH is set to 7.5. The solution is kept at 4°C.

2x HBS (HEPES-buffered saline) contains 0.8g NaCl, 0.027 g $\text{Na}_2\text{HPO}_4 \cdot \text{H}_2\text{O}$, 1.2 g HEPES in 100 mL miliQ water and pH is set to 7.05. The solution is kept at -20°C in aliquots. Freeze thaw is avoided.

1.5 mM Tris for SDS-gel preparation contains 91 g Tris, 2 g SDS in 1 L miliQ water, and pH is set to 8.8. The solution is kept at 4°C.

0.5mM Tris for SDS-gel preparation contains 6.05 g Tris 0.4 g SDS in 100 mL miliQ water, and pH is set to 6.8. The solution is kept at 4°C.

Western Blot loading buffer contains 9 μL Laemmli buffer (Biorad #1610747) and 1 μL NuPage reducing agent (ThermoFisher).

Luria-broth (LB) contains 20 g LB mix in 1 L miliQ water and pH is set to 7.0 and autoclaved.

LB-agar contains 0 g LB mix in 1 L miliQ water and pH is set to 7.0, then 15 g agar is added and autoclaved.

1 g ammonium persulfate is dissolved in 10 mL miliQ water and stored at 4°C.

The following materials have been used during the study.

Protein expressing vectors:

- FLAG-TBK-1 (backbone: pcDNA3.1)
- EGFP-OPTN (WT/E478G/Q398X/E50K) (backbone: pEGFP-C3)
- LC-3 dsRed (backbone: pDsRed-Monomer-C1 vector)

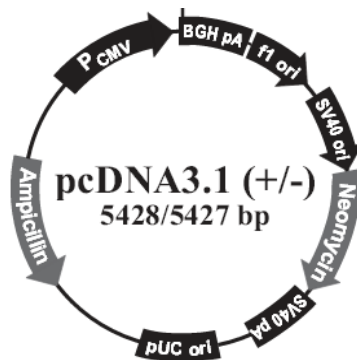


Figure 3.1: Diagram of pcDNA 3.1 vector from Invitrogen.

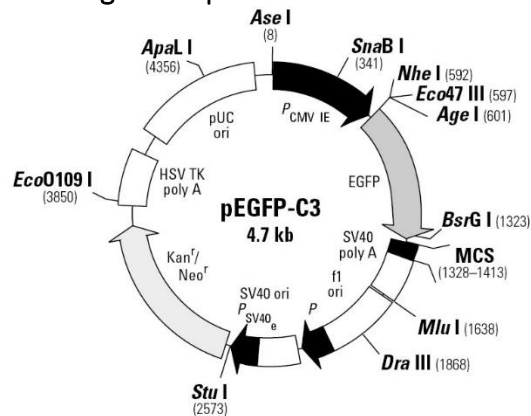


Figure 3.2: Diagram of EGFP-C3 vector from Addgene.

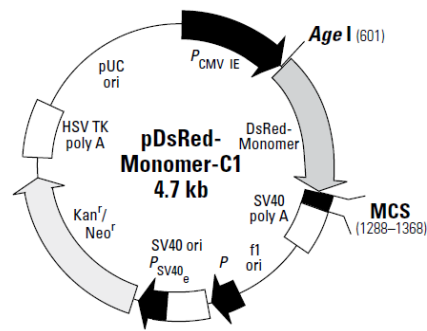


Figure 3.3: Diagram of pDsRed-monomer-C1 vector from Clontech.

3.2 Methods

3.2.1 General cell maintenance

Cells were maintained in DMEM (Sigma) supplemented with 10% FBS (fetal bovine serum) in tissue culture flasks (Falcon). The media of cultured cells was regularly tested for Mycoplasma contamination (Lonza), and only cells that tested negative were used. Cells were incubated at 37°C under 5% CO₂. Cells were passaged before reaching confluence by briefly rinsing in sterile PBS, followed by incubation with trypsin-EDTA solution (Gibco) for ~2min, resuspension in DMEM with 10% FBS and centrifugation for 5' at 1000rpm. The cell pellet was resuspended in DMEM with 10% FBS and the concentration was determined using a Scepter™ 2.0 Handheld Automated Cell Counter from Milipore. Cells were plated in 24-well or 6-well plates as required, and sub-cultured into fresh T75 flasks at 1:5-1:10 dilution.

The following mouse and human cell lines were used for in the in-vitro experiments in this study; mouse motor-neuron like cell line; NSC-34, human neuroblastoma cell line; SH-S5y5, and human embryonic kidney cell line; HEK293.

3.2.1.1. Cell plating

For transfection purposes HEK293, SH-s5Y5, NSC-34 cells were plated at 40,000cell/cm², 40,000cell/cm² and 42,000cell/cm² density, respectively. For immunoblotting experiments, cells were plated in 6-well plates. For immunostaining cells were grown on autoclaved coverslips placed in the bottom of 24-well plates.

3.2.1.2. Transient transfection

Plated cells were allowed to adhere overnight. The following day Lipofectamine 2000 (Invitrogen) reagent was used to transiently transfect cells according to protocols outlined in *Table 3.1*. After 16 h incubation, cells received fresh media to recover, and were placed back at the incubator for another 32 hours or treated as necessary.

Table 3.1: Standard operating protocol (SOP) for Lipofectamine transfection

Lipofectamine transfection				
6-well plate		Plasmid	Lipofectamine	Opti-MEM
	Sol. A	2 ug	-	100 uL
	Sol. B	-	2 uL	100 uL
Solution A and B were prepared in separate tubes and incubated for 5' at RT. Solution A and B were mixed gently and incubated for 20' at RT. 200 uL were added to each well drop by drop and plates were placed back in the incubator for 16 h.				
24-well plate		Plasmid	Lipofectamine	Opti-MEM
	Sol. A	1 ug	-	50 uL
	Sol. B	-	1 uL	50 uL
Solution A and B were prepared in separate tubes and incubated for 5' at RT. Solution A and B were mixed gently and incubated for 20' at RT. 200 uL were added to each well drop by drop and plates were placed back in the incubator for 16 h.				

Calcium phosphate transfection was performed according the methods as follows; 2 µg of each plasmid was mixed with 6.2 µl 2 M CaCl₂, adjusted to 50 µL with

filtered sterile H₂O and gently mixed. Then 50 µl of 2xHBS was added. 100 µL mixture was prepared for one well in 6-well plates and placed drop by drop on to the cells. The plates were incubated for 16 hr in the incubator and the following day fresh media was added to the cells which were placed back in the incubator.

3.2.1.3. Autophagy induction

Autophagy was induced by serum starvation with or without Bafilomycin treatment (Sigma). For serum starvation, serum supplemented media was removed and cells were gently rinsed with PBS for 5 sec. DMEM without serum was added and cells were incubated for 20 h. Cells were treated with 100 nM Bafilomycin for 4 h in serum free media.

3.2.2. Immunoblotting and immunoprecipitation

3.2.2.1. Cell lysis

Cells were rinsed with PBS to remove traces of media and serum and then incubated with approximately 500-800 µL of cell-lysis buffer for 15' on ice. Then cells were removed and placed into Eppendorf tubes and stored at -20°C overnight. The following day lysates were thawed on ice and centrifuged at 15000 rpm for 15' at RT to pellet insoluble material. Soluble protein supernatant was collected and used for protein quantification.

3.2.2.2. Protein quantification

Protein lysates were quantified using bicinchoninic acid *assay* (BCA- Thermo Scientific) by comparison with a bovine serum albumin (BSA) standard curve using concentrations ranging from 0-2 mg/mL, following the manufacturer's protocol. All samples were analyzed in duplicate in 96-well plates, and the absorbance at 560 nm was determined using PHERAStar FS.

3.2.2.3. Protein sample preparation for SDS-gel separation

Cell lysates, containing 40 ug of protein were mixed with 10uL of western blot loading buffer and boiled at 95°C for 5', then loaded on gradient or 6% SDS-polyacrylamide gel.

3.2.2.4. SDS-gel

Precast gradient gels and home-made gels were both used for electrophoresis of protein samples in this study. Precast gradient gels (4-15%) were purchased from Biorad. Home-made gels were poured in Invitrogen cassettes according to the formula in *Table 3.2* depending on the acrylamide % required. Samples were electrophoresed at 100-120V for 2-6 h depending on the degree of separation required.

Table 3.2 Preparation of SDS-polyacrylamide gels.

<i>Solutions</i>	<i>15% gel</i>	<i>12% gel</i>	<i>10% gel</i>	<i>7.5% gel</i>	<i>6% gel</i>
<i>Acryl/bisacryl sol. 30%</i>	5.00	4.00	3.33	2.50	2.00
<i>1.5M Tris pH8.8</i>	2.50	2.50	2.50	2.50	2.50
<i>H2O</i>	2.50	3.50	4.17	5.00	5.50
<i>APS (μL)</i>	100	100	100	100	100
<i>Temed (μL)</i>	10	10	10	10	10
<i>total (in ml)</i>	10	10	10	10	10

Stacking gel (5%) was prepared as follows: 3.5 mL H₂O, 1.5 mL 0.5 mM Tris pH6.8, 1 mL acrylamide (30%), 50 μL APS, and 5 μL TEMED were mixed and immediately poured into the cassette, then combs containing ten wells were placed in the gel. Gel were allowed to polymerize for at least 1 h.

Electrophoretically separated proteins were transferred to nitrocellulose membranes using a semi dry TransBlot® Turbo™ Transfer System from Biorad.

3.2.2.5. Antibody incubation

Membranes were blocked in 5% skim milk-TBS-T or 5% BSA-TBS-T for 1h. Primary antibody was then added to the membrane followed by incubation at 4°C overnight on a rotation stand. The primary antibody concentrations are listed in *Table 3.3*. Membranes were then washed with TBS-T once and TBS twice for 4min, followed by incubation with HRP-conjugated secondary antibody in TBS-T for an additional 1h. After washing with TBS and TBS-T as described above, membranes were then incubated 2ml of Clarity ECL reagent and the signals were detected using Chemidoc system by Biorad. Blots were stripped using 10ml of 1x ReBlot Plus solution (Chemicon) for 10 min and re-probed as above.

Table3.3: Antibody concentrations used in this study.

<i>Antibody</i>	<i>Species</i>	<i>Dilution</i>	<i>Manufacturer</i>
TBK-1	Rabbit	1/500	Abcam
OPTN	Rabbit	1/500	Cayman chemicals
LC-3	Rabbit	1/5000	Novusbio
GAPDH	Mouse	1/1000	Calbiochem
CHOP	Mouse	1/400	Santa Cruz
p-TBK1	Rabbit	1/500	Abcam
p-PERK	Rabbit	1/500	Santa Cruz
PERK	Rabbit	1/500	Santa Cruz
FLAG	Mouse	1/1000-1/10000	Sigma
FLAG	Rabbit	1/1000-1/2000	Sigma

3.2.2.6. Protein immunoprecipitations

GFP-conjugated proteins were precipitated using GFP-Trap (Bionovus Life Sci.). Briefly, 500ug of cell lysate was mixed with 20uL GFP-Trap, and then the volume was adjusted to final volume of 1ml with GFP-trap buffer, and incubated overnight at 4°C on a rotating wheel. The following day samples were centrifuged at 2000rcf for 2 min and then beads were washed with GFP-Trap buffer for 3 times after removing supernatant, and eluted using 30ul of western blot loading buffer by

boiling the beads at 95°C for 5min. Eluted samples were directly loaded on to SDS-polyacrylamide gel, transferred and immunoblotted as described above.

Proteins were immunoprecipitated using protein G/A coated magnetic Dynabeads (Life Technologies). 2 μ g of appropriate antibody was added to 500 μ g of protein lysate and the volume was adjusted to 1ml with GFP-Trap, followed by incubation overnight at 4°C on a rotating wheel. The following day 30 μ L of Dynabeads was added to the antibody/protein lysate mix and incubated for an additional 4 h at 4°C on a rotating wheel. Beads were then washed 3 times with GFP-trap buffer using a magnetic rack. Proteins were then eluted using 30 μ L of western blot loading buffer by boiling the beads at 95°C for 5min. Eluted samples were directly loaded on SDS-polyacrylamide gels, transferred and immunoblotting was performed as described above.

3.2.3. Immunocytochemistry and microscopy

The cells were grown on coverslips and fixed in 4%(w/v) paraformaldehyde-PBS for 10min at RT. Then cells were permeabilized with 0.1%(v/v) Triton-PBS for 1 min, and blocked with 3%(w/v) BSA-PBS for 1h on a shaker. The appropriate antibodies were added then in 1% BSA(w/v)-PBS and incubated overnight at 4°C. The following day coverslips were washed 3 times with PBS, then incubated with fluorescently labelled secondary antibodies in PBS for 1 h at RT on a vertical shaker. After repeated washing, nuclei were stained with Hoechst solution for 5 min at RT using with dilution factor of 1/3300. Coverslips were washed again with PBS then mounted using Dako fluorescent mounting medium.

3.2.3.1. Microscopy

Following immunocytochemistry fluorescently labelled cells were visualized initially using a Zeiss epifluorescence microscope (Z1, Goettingen, Germany).

Subsequently representative images were taken using Zeiss confocal microscope (Zeiss LSM 880).

3.2.4. Mutagenesis, bacteria transformation and plasmid purification

3.2.4.1 Site-directed mutagenesis

Single point mutations were introduced into WT-TBK-1 using pcDNA3.1-FLAG-WT-TBK-1 plasmid as a template (kind gift of Jean-Laurent Casanova -The Rockefeller University, New York). Site directed mutagenesis was performed using Q5® Site-Directed Mutagenesis Kit (New England Biolabs), following manufacturer's instructions (detailed below).

Primers (Sigma) were designed to introduce nucleotide substitutions into WT-TBK-1 sequence using NEBaseChanger (<http://nebasechanger.neb.com/>) using NCBI database. (NCBI Reference Sequence: NM_013254.3).

Table 3.4: Primer sequences to introduce mutations to TBK-1 gene. Base pairs coding the mutated amino acid are in bold. Ta: annealing temperature.

Mutations	Forward primer	Reverse primer	Ta
R308Q	5'-tatacttcacca aa atggtaattcatg-3'	5'-tcactagtttctgcaaaaaaac-3'	58 °C
R357Q	5'-ctacgaaggg ca acgcttagtct-3'	5'-ataagttcttgattgaagaaataatttgg-3'	62 °C
E696K	5'-attaaaggaa aag atggaagggg-3'	5'-ttcttcataccaagagtcatttc-3'	61 °C
E643X	5'-tattgaaga aa gta tcaaaatatcaagaatatac-3'	5'-tcaaaacactgattagtcagc-3'	60 °C

PCR reaction was prepared according to manufacturer's protocol (*Table 3.5*). The precise PCR conditions were optimized for each pair of primers according to the annealing temperature (Ta) for each primer. (*Table 3.6*)

Table 3.5: PCR reaction for site-directed mutagenesis

<i>Product</i>	<i>For 25 μl</i>	<i>Final conc.</i>
Q5 Hot Start High-Fidelity 2X Master Mix	12.5 μ l	1X
10 μ M Forward Primer	1.25 μ l	0.5 μ M
10 μ M Reverse Primer	1.25 μ l	0.5 μ M
Template DNA (1–25 ng/ μ l)	x μ l	1-25 ng
Nuclease-free water	9.0-x μ l	

Table 3.6: PCR cycles for site-directed mutagenesis.

<i>Step</i>	<i>Temp.</i>	<i>Time</i>
Initial Denaturation	98°C	30 seconds
25 Cycles	98°C	10 seconds
	Ta*	10–30 seconds
	72°C	10min
Final Extension	72°C	2 minutes
Hold	4–10°C	

Ta*: annealing temperature, which is specific for each primer.

In order to digest the parental (WT-mutation-free) plasmid DNA thus leaving only the mutant plasmid intact, PCR products were exposed to KLD (kinase-ligase-DpnI) digestion. PCR product (4 μ L) was incubated for 1h at RT according to *Table 3.7.*

Table 3.7: Protocol for KLD-reaction.

<i>Product</i>	<i>Volume</i>	<i>Final conc.</i>
PCR Product	4 μ l	
2X KLD Reaction Buffer	5 μ l	1X
10X KLD Enzyme Mix	1 μ l	1X
Nuclease-free Water	-	

3.2.4.2. Bacteria transformation with plasmid DNA

Heath shock transformation of alpha chemical competent *E. coli* (Bioline) was carried out as follows. Alpha chemically competent cells (50 μ L) were thawed on ice,

and 500 ng of DNA was added. Cells were heat shocked at 42°C for 30 sec, then placed back on ice for additional 5'. Then 100 uL of SOC (super optimal broth supplemented with 20 mM glucose) media was added and the E.coli was incubated for 1 h at 37°C on shaker. Bacteria pre-cultures were then plated on LB brot agar plates containing the appropriate selective antibiotics (ampicillin/kanamycin) and incubated overnight at 37°C. Agar plates were stored at 4°C for further experiments.

3.2.4.3. Plasmid DNA amplification

Single bacteria colonies were selected and amplified in LB-broth media overnight containing selective antibiotics at 37°C on a shaker. Plasmid DNA was purified by using Qiagen Midi/Mini plasmid kit following manufacturer's instruction. Briefly, overnight E.coli cultures were centrifuged at 4000 RPM for 20 min. Cell pellet was resuspended and lysed in solutions provided by Qiagen (composition unknown). Bacteria lysate were centrifuge at 15000 RCF for 30 min. DNA plasmids were washed using spin-columns. Plasmids were eluted from the columns in H₂O. The quantity and quality of plasmid was analyzed with Nanodrop. The ratio of absorbance, measured by Nanodrop, at 260 nm and 280 nm is used to assess the purity of DNA and RNA. Only plasmids with a 260/280 ratio above 1.8 was used in this study.

3.2.4.4. Sequencing

Each purified plasmid DNA (1 µg) was sent for sequencing to Australian Genome Research Facility, Melbourne. Two forward and three reverse primers were designed specifically for this study, to sequence the entire TBK-1 cDNA region. Primers are listed in *Table 4.3* in the Results section of this thesis.

Table 3.8. Sequencing primers for *TBK-1*. Two forward and three reverse primers were designed to sequence the entire *TBK-1* cDNA inserted in the vector. The *TBK-1* gene is 2193 nucleotides long, including the STOP codon, and the initiating methionine sequence.

Primer	Sequence	Position of binding on <i>tbk-1</i>
Forward 1	5'-atgcagagcacttctaatacatcatct-3'	1-26
Forward 2	5'-agcggcagagtttaggtgaaa-3'	1710-1730
Reverse 1	5'-gatgattcattccaccacc-3'	376-357
Reverse 2	5'-ttcacctaactctgccgct-3'	1492-1473
Reverse 3	5'-gccacatccatgggttaaag-3'	2166-2147

3.2.5. Statistical analysis

An unpaired student t-test was used where indicated in the Result sections. Difference was determined as significantly different if p-value was less than 0.05.

4 Results

4.1 Intracellular levels and localization of TBK-1 in the presence of ALS-mutant optineurin

Optineurin and TBK-1 are two proteins that were independently associated with ALS, yet they have been identified as binding partners¹⁶⁵. Optineurin is an autophagy adaptor protein, which recruits LC3 to autophagosomes¹⁶³, and our laboratory has previously shown that ALS-associated mutations, E478Q and Q398X, induce autophagy defects in NSC-34 cells¹⁶¹. As TBK-1 and optineurin mutually participate in xenophagy¹⁶³, and are both linked to ALS, we first investigate whether ALS- optineurin mutations influence the role of TBK-1 in autophagy, using neuronal cells over-expressing wildtype/mutant optineurin.

We chose the mouse hybridoma cell line NSC-34 for this purpose, which was generated from the fusion of a mouse neuroblastoma cell line, N18TG2, with mouse MN-enriched embryonic spinal cord cells¹⁷⁹. NSC-34 is therefore a hybrid cell line which has previously been shown to bear several characteristics of MNs, including the accumulation and release of acetylcholine, generation of action potentials and expression of neurofilaments¹⁷⁹. NSC-34 cells were transiently transfected using Lipofectamine for 48 h, with previously generated constructs overexpressing either wildtype or ALS-mutant optineurin, conjugated to *enhanced green fluorescent protein* (EGFP) (E478G-EGFP or Q398X-EGFP)¹⁶¹. An empty vector control (pEGFPC3), expressing EGFP only, was also used. A control mutant optineurin was also included, E50K-optineurin, which is linked to glaucoma, to allow us to differentiate the specific effects of ALS-causing mutations from any non-specific effects of a general mutation. Furthermore, unlike the ALS-optineurin mutants, the E50K mutant did not affect autophagosome and lysosome fusion in our previous study¹³³. At 48 h post-transfection, cell lysates were prepared and immunoblotting was performed using anti-human optineurin and TBK-1 antibodies. These analyses demonstrated that the optineurin-EGFP proteins were successfully expressed and that endogenous mouse TBK-1 was present in NSC-34 cells (*Figure 4.1*). The molecular weight (MW) of EGFP-conjugated

optineurin is approximately 92 kDa, hence the presence of the EGFP tag allowed visualization of the over-expressed optineurin distinct from the endogenous optineurin. *Figure 4.1* demonstrates that a band of approximately 92 kDa was present in WT, E50K and E478G transfectants but not controls, consistent with expressed optineurin-EGFP. The Q398X mutant contains a premature stop codon, resulting in expression of a truncated form of optineurin, with a smaller size (75kDa) than the other optineurin-EGFP proteins, and a band of this approximate size was also detected for Q398X. The blots were then stripped and re-probed for endogenous TBK-1; anti-human TBK-1 antibody was used because the reactivity of this antibody to both human and mouse TBK-1 has been previously demonstrated¹⁸⁰. The MW of mouse TBK-1 was detected at 84 kDa as expected. Blots were stripped and re-probed for GAPDH as a loading control, demonstrating similar loading in each case.

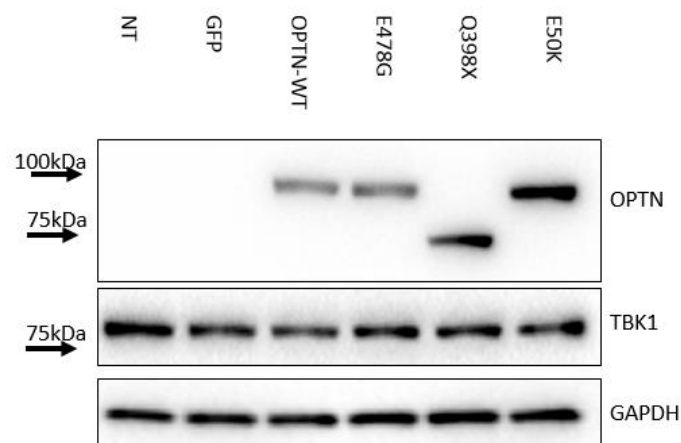


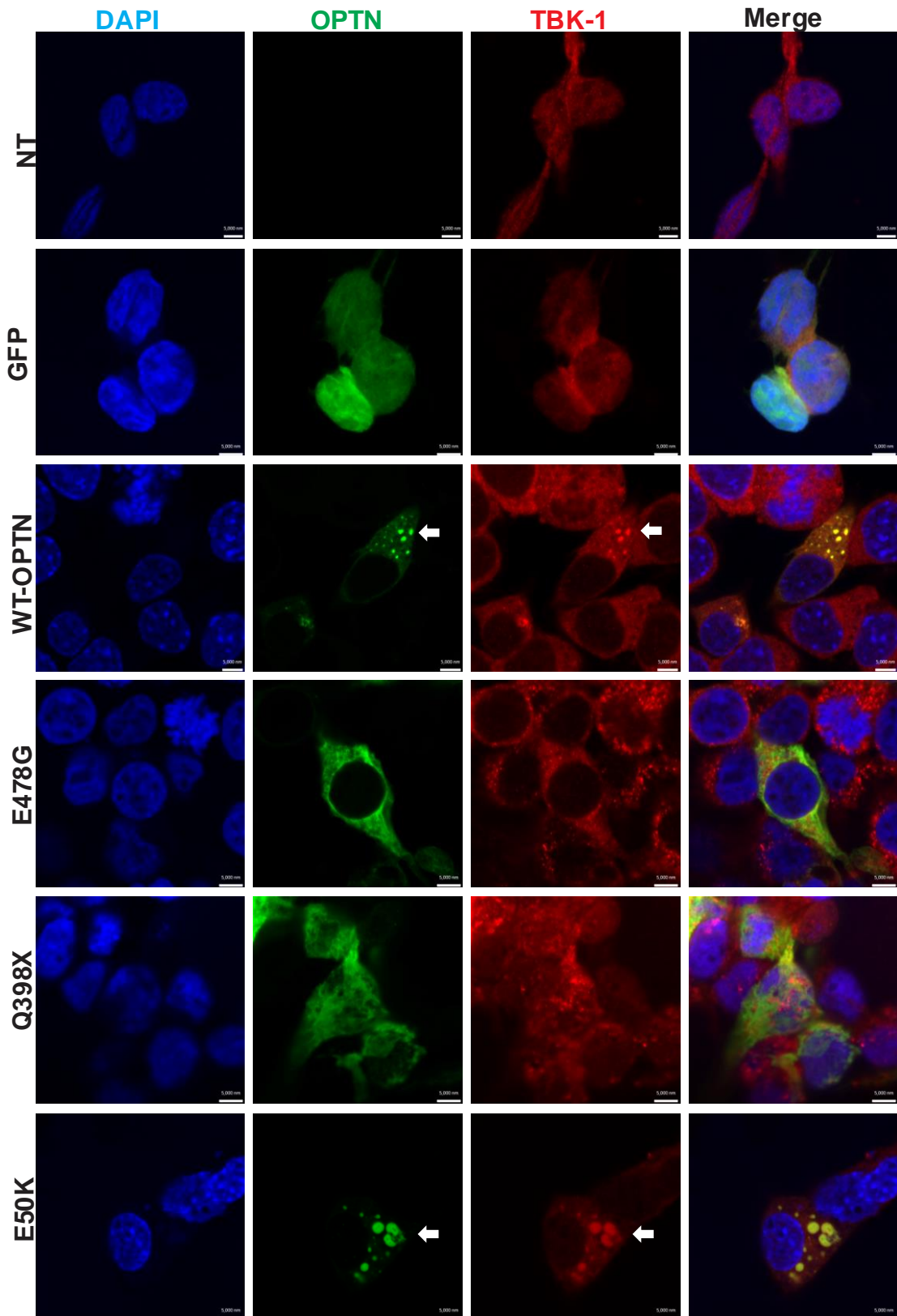
Figure 4.1: Optineurin-EGFP and TBK-1 expression in NSC-34 cell lysates from cells transiently transfected with optineurin-EGFP constructs. Blots were probed for optineurin, then stripped and re-probed for TBK-1 and GAPDH as a loading control. NT; non-transfected, WT; wildtype. OPTN; optineurin.

Next, we examined the intracellular localization of endogenous TBK-1 in NSC-34 cells, and whether it colocalizes with optineurin¹⁶⁵. NSC-34 cells were transiently transfected with optineurin-EGFP constructs (WT/E478G/Q398X/E50K) and immunocytochemistry using anti-TBK-1 antibodies was performed at 48 h post-

transfection. The endogenous mouse TBK-1 was expressed in a punctuate fashion in NSC-34 cells, apparent in non-transfected (NT) and empty vector (EGFP only) transfected controls (*Figure 4.2*). Wildtype optineurin was also expressed in a vesicular pattern, as previously demonstrated¹⁶¹. In contrast, the two ALS-mutants, E478Q and Q398X, displayed diffuse cytoplasmic staining, consistent with our previous observations¹⁶¹. The E50K control mutant also displayed typical vesicular appearance and was similar to wildtype optineurin¹⁶¹.

The colocalization between wildtype or mutant optineurin and TBK-1 was then examined and quantified in transfected NSC-34 cells using fluorescent microscopy. Only transfected cells were included in the analysis, indicated by the presence of positive EGFP-staining. Cells with colocalization of red and green signals (representing TBK-1 and optineurin respectively) in these vesicular structures were counted as colocalized. In contrast, cells displaying either the red or green signal only in these vesicles were not counted. NSC-34 cells overexpressing the EGFP vector showed punctuate TBK-1 staining without any vesicular colocalization of EGFP and TBK-1. Hence EGFP alone does not colocalise with TBK-1, as expected. In contrast, vesicles formed by wildtype optineurin colocalized with TBK-1 in 86.2 % of transfected cells (*Figure 4.2A/B*), as expected, based on their binding ability to each other¹⁶⁵. Similarly, the control glaucoma E50K mutant also formed typical vesicular structures that colocalized with TBK-1 in 82.2% of transfected cells: no statistically significant differences were detected between wildtype or E50K expressing cells ($p=0.47$) (*Figure 4.2*). In contrast, in cells overexpressing ALS-mutant E478Q and Q398X, TBK-1 did not form the prominent vesicles present in WT optineurin overexpressing cells, despite TBK-1 displaying typical punctuate staining in NT and EGFP–vector transfected cells. Hence, no optineurin vesicles were detected colocalizing with TBK-1 in cells overexpressing ALS-mutants E478G, Q398X.

A



B

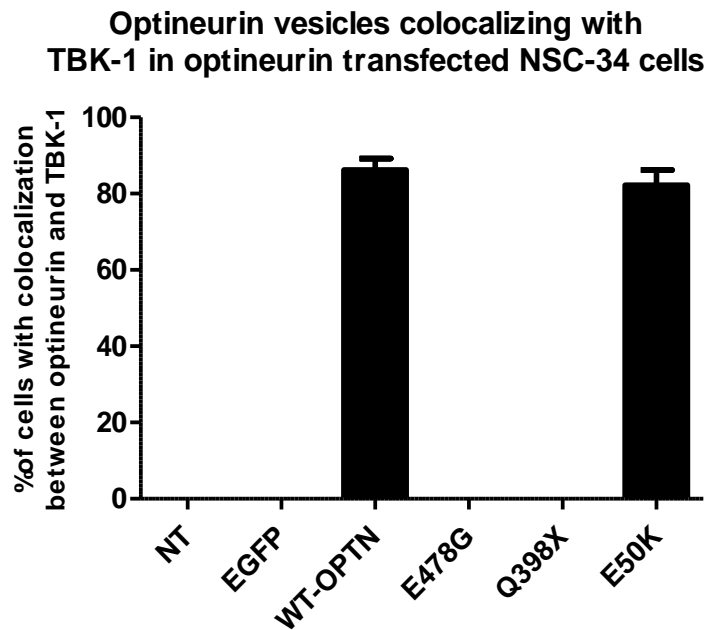


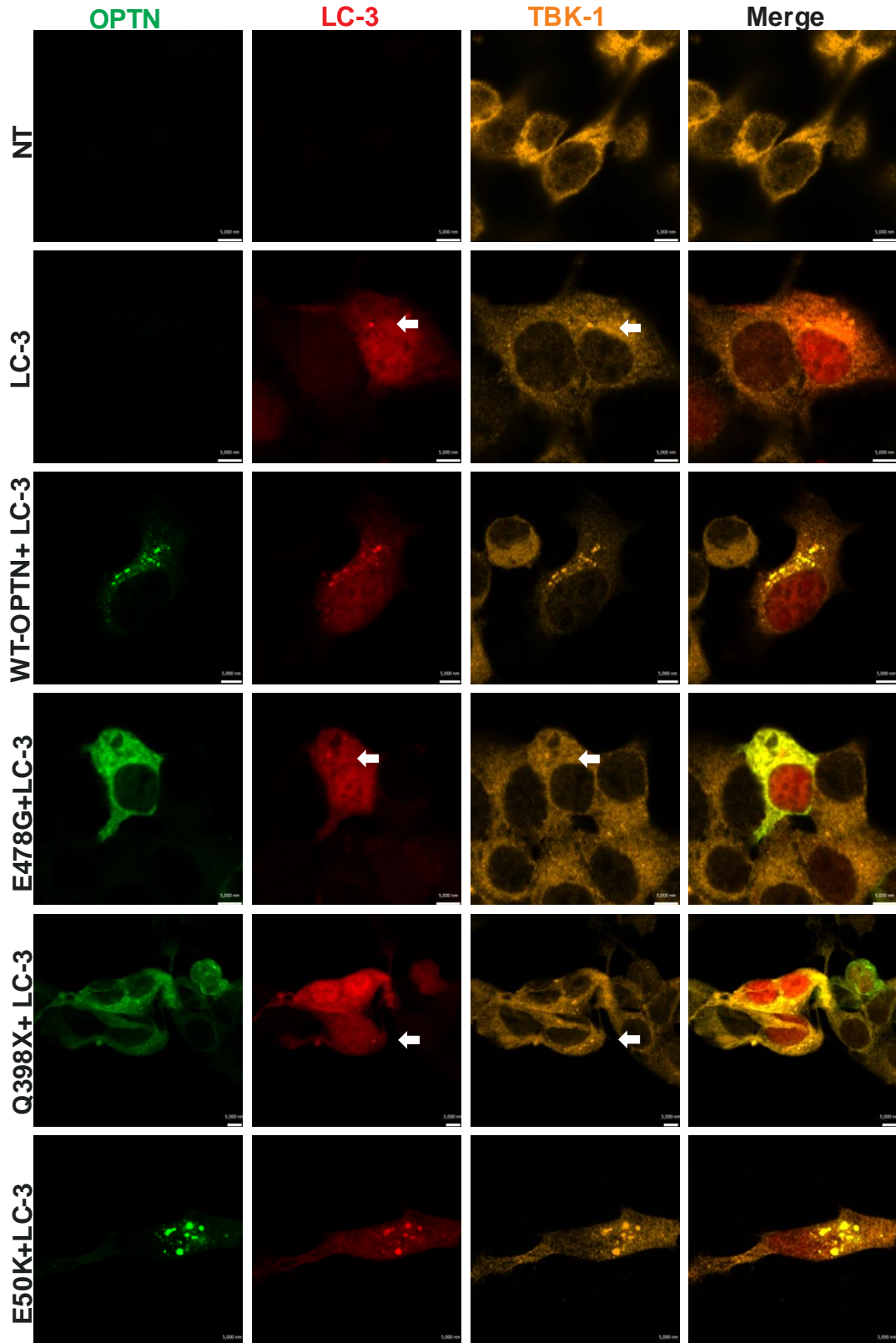
Figure 4.2: Wildtype and control mutant E50K optineurin-EGFP and TBK-1 colocalize in typical vesicular structures in NSC-34 cells, unlike the ALS-optineurin mutants. A) Representative confocal microscopy images of NSC-34 cells expressing WT/ALS and glaucoma mutant optineurin. Immunocytochemistry for endogenous TBK-1 and counter-staining with Hoechst was also performed. WT and E50K mutant optineurin formed vesicles that colocalized with endogenous TBK-1 (indicated by white arrows), while ALS-mutant optineurin did not. B) Quantification of colocalization between optineurin positive vesicle and TBK-1 in (A), N=3. Scale bar: 5 μ m NT; non-transfected, WT; wildtype.

Optineurin recruits LC3 to autophagosomes, suggesting that optineurin should colocalize with autophagosomes. Hence, we next examined whether the TBK-1-positive vesicles detected in wildtype and E50K overexpressing cells were autophagosomes. NSC-34 cells were co-transfected with EGFP-WT/E478G/Q398X/E50K and LC3-overexpressing vectors tagged with dsRed. Autophagy can be induced *in vitro* by serum-starvation or alternatively, treatment with pharmacological agents, such as rapamycin. Rapamycin is an inhibitor of mammalian target of rapamycin (MTOR), a multi-functional serine-threonine protein kinase with roles in cell growth, proliferation, motility and survival, that also negatively regulates autophagy¹⁸¹. In this study, serum-starvation was chosen as the method to induce autophagy, as it is reproducible, easy to carry out, and recommended in the recently (2016) revised, standardised, international guidelines for autophagy¹⁸². Furthermore, in order to reliably examine autophagy in this study, we

followed these guidelines in all experiments performed, to most accurately detect and monitor autophagy.

To induce autophagy, cells were serum-starved for 20 h using serum-free media, then fixed and immunocytochemistry for endogenous TBK-1 was performed. In cells without serum starvation, LC-3 was expressed in a diffuse pattern as expected, due to the lack of autophagy induction in these cells. However, upon serum-starvation, LC-3 positive vesicles, indicating autophagosomes, were found to accumulate in the cytoplasm. Quantification of the number of cells with LC-3-positive vesicles revealed that 30.7% of control cells displayed TBK-1 colocalized with LC-3 vesicles, in those cells that were only expressing LC-3-dsRed and not optineurin (*Figure 4.3 A/B*). However, in cells overexpressing both wildtype optineurin and LC3-dsRed, 81.6% of cells displayed optineurin-positive vesicles that colocalized with TBK-1, and most of these vesicles were also positive for LC3 (80.3%), suggesting autophagosomes. Similarly, in E50K cells, TBK-1 colocalized with optineurin in 73.6% of cells expressing E50K, and these vesicles were also positive for LC3 in 68.9% of cells. These findings were not significantly different ($p=0.81$, $p=0.42$) from the % of cells with TBK-1/optineurin/LC3 co-localisation in WT-optineurin transfected NSC-34 cells. Interestingly, however, in E478Q and Q398X cells, only 32% and 27.2% of cells respectively displayed vesicles that were TBK-1 and LC3 positive, which was significantly less than in wildtype-optineurin cells ($p<0.05$). The numbers of cells with TBK-1/LC3-positive vesicles in E478G/Q398X overexpressing cells were not significantly different from those expressing the LC3-dsRed construct only. These data suggest that another, unknown, protein endogenously expressed in NSC-34 cells, can partially recruit TBK-1 to autophagosomes, independently of optineurin. Hence these data suggest that TBK-1 is recruited to autophagosomes in an optineurin-dependent manner, which is disrupted in the presence of ALS-mutant optineurin.

A



B

TBK-1 colocalization with LC3 vesicles in optineurin transfected NSC-34 cells

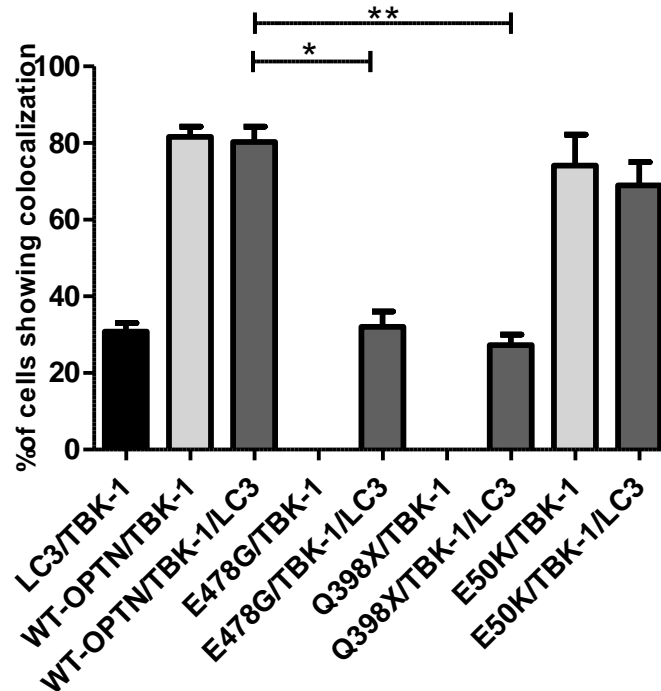
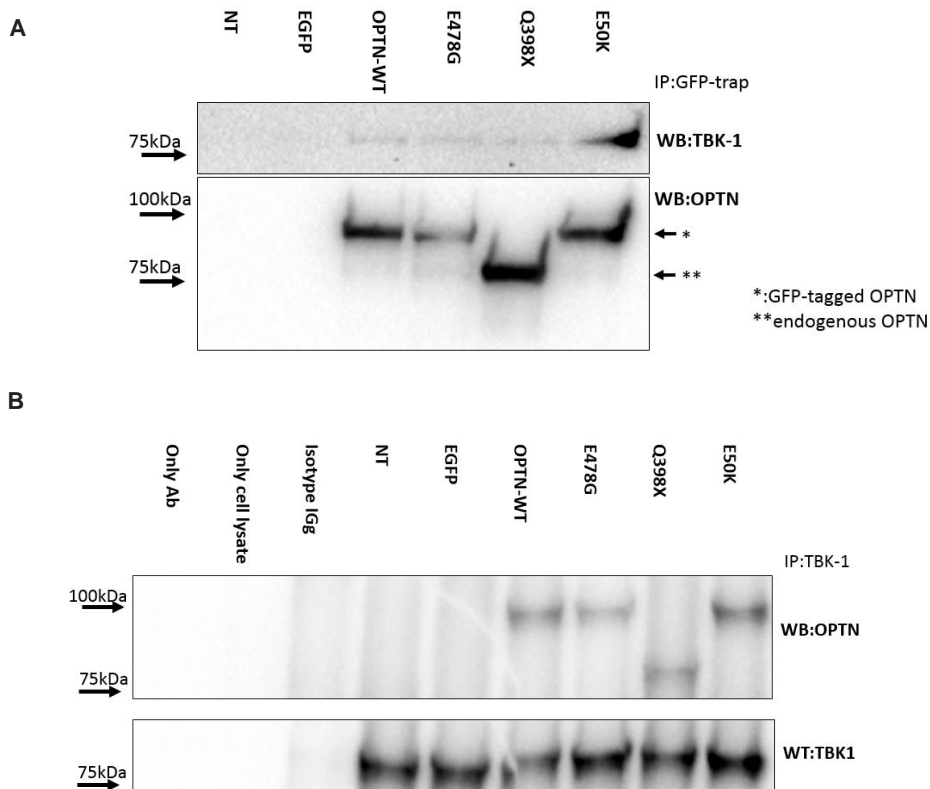


Figure 4.3: Wildtype and E50K control mutant optineurin and TBK-1 are recruited to autophagosomes, unlike ALS mutant optineurin. A) Representative confocal microscopy images of NSC-34 cells co-expressing WT/ALS and glaucoma mutant optineurin with LC-3-dsRed, followed by immunocytochemistry for endogenous TBK-1. Colocalization of optineurin and TBK-1 with LC-3 positive vesicles, indicating autophagosomes, in NSC-34 cells is indicated by the white arrows. B) Quantification of the colocalization between optineurin and TBK-1, and between optineurin, TBK-1 and LC-3. N=3 Mean \pm SEM is represented on the graph. P<0.05:*, P<0.005:**. (Unpaired student-t test Scale bar: 5 μ m NT; non-transfected, WT; wildtype, OPTN; optineurin.

As TBK-1 did not colocalize with optineurin in ALS-mutant cells, compared to wildtype and E50K expressing cells, we next questioned whether this was due to a loss of association between optineurin and TBK-1 in ALS-mutants compared to wildtype. Hence, immunoprecipitation experiments were performed to investigate this possibility. Cell lysates containing 500 μ g of total protein were prepared from optineurin-EGFP expressing NSC-34 cells, and immunoprecipitations were performed using GFP-Trap. Immunoblotting using anti-optineurin antibodies revealed that optineurin was

immunoprecipitated in all optineurin overexpressing conditions, but not in NT or EGFP transfected control conditions as expected, confirming the specificity of the GFP-Trap precipitation (*Figure 4.4 A, bottom panel*). Immunoblotting using anti-TBK-1 antibodies revealed that TBK-1 was immunoprecipitated similarly in each case: TBK-1 was pulled down in wildtype and mutant ALS optineurin-EGFP cells (*Figure 4.4 A, top panel*), slightly more was precipitated in glaucoma mutant cells. To confirm this result, reverse immunoprecipitations were performed using anti-TBK-1 antibodies, followed by immunoblotting using anti-optineurin antibodies. Immunoblotting for TBK-1 demonstrated that endogenous mouse TBK-1 was immunoprecipitated using human TBK-1 antibodies (conjugated to protein A coated Dynabeads) in all cell populations examined, as expected (*Figure 4.4 B, bottom panel*). Moreover, similar levels of optineurin were precipitated from cell lysates from wildtype, ALS or glaucoma-mutant cells (*Figure 4.4 B, top panel*), demonstrating that the association between optineurin and TBK-1 was similar in all conditions. Hence these data imply that the ALS-mutant optineurin and TBK-1 associate equally well as with wildtype optineurin.



These results were not surprising because the E478G and Q398X mutations are present in the C-terminus of optineurin, whereas the TBK-1 binding site is located at its N-terminus. Therefore, together these data suggest that recruitment of TBK-1 to autophagosomes is inhibited in cells expressing ALS-mutant optineurin. However, although immunoprecipitations are only indicative of a physical association between two proteins, these findings imply that this lack of recruitment of TBK-1 to autophagosomes is not due to disruption of TBK-1 and optineurin in the mutants compared to wildtype.

4.2. TBK-1 and its role in autophagy

Several binding partners of TBK-1, including NDP52, optineurin and p62, are autophagy receptors, implying that TBK-1 functions in autophagy, but no previous study has examined the ALS-associated TBK-1 mutants in terms of autophagy in ALS. TBK-1 normally regulates autophagy receptors through phosphorylation, moreover its substrate optineurin is implicated in ER-stress¹³³. Autophagy and ER-stress are two well documented and closely related ALS cellular pathologies¹⁸³. Therefore, we next examined the TBK-1 mutants in relation to these mechanisms. To do this, it was first necessary to generate ALS/FTD mutations in TBK-1 and overexpress these mutants in mammalian cells.

Figure 4.4: Co-immunoprecipitations between optineurin and TBK-1 in cells expressing optineurin-EGFP proteins, demonstrates a similar association between wildtype and ALS-mutant optineurin to TBK-1. A) EGFP-conjugated optineurin was immunoprecipitated using GFP-trap, and immunoblotting using TBK-1 and optineurin antibodies was performed. TBK-1 was co-immunoprecipitated with both wildtype, ALS and glaucoma mutant optineurin; wildtype and ALS mutants to a similar extent. B) Reverse immunoprecipitations using an anti-TBK-1 antibody conjugated to magnetic beads, demonstrated that TBK-1 co-precipitates with each of the mutant optineurin proteins to a similar extent. NT; non-transfected, WT; wildtype, OPTN; optineurin.

4.3. Site-directed mutagenesis of TBK-1

4.3.1 Design of TBK-1 mutations

The following mutations identified in ALS and FTD patients were chosen for this study; R308Q, R357Q, and E696K (*Figure 4.5, Table 4.1, Table 1.3*). R308Q was identified in sALS, R357Q in fALS, while E696K is found in fALS, sALS, and FTD. The two former mutations, R308Q and R357Q, have impaired kinase activity, based on decreased phosphorylation of its substrate IRF3, detected previously¹⁶⁷. Hence, the R308Q and R357Q mutants are predicted to display decreased phosphorylation of TBK-1 substrates, and hence may perturb autophagy. In contrast, E696K mutant has normal kinase activity, but the location of this mutation in the substrate binding domain should result in an inability to bind optineurin, and hence prevent the recruitment of TBK-1 into autophagosomes, although it retains binding capacity for IRF3¹⁶⁷. This mutant was chosen to examine the relationship between TBK-1's kinase activity and optineurin binding in autophagy and ER-stress. In addition to the ALS/FTD mutations, three other non-ALS/FTD mutations were examined as controls; D50A, G159A, and E643X, to examine the specificity of the ALS/FTD mutants on cellular events. D50A and G159A are mutations associated with childhood herpes simplex virus-1 encephalitis (HSE)¹⁸⁴. G159A-TBK-1 displays a complete loss of kinase activity, while the D50A mutant results in lower expression of TBK-1, as detected by lower mRNA and protein levels in HSE patient-derived fibroblasts¹⁸⁴. Finally, E643X-TBK-, is a truncation mutant in which a stop codon is inserted near the C-terminus of TBK-1, resulting in deletion of the entire C-terminus of the protein, from residue 643 onwards. The deleted region is responsible for binding several TBK-1 substrates, and this mutation is not disease-related, but was designed to examine the effect of loss of several substrates, not just optineurin. *Table 4.1* lists the nucleotide substitutions designed to create the specific TBK-1 mutations.

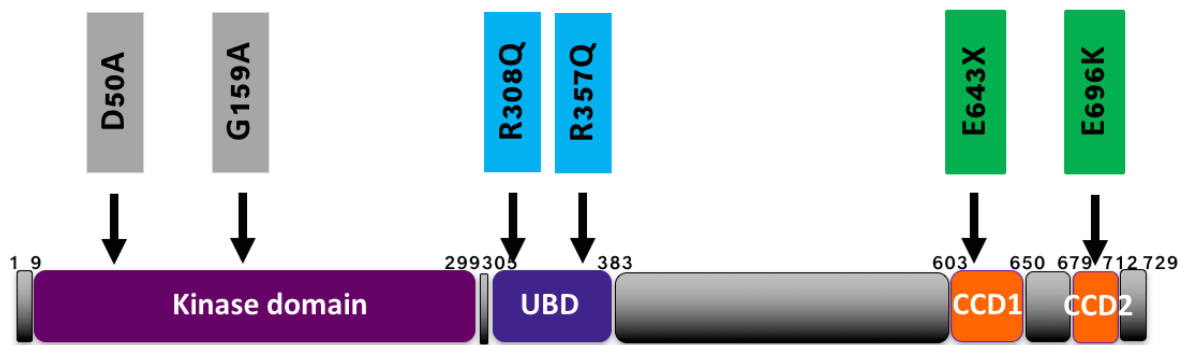


Figure 4.5: Location of the mutations in the TBK-1 protein selected in this study. The D50A and G159A mutations are localized within the kinase domain of TBK-1. In contrast, the R308Q and R357Q mutations are present within the ubiquitin binding domain (UBD), while the E643X and E696K mutations are located within the coiled-coiled domains (CCD) of TBK-1. The R308Q, R357Q, and E696K mutations are present in ALS/FTD patients whereas the D50A, G159A and E643X mutations were used as controls.

Table 4.1: The TBK-1 mutations used in this study, illustrating both the altered nucleotide and amino acid sequences.

Mutation	Codon change	Amino acid change
R308Q	cga>caa	Arginine→Glutamine
R357Q	cga>caa	Arginine→Glutamine
E696K	gag>aag	Glutamic acid→Lysine
E643X	gaa>taa	Glutamic acid→Stop
D50A	gat>gct	Aspartic acid→Alanine
G159A	ggt>gct	Glycine→Alanine

4.3.2 Generation of TBK-1 mutations

Three pc.DNA3.1 –TBK-1 overexpressing constructs (tagged with FLAG, DYKDDDDK) encoding human WT TBK-1 cDNA, or mutants D50A and G159A, were a kind gift of Professor Jean-Laurent Casanova, Rockefeller University, New York¹⁸⁴. In order to produce the mutations R308Q, R357Q, E696K and E643X, single nucleotide substitutions were introduced into the pc.DNA3.1-FLAG WT TBK-1 construct using site-directed

mutagenesis. PCR Primers for site-directed mutagenesis were designed using the software 'NEBaseChanger' (<http://nebasechanger.neb.com/>), as shown in *Table 3.4*.

Mutations were introduced into the pc.DNA3.1-FLAG/WT/TBK-1 construct using a Q5 site-directed mutagenesis kit (New England Biolabs), the resulting products were transformed into alpha select chemically competent cells (Bioline) and miniprep DNA was prepared. Following mutagenesis, the presence/absence of the mutations was examined by Sanger DNA sequencing, at AGRF (Australian Genome Research Facility, Melbourne). Two forward and three reverse primers were designed to sequence the entire TBK-1 region (*Table 3.8*). The resulting sequences were aligned to the WT TBK-1 sequence, using the software 'Ape' (<http://biologylabs.utah.edu/jorgensen/wayned/ape/>). As shown in the chromatographs present in *Figure 4.6*, mutagenesis was successful in each case. Plasmid clones were only used for further experiments if no other additional nucleotide changes were detected in the entire TBK-1 sequence, except for the chosen mutations.

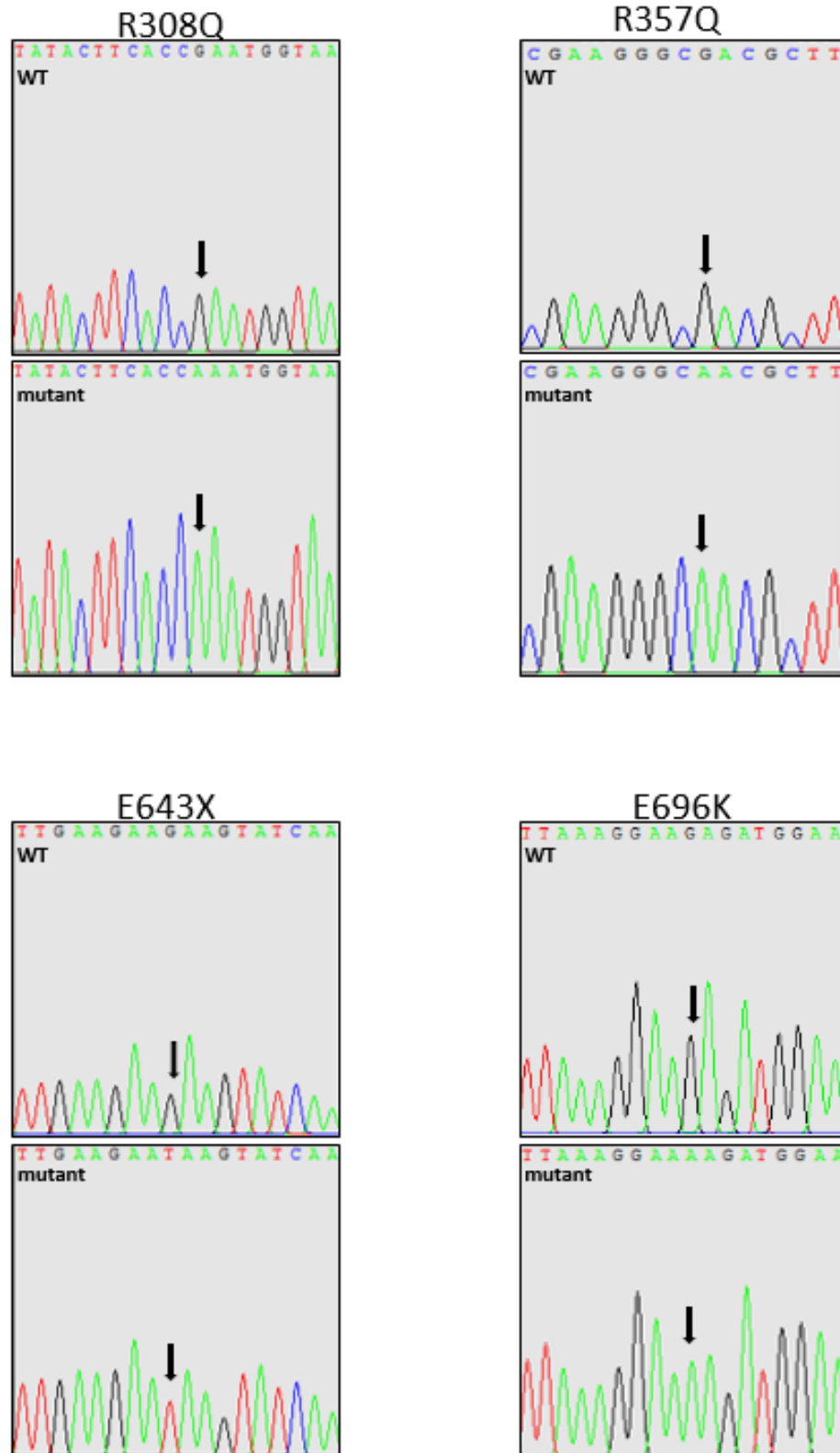


Figure 4.6: Sequencing of the newly generated R308Q, R357Q, E643X, and E696K mutant constructs. Mutagenesis was successful in each case, as indicated by the presence of the altered nucleotides at the appropriate position in the TBK-1 sequence, as indicated by the black arrows.

4.4. TBK-1 overexpression in mammalian cell lines

4.4.1. TBK-1 detection using the FLAG-tag

Having successfully generated each of the four TBK-1 mutants by site-directed mutagenesis, the first aim was to confirm that the newly generated constructs express protein. Firstly, MN-like NSC-34 cells were used, as above. The cells available at the start of this study were of passage number >15, and these cells were used here. However, as discussed later, it is preferable to use a low passage number, as in later studies.

We first examined expression of TBK-1 in NSC-34 cells by immunoblotting using anti-TBK-1 antibodies, although the expected size of endogenous mouse TBK-1 is similar size to overexpressed TBK-1. NSC-34 cells were transfected with TBK-1 constructs for 48 h and immunoblotting of cell lysates using anti-TBK-1 antibodies was performed. These analyses revealed the presence of a band in all cell lysates as expected, however in cells transfected with TBK-1 constructs, this was noticeably stronger than in control non-transfected cells or cells expressing pcDNA3.1 only, suggesting that transfection was successful. We next examined expression of TBK-1 further by immunoblotting using anti-anti-FLAG antibodies, because TBK-1 is conjugated to the FLAG tag in these constructs. This method was preferred rather than detecting expression using anti-TBK-1 antibodies, because it should allow us to detect only the overexpressed TBK-1 proteins, separate from endogenous mouse TBK-1. Hence, NSC-34 cells were transfected with TBK-1 constructs for 48 h and immunoblotting of cell lysates using mouse anti-FLAG antibodies (Sigma) was performed. The expected size of TBK-1-FLAG was 85 kDa, and whilst there was a band present of this size in transfected cells, it was also present in non-transfected cells, indicating that it was non-specific and hence not TBK-1-FLAG. Similarly, several other non-specific bands were present in both transfected and non-transfected lysates (>300kDa, ~180kDa), indicating that they were also non-specific (*Figure 4.7 A, second panel*). Despite several optimization steps, no

better results could be obtained using the mouse anti-FLAG antibody: in each experiment, many non-specific bands that were also present in the non-transfected cells were obtained. An alternative anti-FLAG antibody was also tried, rabbit anti-FLAG antibody (Sigma). However, similar results were obtained; several non-specific bands were obtained in non-transfected cells, none of which were of the expected size (85 kDa) for TBK-1-FLAG (*Figure 4.7 A, third panel*). We next performed immunocytochemistry using the anti-FLAG rabbit antibodies to ascertain if a more specific signal could be obtained. However, again high levels of non-specific staining were obtained in the non-transfected cells (data not shown). Hence we could not confirm expression of the FLAG-tag TBK-1 in the transfected cells.

We next examined whether the FLAG tag was actually present in the expressed TBK-1 protein, which would explain these results. However, the sequencing results obtained (section 4.3.2) demonstrated that the FLAG-tag, DYKDDDDK, was correctly conjugated to TBK-1 at its N-terminus, as expected (*Figure 4.7 B*). This result therefore demonstrated that the FLAG tag was indeed present in the TBK-1 constructs, implying that the available anti-FLAG antibodies were not specific enough to detect the FLAG epitope in the expressed TBK-1 proteins previously. Hence, as we were not able to detect exogenous TBK-1 by the presence of the FLAG-tag, we used another method, as detailed in section 4.4.3. Hence, in the remaining part of this study, only anti-TBK-1 antibodies were used to detect the over-expressed TBK-1 proteins.

4.4.2. TBK-1 overexpression in neuronal low passage NSC34 and SH-SY5Y cells

For the next experiments, a low passage (P4) of NSC-34 cells was used, because our laboratory has previously observed that the MN phenotype of these cells are lost during long periods in culture. Hence, NSC-34 cells of low passage should bear more similarities to MNs compared to those of higher passages. It was first necessary to develop an alternative approach to specifically confirm that transfection was successful, given that the FLAG epitope could not be used. For the initial optimisation experiments, NSC-34 cells were transfected with WT-TBK-1 and R308Q-TBK-1 constructs only using Lipofectamine for 48 h. Cell lysates then were prepared and subjected to immunoblotting using anti-TBK-1 antibodies. However, no differences in the levels of TBK-1 protein were present in the low passage number, non-transfected control cells or WT-TBK-1 or R308Q-TBK-1 cells (*Figure 4.8 A*). These data suggest that TBK-1 WT and mutant R308Q cannot be easily transfected in p4 NSC-34 cells, unlike other ALS proteins used by our laboratory^{161,133}. Interestingly, however, again if cells of a high passage number were transfected (P>15), increased levels of TBK-1 in WT-TBK-1 transfectants were observed by immunoblotting, compared to control cells (non-transfected or transfected with empty vector) (*Figure 4.8 B*). Hence the high passage number NSC-34 cells could be successfully transfected, unlike the low passage number cells.

These results therefore suggest that expression of TBK-1 using Lipofectamine transfection for p4 NSC-34 cells was inefficient. Hence, to improve expression levels, an alternative method; calcium phosphate transfection; was trialled instead¹⁸⁵. Lipofectamine and calcium phosphate transfection methods work in different ways. Lipofectamine is a cationic liposome that binds to negatively charged plasmids, and can overcome the electrostatic repulsion of the cell membrane¹⁸⁶. In contrast, during calcium phosphate transfection, calcium phosphate-DNA precipitates form, which are introduced to the cell through endocytosis. As some cell types are more readily transfected using one of these techniques rather than the other¹⁸⁷, we next examined whether using the calcium phosphate transfection method could give higher efficiencies

than Lipofectamine in NSC-34 cells. As a control, wildtype optineurin-EGFP was expressed using calcium phosphate, because this construct previously expressed efficiently using Lipofectamine (section 4.1 above)¹⁶¹.

Transfection of NSC-34 cells with TBK-1 and optineurin vectors was performed in parallel using identical conditions, to directly compare expression of each protein. Immunoblotting using anti-human optineurin antibodies demonstrated successful overexpression of EGFP-tagged optineurin using either Lipofectamine or calcium phosphate transfection methods (*Figure 4.8 C*). Optineurin-EGFP was easily detected compared to endogenous optineurin, because the EGFP tag adds an additional 26kDa to the size of the protein (92kDa compared to 66kDa). Endogenous optineurin is not shown on the blot in *Figure 4.8C* for clarity. Similar levels of optineurin were expressed using either technique, indicating that optineurin was efficiently transfected using Lipofectamine or calcium phosphate methods. For unknown reasons, optineurin was detected at different molecular weight between the different transfection methods, but this was not examined further. However, in contrast, little TBK-1 was expressed using either Lipofectamine or calcium phosphate methods, which was barely visualised against the endogenous TBK-1 background (*Figure 4.8 D*). These data therefore suggested that low passage NSC-34 cells are resistant to overexpression of TBK-1 upon transfection. n

Hence, next we decided to try a different neuronal cell line, the widely used human SH-SY5Y neuroblastoma cells, with the premise that a human cell line is more responsive to transfection with human proteins than a mouse cell line. Using Lipofectamine, SH-SY5Y cells were transfected with TBK-1-FLAG tagged vectors (WT/R308Q) for 48 h (*Figure 4.8 E*), followed by immunoblotting with anti-TBK-1 antibodies. Unfortunately, the TBK-1 levels were not elevated in any of the SH-SY5Y cells transfected with FLAG-tagged TBK-1 constructs, above the level of endogenous TBK-1, again suggesting that the transfections were all unsuccessful (*Figure 4.8 E*). Hence these data reveal that TBK-1, at least using the constructs available in this study, could not be

efficiently expressed in two neuronal cell lines examined; low passage mouse NSC-34 and human SH-SY5Y cell lines.

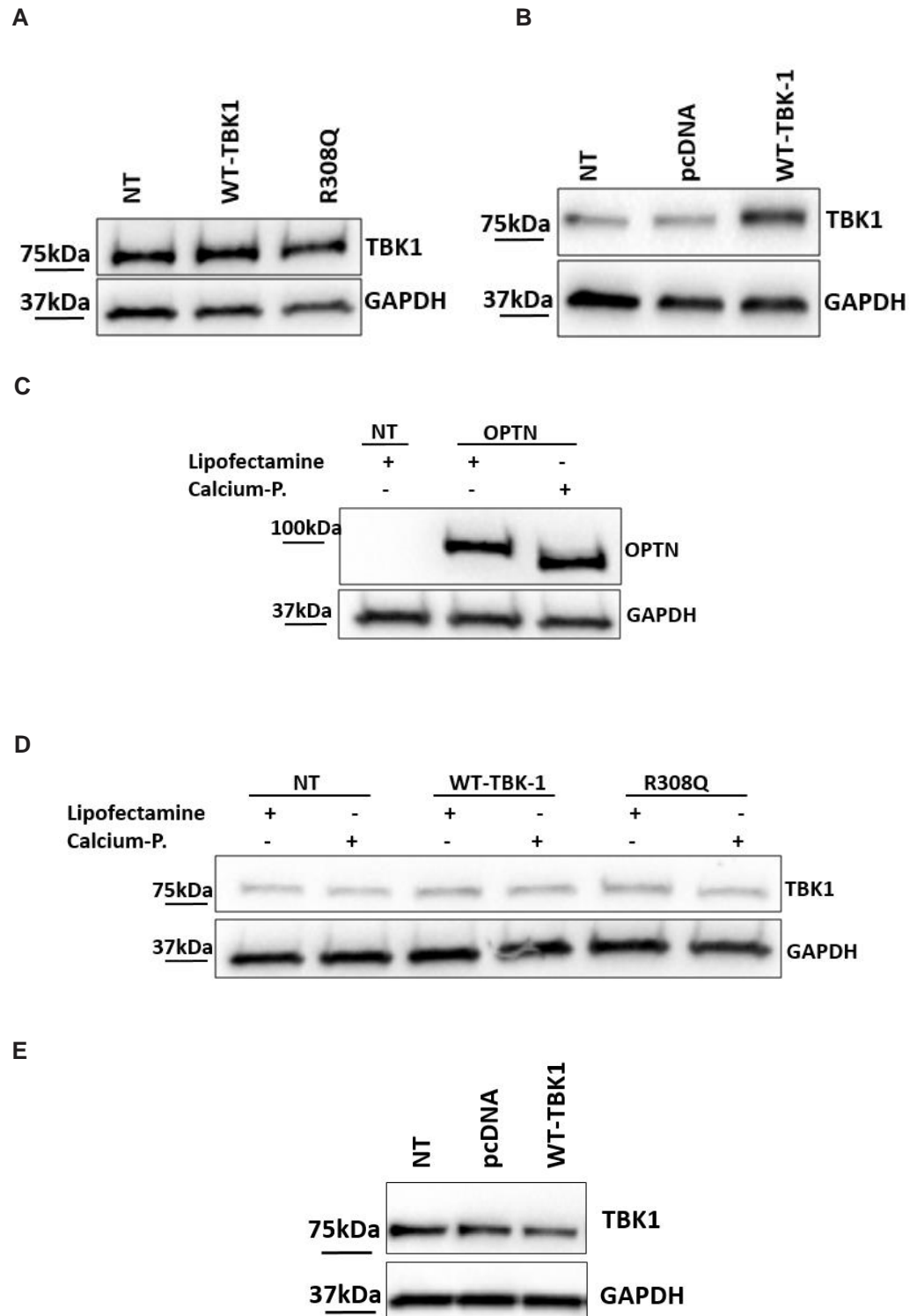


Figure 4.8: Expression of TBK-1 in NSC-34 and SH-S5Y5 cell lines using Lipofectamine and calcium phosphate transfection methods. A) TBK-1 expression in transfected, low-passage NSC-34 cells (P=4), 48 h post-transfection. B) TBK-1 expression in transfected high passage NSC-34 cells (P>15), 48 h post-transfection. Slightly more TBK-1 is detected in cells transfected with WT TBK-1 compared to the other populations. C) OPTN-EGFP expression in Lipofectamine and calcium phosphate transfected low passage NSC-34 cells (P=6), 48 h post-transfection. Efficient expression of OPTN is denoted by the presence of the 92kDa OPTN-EGFP band in the WT optineurin transfectants D) TBK-1 expression in Lipofectamine and calcium phosphate transfected low passage NSC-34 cells. P=6 E) TBK-1 expression in transfected SH-s5Y5 cells. NT; non-transfected, WT; wildtype, OPTN; optineurin. Blots were stripped and reprobed for GAPDH as a loading control.

4.4.3. TBK-1 overexpression in HEK293 cells

Whilst the use of a neuronal cell line is the preferred way to examine TBK-1 mutations in ALS/FTD, due to the strict time restrictions for this project and low expression levels obtained in the neuronal cells, we then decided to examine an alternative cell line known for to express exogenous proteins to high levels; HEK293 cells; so we could perform initial investigations into the effect of TBK-1 mutations. HEK293 is a widely used human kidney embryonic cell line, which has been immortalized by transduction with sheared adenovirus 5 DNA¹⁸⁸. HEK293 cells bear little neuron-like characteristics, although these cells express neurofilament subunits, which are typically found in neurons¹⁸⁹. Although HEK293 cells are not an ideal cell line to examine pathogenic mechanisms in ALS, they nevertheless allowed us to investigate the mutations. However, the effect of the TBK-1 mutants should be subsequently examined in neuronal cells, ideally in primary neurons.

To examine how efficiently HEK293 cells express exogenous TBK-1, cells were transfected with empty vector, WT, and R308Q-TBK-1 constructs using Lipofectamine. Cell lysates were prepared at 48 h post-transfection, followed by immunoblotting using human anti-TBK-1 antibodies as above. Clear overexpression of TBK-1 in HEK293 cells was obtained relative to cells transfected with empty vector pcDNA3.1 (*Figure 4.9 A*). In comparison to the overexpressed TBK-1, HEK293 cells express endogenous human TBK-1 at much lower level, as shown in the empty vector, pcDNA3.1, lane (*Figure 4.9 A*). To

confirm that both endogenous and exogenous TBK-1 were expressed in these cells, the experimental conditions were then optimised for visualisation of both proteins on the same gel. Despite the FLAG tag not being detectable by immunoblotting (*Figure 4.7 A*), the eight additional amino acids within the FLAG sequence, DYKDDDDK, should result in overexpressed TBK-1 proteins possessing approximately 1 kDa higher MW compared to endogenous TBK-1 (83,642Da MW for endogenous TBK-1 vs. 84,637Da MW for FLAG-tagged TBK-1). Whilst this is only a very small difference in size, using suitable conditions for electrophoresis, it is possible that this could be resolved. Hence, we then modified the immunoblotting conditions, in order to separate over-expressed TBK-1 from endogenous protein. Optimisation experiments demonstrated that the following conditions allowed visualisation of two separate bands (endogenous and overexpressed TBK-1) in the TBK-1 transfectants: running on a 6% SDS-PAGE (rather than a gradient gel), using Invitrogen apparatus rather than Biorad, which enables longer gels to be run, and the gels were electrophoresed for approximately 4-5h at 100V. *Figure 4.9 B* shows cell lysates from cells transfected with empty vector, WT-TBK-1, and R308Q constructs, subjected to TBK-1 immunoblotting using these conditions. The presence of two bands can be seen in the FLAG-TBK-1 transfectants, with a small shift in MW compared to endogenous TBK-1 (*Figure 4.9 B*). Due to low levels of endogenous TBK-1, observed in empty vector transfectants, the strong exogenous FLAG-TBK-1 signal slightly covers the endogenous TBK-1 in WT-TBK-1 and R308Q cells, but the presence of two bands with slightly higher MW than endogenous TBK-1 is clearly visible, suggesting that the FLAG-tag is present in these cells. Further evidence and a more precise separation of endogenous and exogenous TBK-1 is presented in section 4.4 (*Figure 4.11*) of this thesis. These data therefore suggest that the increase in band intensity in TBK-1 transfectants is due to exogenous, over-expressed TBK-1. These data therefore suggest that TBK-1-FLAG has been successfully transfected in HEK293 cells. The reason for the presence of two TBK-1 bands was unclear. However, it is known that TBK-1 goes through several post-translational modifications, including SUMO-ylation¹⁹⁰ and ubiquitination¹⁹¹. Hence, the upper TBK-1 band appearing *Figure 4.9 B* may represent different post-translationally modified versions of TBK-1.

It is not clear why the FLAG epitope could not be detected in either the immunoblotting or immunocytochemistry, as the same antibodies and methods have been used in our laboratory to detect other FLAG-tagged proteins. However, it is possible that the specific conformation adopted by the FLAG tag in overexpressed TBK-1, means it is inaccessible to the anti-FLAG antibodies available in this study.

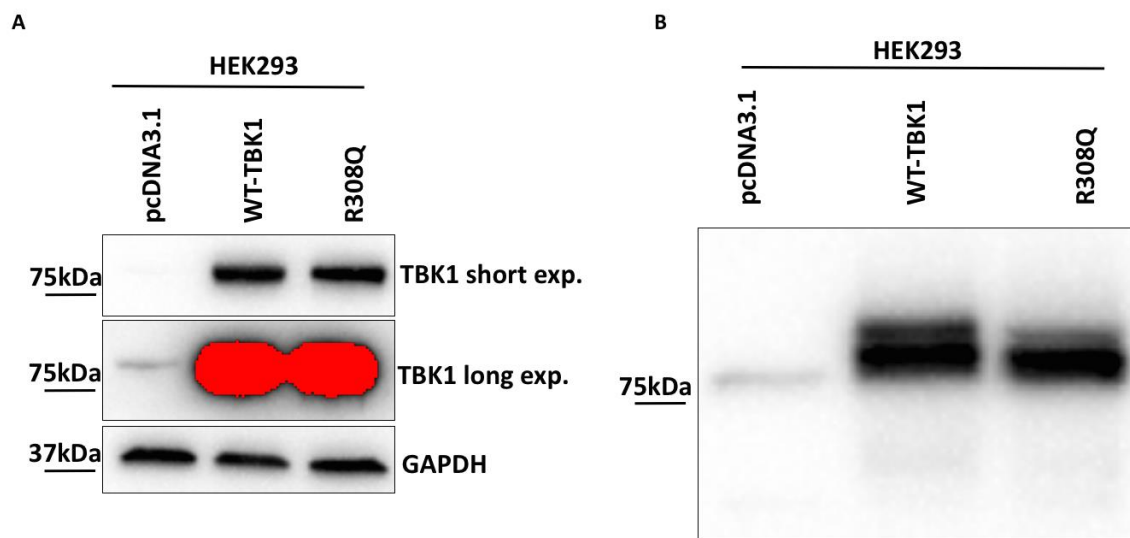


Figure 4.9: TBK-1 overexpression in HEK293 cells, and separation of exogenous and endogenous TBK-1 on 6% SDS-PAGE gels. A) Increased TBK-1 expression levels are detected in transfected HEK293 cells compared to vector (pcDNA3.1) only transfected cells, separated on a gradient gel (4-15%). Blot was stripped and reprobed with GAPDH as a loading control. B) TBK-1 positive bands, of slightly higher MW than endogenous TBK-1, are present only in TBK-1 transfectants when cell lysates are run on a 6% SDS-PAGE gel, suggesting that the FLAG-TBK-1 has been separated from endogenous protein under these conditions. WT; wildtype.

4.4. Characterisation of expression of WT and mutant TBK-1 in HEK293 cells by immunoblotting and immunofluorescence

After establishing the conditions for detection of TBK-1-FLAG proteins, we next needed to confirm that the remaining TBK-1 constructs also express in HEK293 cells, using the optimised conditions. The panel of WT, ALS mutant and control mutant TBK-1

overexpressing vectors were therefore transfected into HEK293 cells using Lipofectamine, and cell lysates were prepared at 48 h post-transfection. Immunoblotting using anti-human-TBK-1 antibodies demonstrated overexpression of all TBK-1 proteins compared to non-transfected cells and empty vector transfectants: a band of slightly higher MW than endogenous TBK-1 was present in all lanes, except E643X, which being a truncation mutant, was expressed at a slightly lower MW, as expected (predicted size 68kDa) (*Figure 4.10 A*). Image J was used to quantify the band intensities using densitometry for each protein, from at least three independent experiments (*Figure 4.10 B/C*). For this quantification, protein samples were separated on gradient SDS-PAGE gels, hence the endogenous and exogenous TBK-1 were quantified together.

WT-TBK-1 and all mutants showed increased expression of TBK-1 compared to non-transfected and empty vector transfected cells, implying that each transfection was successful (*Figure 4.10 A, B*). Interestingly, R357Q, E643X and D50A mutants were expressed to significantly lower levels than WT-TBK-1 ($p > 0.05$). WT-TBK-1 showed an average 15-fold increase in expression level compared to endogenous TBK-1 represented in NT and empty vector conditions, while the expression of R357Q and E643X mutants was increased on average only 5 and 3.8-fold compared to both controls, respectively. D50A expression increased on average 9.5-fold (*Figure 4.10 B*). D50A has been previously described as a 'loss of expression' mutation in patients derived fibroblast, and quantification of expression in HEK293 cells revealed that expression was indeed significantly less wildtype TBK-1 FLAG expressing cells ($p > 0.05$, *Figure 4.10 B*), consistent with previous findings¹⁸⁴. Similarly, based on the quantification results, the findings obtained here suggest that the ALS mutant R357Q and E643X could possibly also be characterized as a loss of expression mutants.

Next, the phosphorylation status of each expressed TBK-1 protein was examined, which is in tight association with its kinase activity, TBK-1 needs to be phosphorylated, on a serine residue at position 172, in order to be enzymatically active¹⁷⁶. Taking into account this tight association, the phosphorylation status of the mutants should

therefore reflect their kinase activity. At 48 h post-transfection, immunoblotting was performed using a phospho-specific anti-TBK-1 antibody (Abcam) that detects only phosphorylation of TBK-1 at residue 172. These experiments demonstrated that there was no phosphorylated TBK-1 (p-TBK-1) in non-transfected and empty vector conditions or at least, at levels below the limit of detection of immunoblotting (*Figure 4.10 A*). Phosphorylation of TBK-1 requires an initial step, either a higher concentration of protein or of other kinases¹⁷¹. The lack of p-TBK-1 in these controls is therefore not due to impaired kinase activity, it is probably due to TBK-1 not being activated in basal conditions. Similarly, as expected, WT-TBK-1 and E696K mutant TBK-1 were phosphorylated to a much greater degree, represented by a strong positive p-TBK-1 signal on the blot, while kinase deficient mutants, R308Q and R357Q, were phosphorylated significantly less compared to WT-TBK-1 ($p < 0.05$) as expected (*Figure 4.10 C*). Surprisingly, the E643X mutant was phosphorylated less than WT-TBK-1, despite this mutation being present in the substrate-binding domain, and hence it should not affect the phosphorylation status of TBK-1. However, this difference did not reach statistical significance ($p = 0.1$). D50A showed less phosphorylation of TBK-1 compared to WT-TBK-1, but did not reach statistical significance. G159A, appeared not to be phosphorylated at all, similar to previous observations¹⁸⁴.

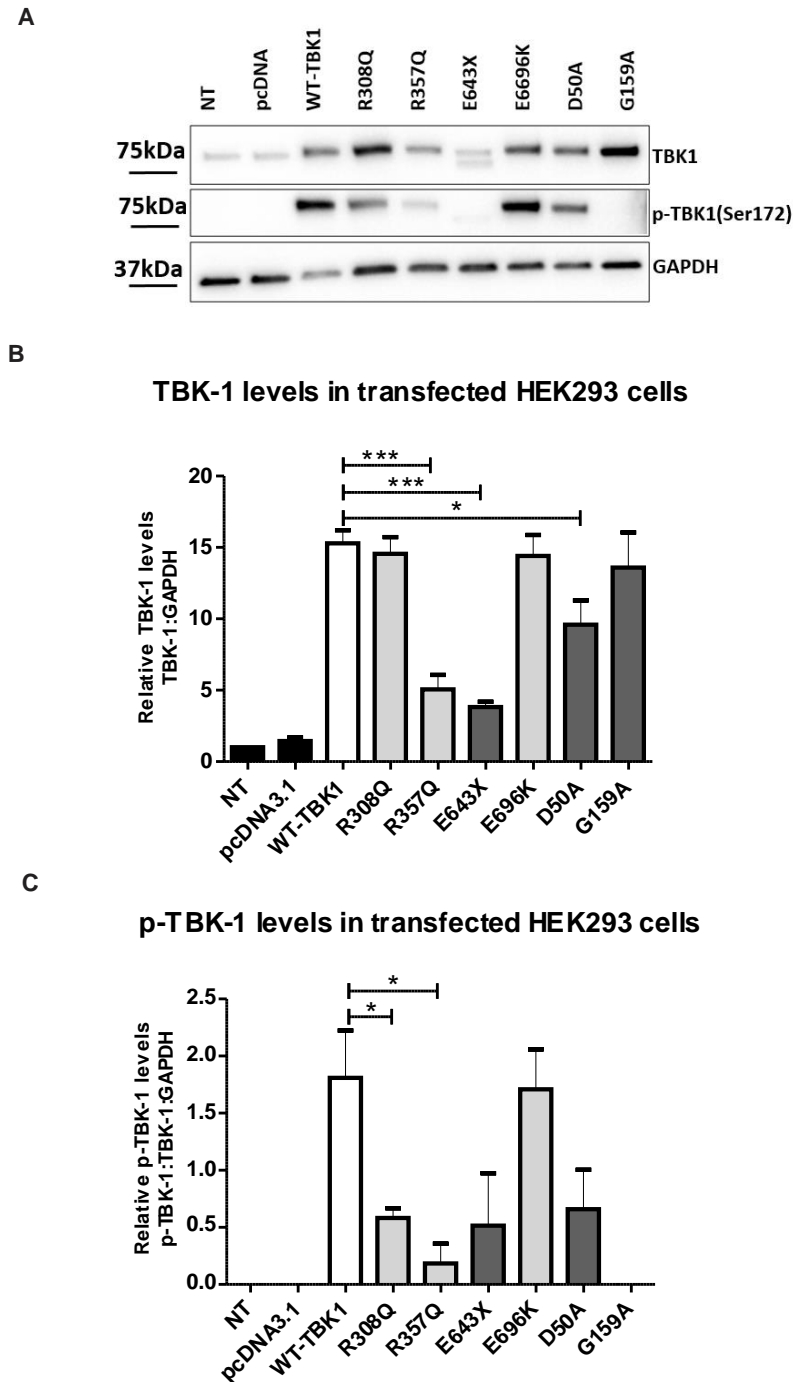


Figure 4.10: Total and p-TBK-1(Ser172) detection in WT and mutant TBK-1 overexpressing HEK293 cells. A) Total TBK-1 and p-TBK-1 detection by immunoblotting in TBK-1 transfected HEK293 cells. Blot was stripped and reprobed for GAPDH as a loading control. B) Quantitative comparison of total endogenous, WT and mutant TBK-1 levels in HEK293 cells using ImageJ. N=4. C) Quantitative comparison of endogenous, WT and mutant p-TBK-1 levels in HEK293 cells using ImageJ. N=3, Mean +/- SEM is presented on the graphs. ***P>0.0005, *P>0.05 (Unpaired Student-t-test). NT; non-transfected, WT; wildtype.

The optimised conditions described in section 4.4.3 were then used to separate endogenous/overexpressed TBK-1 proteins, using 6% (w/v) PAGE gels. Several bands were present in mutant TBK-1 overexpressed cell lysates, similar to those observed previously (Figure 4.5). Further optimization was performed; the concentration of primary antibody was decreased from 1/500 to 1/1000, to increase the discrimination between the additional TBK-1 positive bands. In NT and empty vector (pcDNA3.1) conditions, only one TBK-1 positive band was present, representing endogenous TBK-1, as expected. This 84kDa band was present in all lanes, and is marked with *** on Figure 4.7 in lane WT-TBK-1 and E643X. All overexpressed TBK-1 proteins, except for G159A, were expressed as two additional bands, marked with * and ** on Figure 4.7, with approximate sizes of 85-86kDa. Hence both of these bands should be considered to be overexpressed exogenous TBK-1 as they are absent in NT and pcDNA conditions. The presence of two discrete bands for exogenous TBK-1 is also evident for the truncation mutant, E643X, where two bands are present at lower MW, approximately 64-65 kDa MW. In contrast, the G159A mutant was expressed as one band only. This mutant has a complete loss of kinase activity¹⁸⁴, hence it is possible that the modifications that generate the two bands in each of the other over-expression conditions require some degree of kinase activity. This notion is further supported by the fact that in non-transfected and empty vector transfected non-stressed HEK293 cells, no p-TBK-1 was present, moreover only one TBK-1 band was presented in those conditions.

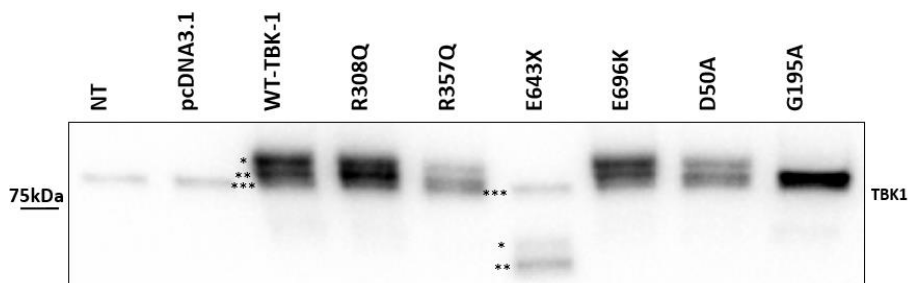


Figure 4.11: Separation of endogenous and overexpressed TBK-1-FLAG by a 6% SDS-PAGE gel. Endogenous TBK-1 is represented by one band, as seen in non-transfected and empty vector transfected conditions, shown by *** in the figure. Exogenous TBK-1 is expressed as two individual bands in all conditions, except for G159A, shown by ** and * in the figure. NT; non-transfected, WT; wildtype.

In order to characterize the overexpressed proteins further, we next analyzed the intracellular distribution of exogenous TBK-1 in HEK293 cells. Cells were fixed, permeabilized and immunocytochemistry using anti-TBK-1 antibodies was performed at 48 h post-transfection. Using confocal fluorescent microscopy, overexpression of TBK-1 proteins could be clearly observed by the stronger immunostaining obtained in transfected cells compared to non-transfected and vector only transfectants. However, the distribution of overexpressed TBK-1 was not as expected. Endogenous TBK-1 was expressed in a punctuate pattern in HEK293 cells, in both non-transfected and empty vector transfected cells (*Figure 4.12 A*), consistent with previous observations¹⁹², and in NSC-34 cells described above (in section 4.1). However, in contrast, overexpressed WT and mutant TBK-1 were expressed in a diffuse cytoplasmic pattern, rather than punctate distribution. This observation will be further discussed in section 4.7 (*Figure 4.12 B*).

A

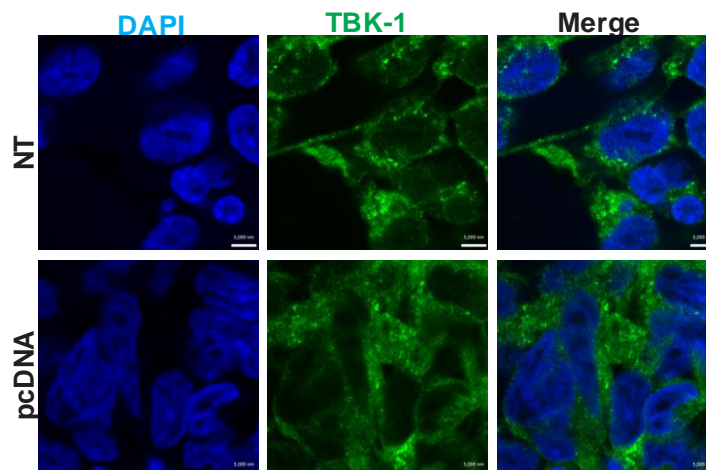
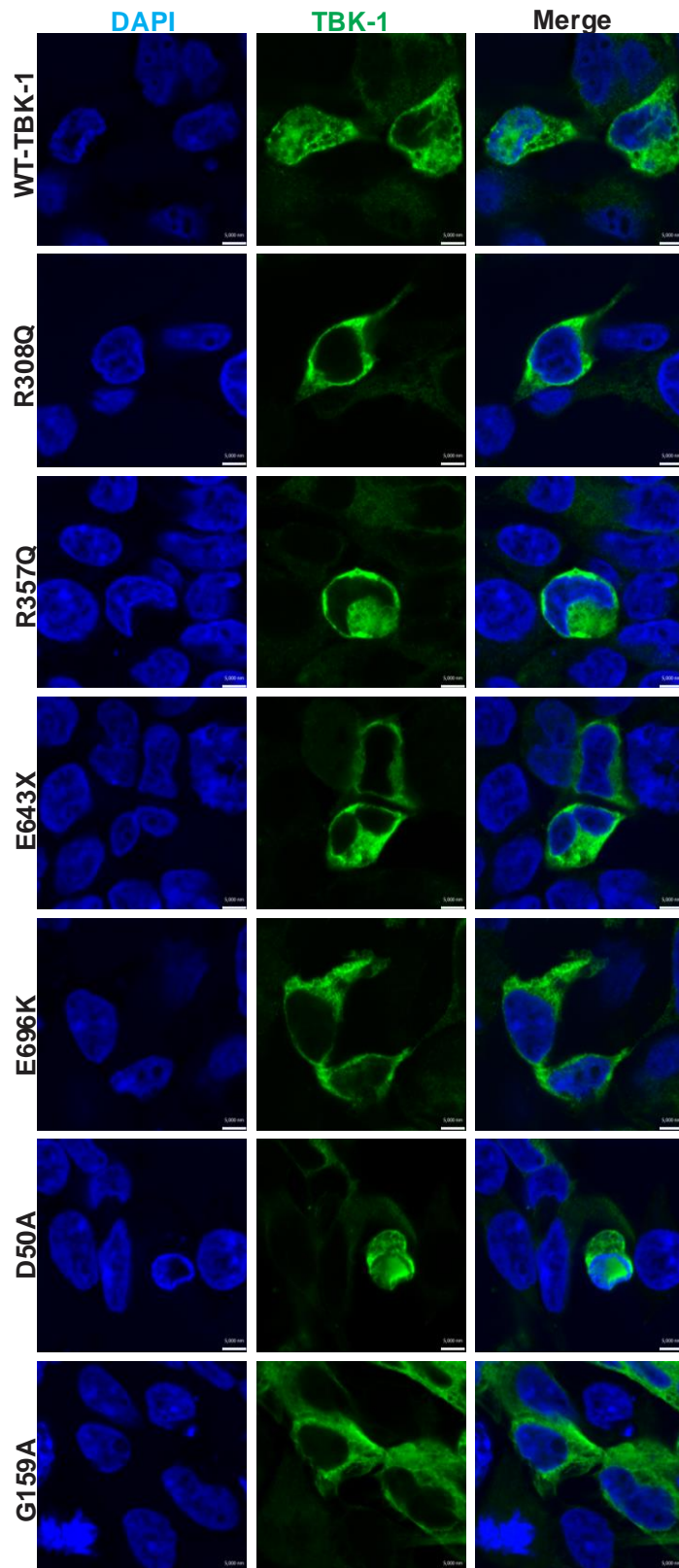


Figure 4.12: Detection of overexpressed TBK-1 via immunocytochemistry and confocal fluorescent microscopy in HEK293 cells. A) Endogenous TBK-1 is expressed in a punctuate pattern in NT and pcDNA3.1 conditions), consistent with previous observations. Every cell examined displayed TBK-1 staining. B) In contrast, overexpressed TBK-1 is expressed in a diffuse cytoplasmic, non-punctuate pattern, in both WT and mutant TBK-1 transfected cells. The microscope settings (gain function) were adjusted to only detect exogenous TBK-1, hence there is an apparent lack of signal in several cells. Scale bar: 5 μm.

B



4.6. Optimisation of conditions to induce autophagy in HEK293 cells

Next, autophagy was examined by investigating the levels of LC-3 in cells expressing TBK-1 proteins using immunoblotting. During autophagy induction, LC3 (LC3-I) is conjugated to phosphatidylethanolamine, to form a LC3-phosphatidylethanolamine conjugate (LC3-II), which is recruited to autophagosomal membranes. Hence, LC3-II is a specific marker of autophagosome formation and the levels of LC-3 can be quantified using immunoblotting. However, following the standardized 2016 autophagy guidelines¹⁸², the levels of both LC3-I and LC3-II levels should be assessed to most accurately detect autophagy, and cells should be treated with Bafilomycin when quantitating LC3, which inhibits autophagosome-lysosome fusion, leading to an accumulation of autophagosomes¹⁸².

In order to establish the baseline levels of autophagy for these experiments, it was first examined how HEK293 cells respond to starvation, and starvation plus bafilomycin treatment, as possible methods to induce autophagy. HEK293 cells were starved for 20 h in serum-free media, or serum-starved for 16 h and treated with 100 nM bafilomycin in serum-free media for 4 h. Following treatment, cell lysates were prepared and subjected to LC3 and TBK-1 immunoblotting. As we were only able to visualize TBK-1-FLAG using anti-TBK-1 antibodies, which recognizes endogenous and exogenous TBK-1 simultaneously, it was first necessary to determine how endogenous TBK-1 is affected by serum starvation and bafilomycin treatment, using non-transfected cells. Following these treatments, the levels of endogenous TBK-1 were quantified by densitometry, revealing that there were no significant differences in the levels of TBK-1 expression, using starvation only or starvation plus bafilomycin (*Figure 4.13 B*). These data indicate that starvation and bafilomycin treatment does not significantly affect endogenous TBK-1 expression, hence we did not consider endogenous TBK-1 in the following experiments.

The levels of total LC3 relative to GAPDH appeared to increase slightly upon starvation only, but this was not statistically significant ($p=0.56$). Moreover, the levels of total LC3 relative to GAPDH were not statistically different in serum-starved and bafilomycin treated conditions either ($p=0.32$) (*Figure 4.13 B/D*). However, these experiments have been performed only twice and hence need to be repeated again to confirm these conclusions. The blots were stripped and reprobed for GAPDH as a loading control, which indicated equal loading between conditions. Similarly, the levels of LC3-I, relative to GAPDH, also showed little change between the treatments, and did not reach statistical significance ($p=0.4$) (*Figure 4.13 B/E*). The levels of LC3-II relative to GAPDH increased three fold on average in starved compared to non-starved cells (*Figure 4.13 B/F*), indicating that autophagy may not be induced, or that intense autophagy flux consumes LC3-II¹⁸². Other studies using HEK293 cells have shown similar results¹⁹³. However, upon bafilomycin treatment together with serum starvation, LC3-II levels appeared to greatly increase compared to basal conditions (*Figure 4.13 B/F*). On average, a 35-fold increase was detectable, but due to large variation between biological replicates, this did not reach statistical significance, ($p=0.35$). However, the conditions used to induce autophagy may not be ideal for HEK293 cells, because previous studies have demonstrated that HeLa cells respond better to serum starvation than HEK293 cells¹⁹³. However the response of HEK293 cells to serum-starvation in this study were similar to previous observations¹⁹³. Unfortunately, due to time constraints it was not possible to perform further optimisation experiments for autophagy induction or to examine the effect of bafilomycin treatment itself.

Hence the conditions used in the upcoming sections were serum starvation for 20 h, and serum starvation for 16 h followed by 4 h 100 nM Bafilomicyn treatment in serum-free conditions.

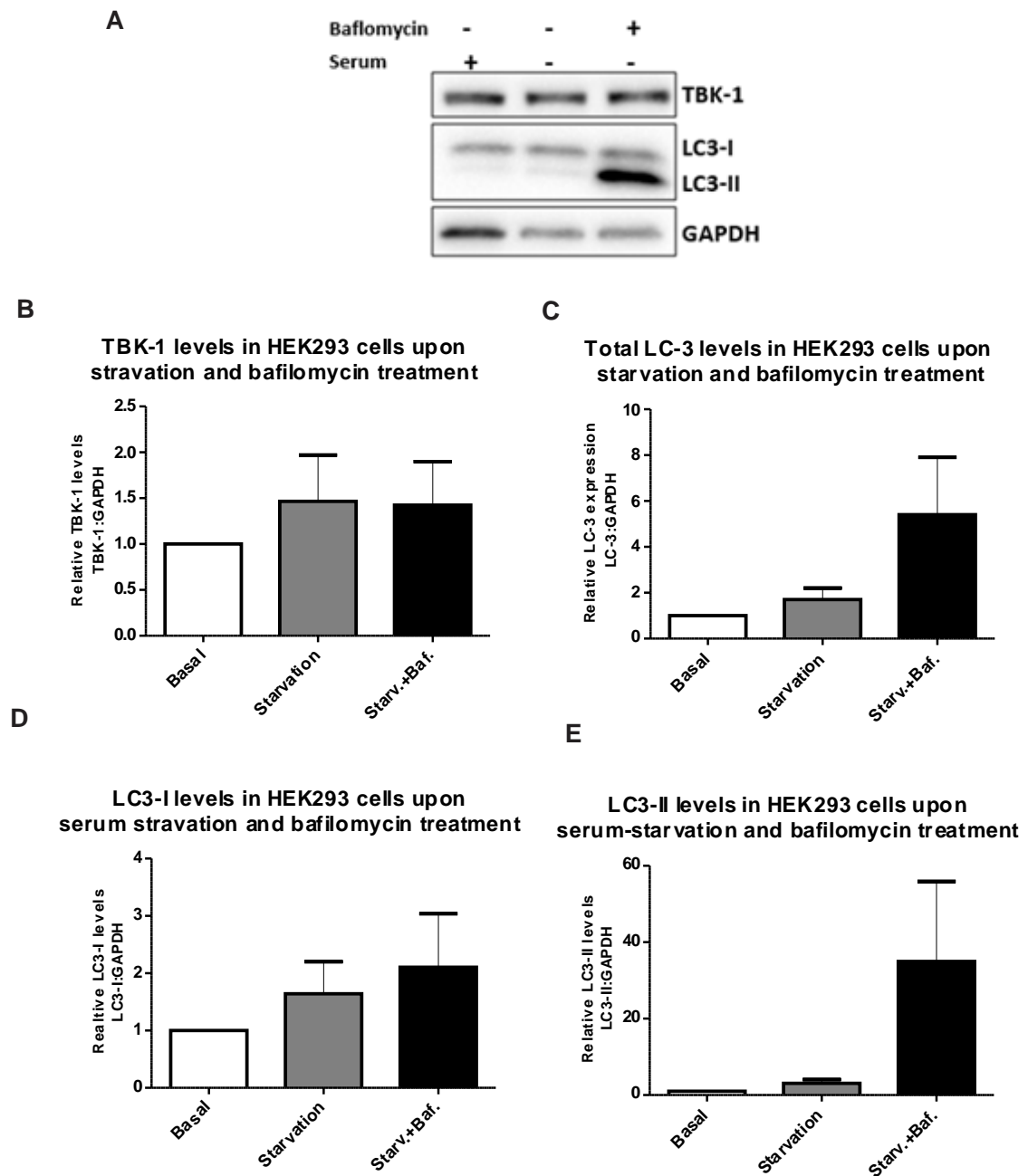


Figure 4.13: Autophagy induction in HEK293 cells A) TBK-1 and LC-3 immunoblotting analysis of starved and bafilomycin treated HEK293 cells. Blots were stripped and reprobbed for GAPDH as a loading control B, C, D, E) Quantification of immunoblotting in (A) for TBK-1 and LC3 in differently treated HEK293 cells, by densitometry. Autophagy induction is occurring, based on the increased LC3-II levels present in serum-starved and bafilomycin treated cells. The levels of TBK-1 and LC3 are represented relative to GAPDH, N=2. Mean +/- SEM is presented in the graphs.

4.7. ALS-associated TBK-1 mutants may dysregulate autophagy in HEK293 cells

To determine whether expression of ALS-associated mutant TBK-1 leads to dysregulation of autophagy of HEK293 cells, cells were transfected with WT, and mutant TBK-1 (ALS [R308Q, R357Q, E696K] and control [D50A, G159A, E643X]) constructs using Lipofectamine. The conditions determined above were used to induce autophagy: serum starvation for 20 h, or serum starved for 16 h then treated for 4 h with bafilomycin.

At 48 h post-transfection, cell lysates were prepared and immunoblotting using anti-LC3 and anti-TBK-1 antibodies was performed. Only those experiments in which TBK-1 was successfully overexpressed, and p-TBK-1 was detected according to the previously described pattern for each protein, indicating the expected impaired or intact kinase activity (*Section 4.5, Figure 4.10*), were examined further for autophagy. As expected, similar to above (*Figure 4.13 B, first lane*), little LC3-II was detected when cells were grown in serum-supplemented conditions (*Figure 4.14 A*). The levels of total LC-3 were quantified but no significant differences were detected in TBK-1 overexpressing cells compared to non-transfected or cells transfected with vector only (*Figure 4.14 B*), implying that TBK-1 does not interfere with basal autophagy in HEK293 cells. This result was unexpected because previous studies have shown that TBK-1 silencing in HeLa cells leads to decreased LC3-II levels¹⁹⁴, which implies a role for TBK-1 in basal autophagy, although these experiments were performed in a different cell line. Hence, further experiments are required to investigate whether TBK-1 functions in basal autophagy in HEK293 cells.

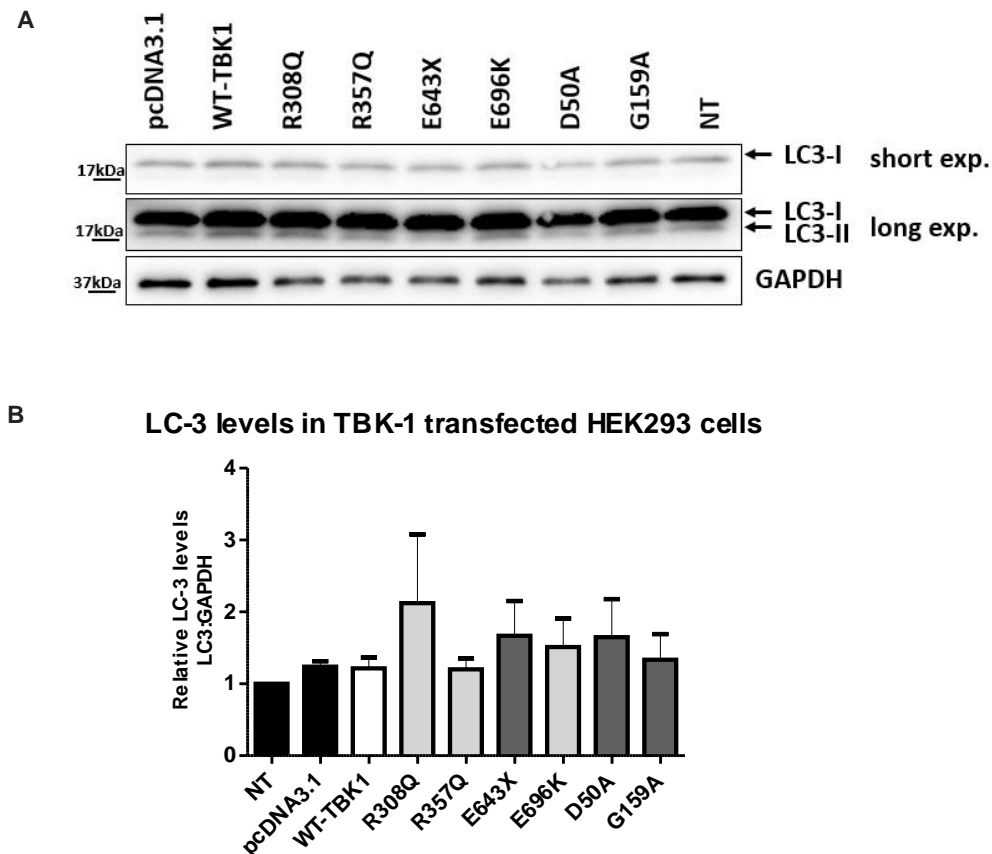


Figure 4.14: Immunoblotting analysis of TBK-1 transfected HEK293 cells A) LC-3 immunoblotting analysis of TBK-1 transfected HEK293 cells. Blots were stripped and reprobbed for GAPDH as a loading control. B) Quantification of LC-3 levels of the blots in (A). LC3 levels are represented relative to GAPDH, N=3, Mean \pm SEM is presented on the graphs. NT; non-transfected, WT; wildtype.

Whilst overexpression of TBK-1 did not interfere with basal autophagy, the levels of LC3-II, were next examined. Hence, TBK-1 transfected HEK293 cells were serum-starved for 20 h, and cell lysates were prepared and then subjected to immunoblotting using anti-LC3 antibodies (*Figure 4.15A*). The levels of total LC3 and LC3-II, relative to GAPDH, were quantified by densitometry. No significant differences in either form of LC3 were detected between the different conditions (*Figure 4.15B/C*). These data suggest that neither wildtype, control mutant nor ALS-mutant TBK-1 proteins affect the accumulation or degradation of LC3-II. However, an alternative explanation is that any differences in LC3-II levels could be masked by the high basal autophagy level of HEK293 cells, indicated by the low LC3-II levels in serum-starved conditions.

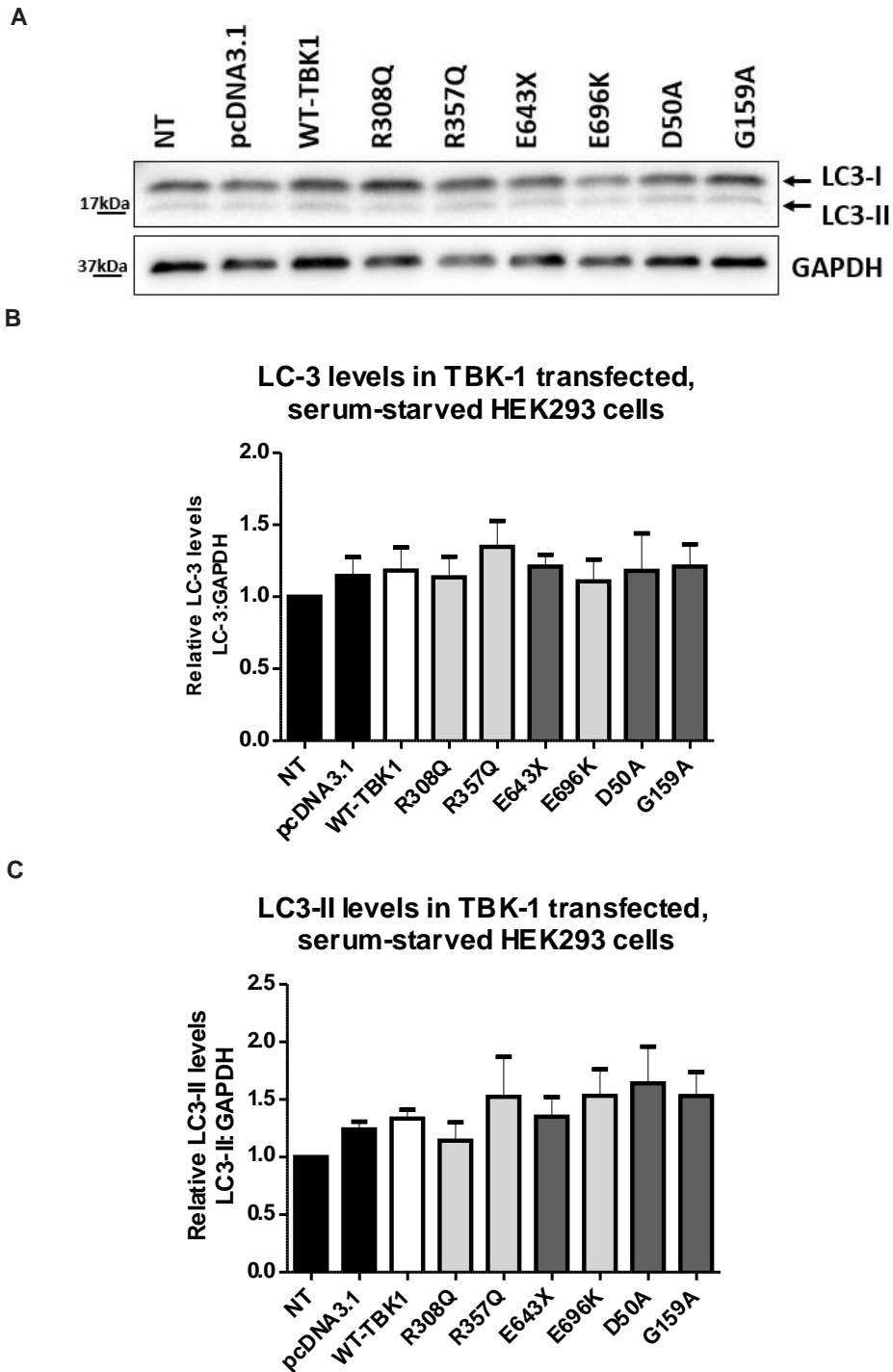
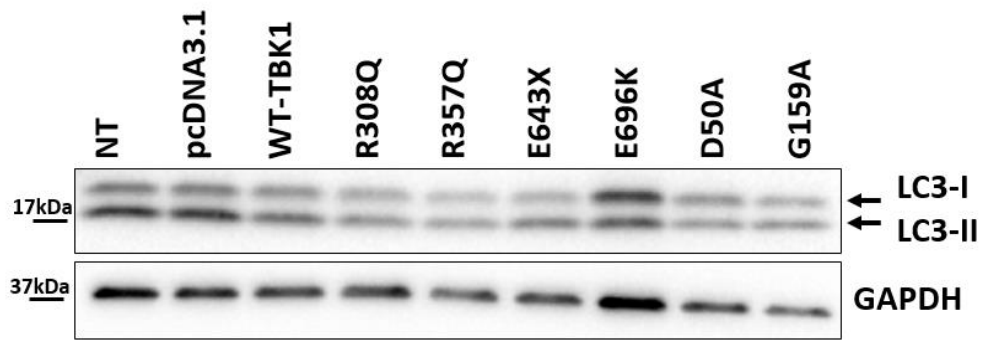


Figure 4.15: Immunoblotting analysis of TBK-1 transfected and serum starved HEK293 cells
 A) LC-3 immunoblotting using anti-LC3 antibodies of TBK-1 transfected and serum starved HEK293 cells. Blots were stripped and reprobed for GAPDH as a loading control.
 B) Quantification of LC-3 levels in the blots in (A). LC3 levels are represented relative to GAPDH
 C) Quantification of LC3-II levels. LC3-II is represented relative to GAPDH, N=3, Mean +/- SEM is presented on the graphs. NT; non-transfected, WT; wildtype

Next, because the only conditions that notably elevated LC3-II levels, so that we could reliably quantify autophagy induction, were serum starvation and bafilomycin treatment together, these conditions were applied to cells transfected with TBK-1 proteins. To assess the accumulation of autophagosomes due to treatment with bafilomycin, immunoblotting was performed using anti-LC3 antibodies on cellular lysates collected at 48 h post transfection. In serum starved, bafilomycin treated cells, the levels of LC3-II were increased compared to untreated conditions, allowing us to reliably quantify these levels as expected (*Figure 4.16A*). Quantification using densitometry revealed a trend towards decreased levels of total LC3 in cells expressing the ALS-mutants, R308Q, R357Q, E696K, compared to WT-TBK-1 overexpressing cells, although this did not reach statistical significance (p values of 0.1, 0.15, 0.19, respectively). Similarly, there was a trend for a slight decrease in total LC3 levels in cells expressing control mutant D50A, (*Figure 4.16B*), but this was also not statistically significant (p=0.43). Interestingly, overexpression of WT-TBK-1 had no effect on total LC3 levels, suggesting that this trend may be mutant-specific, although further experiments are required to investigate this possibility.

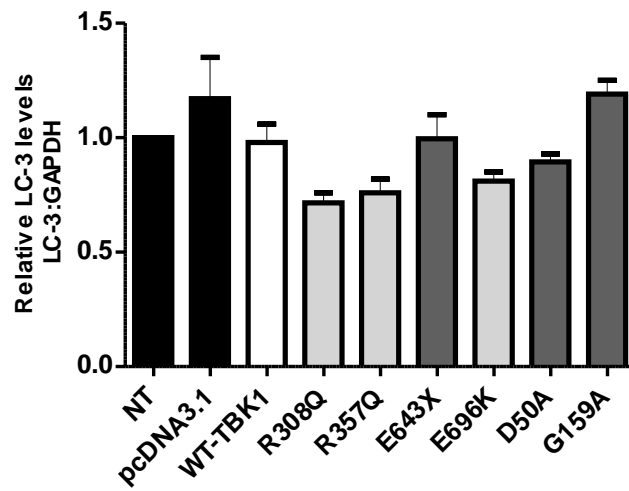
Next, to assess autophagosome formation, the levels of LC-I and LC3-II were quantified. These analyses revealed that LC3-I levels were similar in WT-TBK-1 overexpressing cells compared to non-transfected cells or cells expressing vector only. However, there was a trend towards lower levels of LC3-I in those cells expressing ALS mutants compared to WT-TBK-1 expressing cells (R308Q, R357Q, E696K, *Figure 4.16C*), although this did not reach statistical significance. When the levels of LC3-II were quantified, similar trends were observed: decreased levels of LC3-II in cells expressing ALS mutants R308Q, R357Q, E696K compared to WT-TBK-1 overexpressing cells. Moreover, this difference did reach statistical significance in all ALS-mutant TBK-1 overexpressing cells (R308Q, R357Q, E696K) (p<0.05). In contrast, none of the control mutant-TBK-1 overexpressing cells showed any significant differences in expression levels of LC3-II.

A



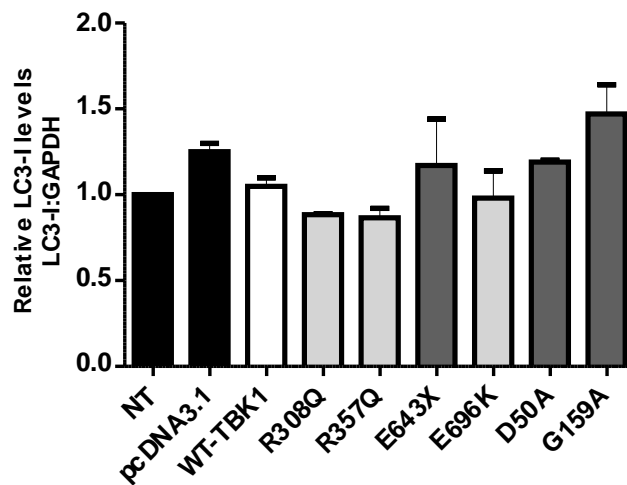
B

LC-3 levels in TBK-1 transfected, serum-starved, and bafilomycin treated HEK293 cells



C

LC3-I levels in TBK-1 transfected, serum-starved, and bafilomycin treated HEK293 cells



D
LC3-II levels in TBK-1 transfected, serum-starved, and bafilomycin treated HEK293 cells

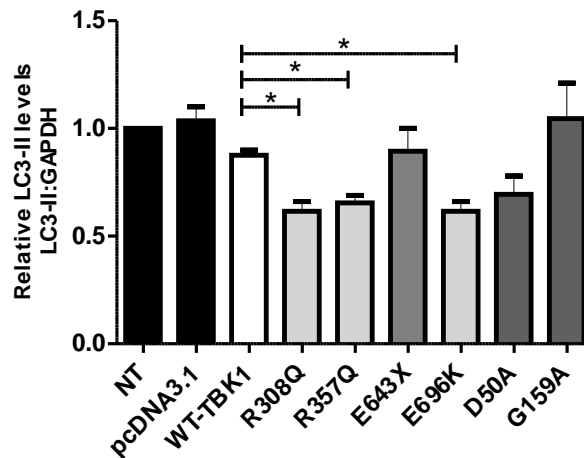


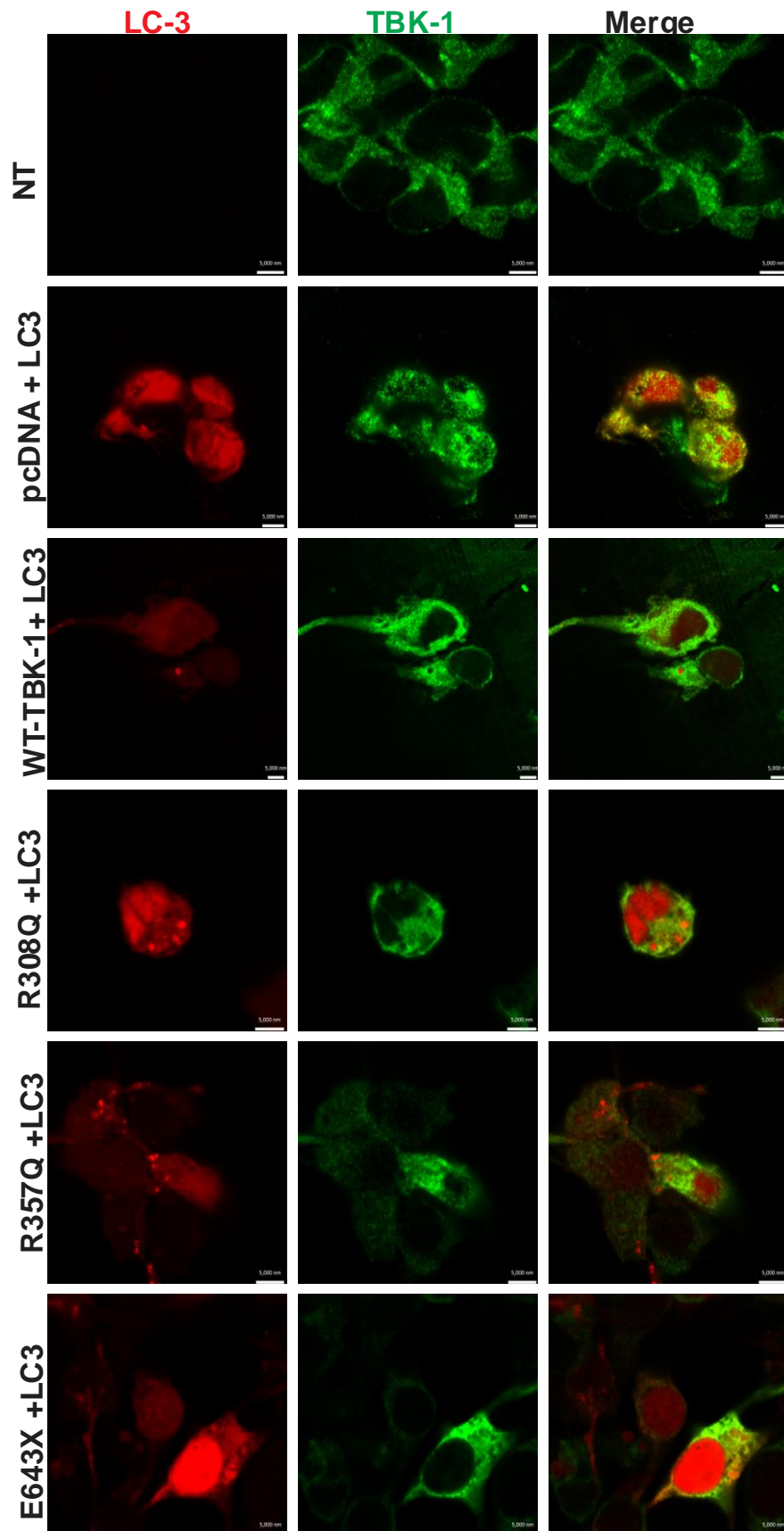
Figure 4.17: Immunoblotting analysis of TBK-1 transfected, serum starved and bafilomycin treated HEK293 cells A) LC-3 immunoblotting analysis of TBK-1 transfected, serum starved and bafilomycin treated HEK293 cells. Blots were stripped and reprobed for GAPDH as a loading control. B) Quantification of LC-3 levels of the blots in (A). LC3 levels are represented relative to GAPDH. C) Quantification of LC3-I levels of the blots in (A). LC3-I is represented relative to GAPDH. D) Quantification of LC3-II levels of the blots in (A). LC3-II is represented relative to GAPDH, N=2, Mean +/- SEM is presented in the graphs. *P>0.05(Unpaired Student-t-test)

Taken together, these initial experiments imply that ALS-associated mutations in TBK-1 may dysregulate autophagy. To investigate this notion further, preliminary experiments were performed using immunocytochemistry. During western blot experiments, the cellular lysates are derived from the whole cell population, containing both transfected (high/low levels) and non-transfected cells due to transient transfection conditions. Hence, it can be difficult to accurately detect cellular changes in transient cell transfections using immunoblotting or other techniques that sample the whole cell population.

Hence, to have a clearer understanding of how mutant TBK-1 influences autophagy, we next visualised autophagosome formation using immunofluorescence microscopy of cells co-transfected with a construct expressing LC3 tagged with dsRed. The use of fluorescently labelled LC3 constructs to detect autophagy is supported by the

Klionsky 2016 guidelines¹⁸², and it allows visualization of autophagosomes directly, which appear fluorescently labelled. Hence, cells were co-transfected with LC3-dsRed overexpressing vectors with either ALS-mutant TBK-1, control mutant TBK-1, WT TBK-1 overexpressing vectors, or empty vector. Similar to the immunoblotting experiments, cells were serum starved for 20 h then fixed, permeabilised and immunocytochemistry using anti-TBK-1 antibodies was performed. Due to time restrictions, it was not possible to also perform serum starvation and bafilomycin treatment together however.

Using fluorescent confocal microscopy, we found that the TBK-1 immunostaining in cells expressing WT TBK-1 or mutant TBK-1 did not colocalize with LC3-positive vesicles in HEK293 cells (*Figure 4.18*). Moreover, the areas staining positive for TBK-1 clearly did not stain positive for the LC3-positive structures, which indicate autophagosomes (indicated by the white arrows on *Figure 4.17*). This was an interesting observation, as in NSC-34 cells, LC-3 positive vesicles did colocalize with endogenous TBK-1 (section 4.1). Furthermore, previous studies have demonstrated that TBK-1 colocalizes with autophagosomes¹⁹⁵. As described previously in section 4.4, over-expressed TBK-1 displays a more diffuse staining in HEK293 cells than expected, unlike endogenous TBK-1, which forms the typical punctuate structures described in previous studies. Hence, these data suggest that as the expression pattern of exogenous TBK-1 is not typical in HEK293 cells, it is not surprising that TBK-1 does not colocalize with autophagosomes as expected. Moreover, this could also explain why we did not detect significant differences in LC3 levels by immunoblotting in TBK-1 transfected HEK293 cells that were exposed to serum-starvation only.



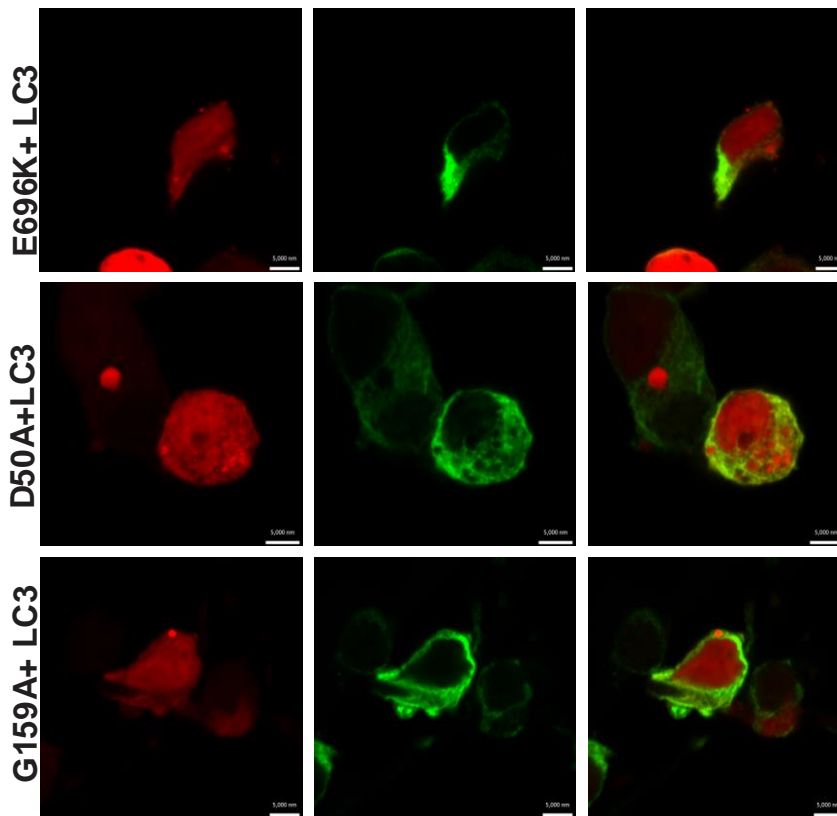


Figure 4.17: LC-3-positive structures and TBK-1 do not colocalize in transfected HEK293 cells. Representative images of HEK293 cells cotransfected with WT/ALS and control mutant TBK-1 and LC3-dsRed constructs and immunostained for TBK-1. TBK-1 does not colocalize with LC3-positive vesicles. White arrows indicate the absence of TBK-1 staining in the LC3-positive vesicles, indicative of autophagosomes. Scale bar: 5 μ m .

There was insufficient time to determine if mutant or WT TBK-1 inhibited the formation of autophagosomes, by quantification of the number of LC-3 positive vesicles per cell. However these data imply that the ALS-TBK-1 mutants dysregulate autophagy, and from the experiment described here, it would be possible to determine if the inhibition of autophagy is due to inhibition of autophagosome formation. In future studies, examining TBK-1 overexpressing cells in the presences of bafilomycin treatment and starvation, should reveal if/how ALS mutant TBK-1 perturbs autophagosome formation in more detail.

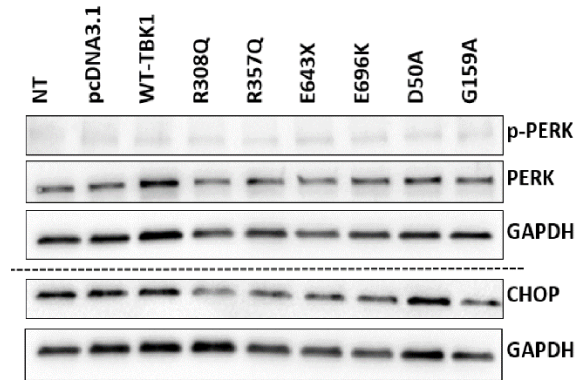
4.8. Kinase deficient mutant TBK-1 affects CHOP-expression

ER-stress and concomitant UPR represent a major pathological pathway leading to apoptosis in ALS¹⁹⁶, and ER stress is also linked physiologically to autophagy¹⁸³. ER-stress is also induced by IFN β production¹⁹⁷ during innate immunity, and as TBK-1 is a major regulator of IFN β production, it is therefore conceivable that mutations in TBK-1 may perturb the UPR. Hence, ER stress was next examined in cells expressing the TBK-1 mutants. Due to time constraints, it was not possible to examine the full UPR, hence we focused on one part of the UPR only, the PERK pathway, as this branch of the UPR is associated with Toll-like receptor signalling¹⁹⁸.

WT, ALS-mutants and control-TBK-1 mutants were overexpressed in HEK293 cells for 48 h, and cell lysates were prepared. Immunoblotting using antibodies against the activated, phosphorylated form of PERK, p-PERK, total PERK, and the UPR-associated pro-apoptotic transcription factor CHOP, was then performed. However, there were no significant differences in the levels of total PERK expressed between the different conditions (*Figure 4.18 A/B*). Moreover, the levels of p-PERK, which is a more specific marker for activation of the UPR than total PERK, was also unchanged between the different cell populations, however it was not quantified. This finding initially suggested that the PERK branch of the UPR is not activated by wildtype or mutant (ALS or control) TBK-1 overexpression. However, surprisingly, the levels of CHOP detected by immunoblotting were significantly decreased in kinase deficient R308Q, R357Q ALS-mutants and E643X control mutant TBK-1 overexpressing HEK293 cells ($p=0.008$, $p=0.001$, $p=0.0005$ respectively) (*Figure 4.18 C*). A trend towards decreased levels of CHOP was also detected in cells overexpressing the control mutant G159A, but this did not reach statistical significance ($p=0.08$). In the previous section, it was shown that the same mutants, R308Q, R357Q, E643X and G159A have lower levels of p-TBK-1, thus implying impaired kinase activity (*Figure 4.10*). Hence these results demonstrate that decreased CHOP expression was detected in cells expressing control or ALS mutants that have impaired kinase activity. Hence, these data suggest that the kinase activity of TBK-

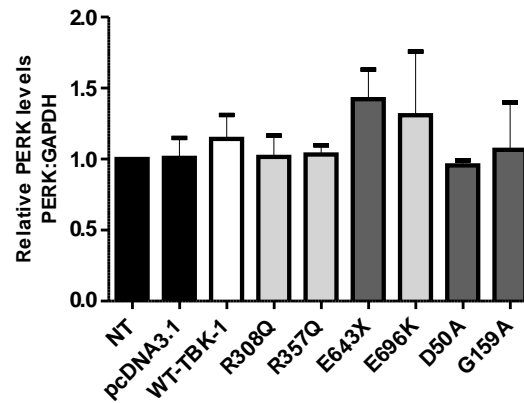
1 may regulate CHOP expression, and therefore possibly the UPR. However, due to time constraints, it was not possible to investigate this further.

A



B

PERK levels in TBK-1 transfected HEK293 cells



C

CHOP levels in TBK-1 transfected HEK293 cells

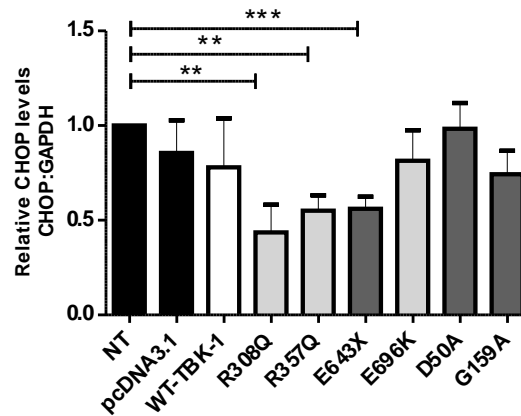


Figure 4.18: Decreased CHOP expression in the presence kinase-deficient TBK-1 mutants.
A) Immunoblotting analysis of p-PERK, PERK and CHOP expression. Blots were stripped and reprobbed for GAPDH as a loading control. B) Quantification of PERK and CHOP protein levels in the blots in (A) by Image J. The levels of PERK and CHOP were quantitated relative to GAPDH N=3, Mean+/- SEM is presented on the graphs. ***P>0.0005, **P.0.005(Unpaired Student-t-test)

5

DISCUSSION

The main findings described in this thesis are that a) recruitment of TBK-1 to autophagosomes is perturbed in cells expressing the optineurin ALS-mutants (E478G, Q398X) in NSC-34 cells; b) ALS-associated mutations in TBK-1 (R308Q, R357Q and E696K) may dysregulate autophagy, because significantly lower levels of LC3-II were detected in serum-starved and bafilomycin treated HEK293 cells; and c) the expression levels of CHOP were significantly decreased in cells expressing TBK-1 mutants with impaired kinase activity. These mutants included both ALS-associated R308Q, R357Q and also control mutant E643X, implying that the kinase activity of TBK-1 is associated with CHOP expression, and that this is unrelated to ALS because it was not specific to the ALS mutants.

5.1 Recruitment of TBK-1 to autophagosomes is inhibited in cells expressing ALS-associated mutant optineurin

Previously, TBK-1 was shown to phosphorylate autophagy receptors optineurin and p62^{163,199}, and TBK-1-mediated phosphorylation of optineurin induced autophagy mediated clearance of Salmonella in HeLa cells¹⁶³. The studies outlined in this thesis also imply that optineurin recruits TBK-1 to autophagosomes in neuronal cells, although additional experiments are required. Optineurin is a substrate of TBK-1, moreover optineurin mutations are also present in ALS and FTD¹⁶⁰. Our laboratory previously demonstrated that ALS-associated E478G, Q398X optineurin mutants inhibit the maturation of autophagosomes¹⁶¹, but these mutants' interaction with TBK-1 has not previously been examined. In this study, it was found that wildtype optineurin formed vesicles that co-localised with TBK-1 in NSC-34 cells. Moreover, colocalisation with LC-3 implied that these vesicles were autophagosomes (*Figure 4.2/4.3*), as expected. In contrast, TBK-1 was recruited to autophagosomes in significantly fewer ALS-mutant cells compared to wildtype optineurin cells. The lack of recruitment of TBK-1 to autophagosomes was not due to disruption in TBK-1 and optineurin interaction, since mutant optineurin and wildtype TBK-1 co-precipitated equally well as wildtype optineurin and wildtype

TBK-1. Hence the reason for the observed inhibition of recruitment of TBK-1 to autophagosomes remains unclear. Nevertheless, these are the first observations that recruitment of TBK-1 to autophagosomes is disrupted if ALS-mutant optineurin is present.

An important role for optineurin and TBK-1 in autophagy has been previously described. The binding between optineurin and TBK-1 is crucial for TBK-1 activation in macrophages²⁰⁰ and HEK293 cells²⁰¹. Furthermore, during *Salmonella* infection, phosphorylation of optineurin, mediated by TBK-1, is crucial for optineurin binding to LC3 and for engulfment of bacteria by autophagosomes¹⁶³. Based on these previous observations, it is possible that the autophagy dysfunction our laboratory previously detected in ALS-mutant optineurin overexpressing cells¹⁶¹ may be related to inhibition of recruitment of TBK-1 to autophagosomes. However, further experiments are necessary to investigate this possibility in the future.

5.2 TBK-1 is an ALS gene

To date, 44 mutations in TBK-1 have been described in ALS and FTD (*Table 1.3*)^{160,167,174,175,202,203}. Out of these, 7 (16%) were identified only in FTD patients, 28 (63%) were detected only in ALS, and the remaining 9 (21%) were present in patients that manifest symptoms of both ALS/FTD. Hence, mutant TBK-1 could be an important factor in the pathology associated with these disorders.

The approach followed in this study was to generate mutant TBK-1 overexpressing constructs, transfect them into mammalian cells, and then examine autophagy and ER-stress. We selected the mutations in TBK-1 based on two criteria: impairment of TBK-1 kinase activity (R308Q, R357Q), and retention of kinase activity but removal of substrate-binding activity, including optineurin. Given that optineurin mutations are present in ALS and FTD¹⁶⁰, we selected the mutant E696K that should abrogate TBK-1 binding to optineurin.

Using WT TBK-1 FLAG/pcDNA3.1 as a template, the ALS mutants (R308Q, R357Q) and ALS/FTD mutant (E696K) were successfully generated using site directed mutagenesis (*Figure 4.6*). Hence these mutants allow investigation of whether the kinase activity or optineurin binding activity, or both, were important in ALS pathogenesis. We also included three control TBK-1 mutants that were not linked to ALS/FTD to examine the specific of the effects of the ALS/FTD mutations. The control mutants D50A and G159A are associated with herpes simplex virus-1 encephalitis, and we obtained previously described constructs expressing these mutants¹⁸⁴. The final control mutant, E643X, is a novel mutant not associated with disease. This mutant was also successfully generated by site-directed mutagenesis in this study using WT TBK-1 FLAG -pcDNA3.1 as a template.

The aim of this part of the study was to investigate how the TBK-1 mutants are related to ALS and hence NSC-34 MN-like cells were initially used. Surprisingly, however, it was difficult to overexpress the TBK-1 constructs transiently in NSC-34 cells (*Figure 4.8*) that were of a low passage number and hence more likely to retain MN characteristics. Moreover, we were also unsuccessful in overexpressing TBK-1 in a human neuroblastoma cell line, SH-SY5Y (*Figure 4.8*). The reasons for this are unclear but there are several possibilities. Firstly, TBK-1 expression could be blocked at the transcriptional or translational level. Although it is unknown why this may occur, it could be related to the specific functional activity of TBK-1. Alternatively, it may be that transfection was inhibited, although we successfully overexpressed optineurin proteins in NSC-34 cells (*Figure 4.1/Figure 4.8*), implying that the transfection procedure itself was efficient in these cells. Another possibility is that the newly synthesised TBK-1 is directed to ubiquitin proteasomal system and becomes degraded soon after synthesis. These possibilities should be investigated in the future to determine why TBK-1 was not successfully expressed in the neuronal cells. Furthermore, future studies should examine alternative methods to express TBK-1 in neuronal cells, including the production of stable cell lines, or the generation of alternative TBK-1 constructs with a different backbone.

As we did not have time to produce stable cell lines during this study, it was decided to use HEK293 cells to investigate the effect of TBK-1 mutants on ER stress and autophagy. HEK293 cells were efficiently transfected with the TBK-1 constructs and all of the mutants were successfully expressed (*Figure 4.10*). Surprisingly, the R357Q and E643X mutants were expressed at significantly lower levels compared to wildtype TBK-1 protein. Although we did not examine the mRNA levels of TBK-1 in our system, immunoblotting experiments suggest that they may be loss-of-expression mutations. It is unclear if this was due to expression of lower levels of protein or transcription of RNA or alternatively, due to these mutants being degraded significantly faster than wildtype TBK-1 and the other mutants.

Overexpression of TBK-1 in HEK293 cell lysates was initially probed using anti-FLAG antibodies. Unfortunately, none of the available anti-FLAG antibodies (rabbit or mouse) could specifically detect overexpressed TBK-1 (*Figure 4.7*). Sequencing of the WT-TBK-1-FLAG construct revealed that the FLAG tag was indeed connected to *TBK-1* at its N-terminus (*Figure 4.7*). The reason for the lack of the detection using the anti-FLAG antibodies is therefore unclear but may be because of the conformation of TBK-1, whereby the FLAG epitope is buried within the core of the protein and hence not accessible to the antibodies. Another possibility is that the FLAG tag was removed during post-translational modification, but we can rule out this scenario because the immunoblotting studies demonstrated that there was a small shift in size between endogenous and exogenous TBK-1, thus implying that the FLAG-tag was present (*Figure 4.9 and Figure 4.11*). Alternatively, the available anti-FLAG antibodies may not be specific enough to detect the epitope, because many non-specific bands were detected in immunoblotting (*Figure 4.7*). Furthermore, the FLAG tag is repeated only once in TBK-1, unlike other expressed recombinant proteins that contain several copies of the FLAG-tag.

Methods were optimised to separate the endogenous and exogenous TBK-1. Although they differ only in 1kDa in size, it was possible to distinguish between the two proteins. In addition, two different MW species of overexpressed TBK-1 were presented in HEK293 cell lysates (*Figure 4.11*), approximately 85kDa and 86kDa.

The identity of these two forms of TBK-1 is unclear. However, TBK-1 undergoes several post-translational modifications, including ubiquitination¹⁹¹ and SUMOylation¹⁹⁰. The two forms of TBK1 may therefore represent distinct ubiquitinated or SUMO-ylated TBK-1 species.

In order for TBK-1 to be enzymatically active it has to be phosphorylated at Ser 172. A previous study¹⁶⁷ characterized several ALS-TBK-1 mutants in relation to their kinase activity, as assessed by phosphorylation of IRF3, a well-characterized TBK-1 substrate. We also assessed the phosphorylation status of our TBK-1 mutants in order to predict their kinase activity. Using an antibody specific for phosphorylated TBK-1, lysates from cells expressing the two kinase deficient mutants (R308Q, and R357Q) contained significantly less p-TBK-1 compared to cells expressing wild-type TBK-1, as expected. Interestingly the control mutant E643X was also phosphorylated less compared to wildtype TBK-1 (*Figure 4.10*), despite retaining the kinase domain. However, Ser-172, which regulates the kinase activity, resides within the classical kinase activation loop of TBK-1¹⁷¹. During trans-autophosphorylation of Ser-172, TBK-1 undergoes conformational changes¹⁷¹ leading to its activation. It is conceivable that due to truncation of TBK-1 at its C-terminus, the E643X-mutant may not be able to undergo the proper conformational changes that are required for its kinase activity. Based on the results obtained in this study, we can hypothesise that the R308Q, and R357Q, TBK-1 mutants display decreased kinase activity. However, examination of additional TBK-1 substrates would be necessary to provide further evidence for this notion. It would also be necessary to perform a kinase assay on the overexpressed mutants, and also the downstream targets of the TBK-1 mutants should be identified.

To characterize the mutant proteins further, we evaluated their intracellular distribution in HEK293 cells. Endogenous TBK-1 demonstrated punctuate staining in both HEK293 and NSC34 cells (*Figure 12A, Figure 4.1*), similar to previous studies¹⁹². Interestingly overexpressed TBK-1 showed more diffuse cytoplasmic staining, in both wild-type and mutant-TBK-1 overexpressing cells (*Figure 4.12 B*), compared to endogenous TBK-1. This may be because of the very high levels of

protein overexpression in HEK293 cells²⁰⁴, because overexpression of TBK-1 in HeLa²⁰⁵ and A549 lung carcinoma¹⁹⁵ cells demonstrates much more punctuate staining. However in the two latter studies, TBK-1 was conjugated to YFP or EGFP, which makes detection of the expressed protein more specific than the immunocytochemistry approached used here, which detects both overexpressed and endogenous protein. One advantage of using a small tag, such as the FLAG tag used here, compared to large fluorescent protein tags, is that they are less likely to modify the activity of the protein due to their smaller size. Further experiments need to be conducted to characterize the overexpressed TBK-1 in more detail.

5.3 ALS-mutant TBK-1 may dysregulate autophagy

Dysfunction in autophagy is gaining increasing importance as a pathogenic mechanism in ALS. The characteristic pathological hallmark of ALS are misfolded protein aggregates, which could therefore indicate failure of autophagy in degenerating MNs in ALS. Further evidence linking autophagy to ALS is that several genes encoding proteins whose normal function is related to autophagy, are mutated in fALS^{49,156}, most recently TBK-1⁵¹, with roles in selective autophagy, including xenophagy¹⁶³ and mitophagy^{192,201}. One of the major functions of TBK-1 is to phosphorylate autophagy receptors including NDP52, optineurin and p62. In our study we focused on non-selective macroautophagy, induced by serum-starvation in HEK293 cells. We evaluated autophagy induction through the widely used marker, LC3, following the latest Klionsky autophagy guidelines (published in 2016)¹⁸². Low levels of LC3-II were detected even in serum-starved cells, implying that under these conditions, HEK293 cells have high basal levels of autophagy (*Figure 4.13*). Hence, LC3-II would be turned over very quickly, thus making its detection difficult. No differences were observed in LC3 (either LC3-I or LC3-II) levels between HEK293 cells expressing TBK-1 proteins, not even if they were starved following transfection (*Figure 4.14, 4.15*). Based on these data, because there was no accumulation of LC3-II in TBK-1 mutant cells, we can hypothesise that TBK-1 does not affect the autophagy stages that are related to LC3-II expression, such as

maturation of autophagosomes into autolysosomes, and degradation of autolysosomes. If mutant TBK-1 had influenced the above mentioned stages, LC3-II would have accumulated upon transfection without additional treatments. LC3-I and LC3-II levels are equally informative indicators of autophagy according to the guidelines¹⁸², and changes in LC3-I and LC3-II levels are cell-type and stress-dependent, hence both need to be monitored for accurate results.

We detected significantly lower LC3-II levels upon ALS-mutant TBK-1 overexpression when cells were starved and simultaneously treated with bafilomycin (*Figure 4.16*), which inhibits autophagosome-lysosome fusion. Upon bafilomycin treatment, autophagosomes accumulate in the cell, hence if there is dysfunction in early autophagy, attenuated accumulation of autophagosomes can be detected. Hence our data suggest, based on the decreased accumulation of total LC3, LC3-I and LC3-II levels in bafilomycin treated cells, that ALS-mutant TBK-1 may negatively influence autophagy at the early stages, such as autophagosome formation. However it should be stated that we have not assessed LC3 at the transcriptional level, which might explain the decrease of LC3-I and LC3-II at the protein level¹⁸². In contrast to our results, Pilli and colleagues demonstrated that in macrophages, TBK-1 was necessary for the maturation of the autophagosomes into lytic bacterial organelles¹⁹². In our experiments, initiation of autophagy may be disrupted, but it should be kept in mind that we used different cell types in this study, and we focused on non-selective macroautophagy rather than the more selective elimination of mycobacteria. It is possible that TBK-1 has different roles in the different types of autophagy.

5.4 Kinase deficient TBK-1 mutants inhibit CHOP expression

The ER is responsible for the folding, post-translational modification and quality control of newly synthesised proteins. Hence it is a key component of cellular proteostasis. There is increasing evidence describing the importance of ER stress and UPR induction in ALS pathology^{129,131,133,206}. TBK-1 plays a major role in the

phosphorylation of IRF3, an inducer of the innate immune response. Moreover, ER stress regulates the innate immune response through IRF3²⁰⁷. Hence in this study we questioned whether the TBK-1 kinase may link the innate immune response to ER stress and the UPR.

It was demonstrated by immunoblotting that CHOP expression was decreased in HEK293 cells expressing the kinase deficient TBK-1 mutants (R308Q, R357Q, E643X, G159A), while no significant differences were detectable in cells expressing wildtype TBK-1 or the substrate binding deficient mutant (E696K) (*Figure 4.18*). This observation should be further confirmed by immunocytochemistry staining using anti-CHOP antibodies in TBK-1 transfected HEK293 cells, a method used previously in our laboratory. This technique would eliminate any possible issues with low transfection efficiency, because it allows specific quantification cells of individual transfected cells with activated CHOP. CHOP is a transcription factor that accumulates in the nucleus when activated; hence nuclear immunoreactivity to CHOP can be used as a specific method to detect ER stress²⁰⁸. CHOP is downstream of the PERK branch of the UPR, but interestingly, activation of PERK, indicated by the production of p-PERK, was not affected by expression of the TBK-1 mutants by immunoblotting. We did not examine the ATF6 branch of the UPR in this study due to time constraints. However, up-regulation of ATF6 is also an upstream mediator of CHOP expression, so it is possible that the inhibition of CHOP is mediated by the ATF6 branch of the UPR.

These data imply that the lower levels of CHOP associated with mutant TBK-1, is due to the loss of TBK-1 kinase activity, rather than ALS pathology, because only the kinase deficient mutants inhibited CHOP expression, and one of these was not an ALS/FTD mutant. In previous studies, ER stress-induced expression of CHOP is inhibited by prior engagement of Toll-like receptor signalling in a TRIF-mediated manner, by decreased activation of ATF4 translation¹⁹⁸. Toll-like receptor signalling is a major pathway activated in innate immunity, and TBK-1 is a major kinase active in innate immune pathways. Hence these findings imply that TBK-1 phosphorylates important elements of the UPR, and this is why we detected lower levels of CHOP in

cells expressing the kinase-deficient mutants. However, whilst the authors of the previous study concluded that CHOP suppression was not TBK-1 mediated, thus arguing against this possibility¹⁹⁸, they only examined the PERK, not the ATF6, pathway. Hence, it is possible that the kinase-dependent TBK-1-mediated CHOP expression is related to the ATF6 branch of the UPR and not the PERK pathway. This should be further analysed to investigate this possibility.

CHOP mediates the transition of UPR from pro-survival to pro-apoptosis. Hence it was unexpected that expression of ALS mutants could result in lower levels of a pro-apoptotic protein. Moreover, surprisingly, we did not detect upregulation of the UPR by the ALS TBK-1 mutants. This is in contrast to other mutants associated with fALS, including SOD1¹³³, TDP-43¹³⁴ and FUS¹³⁵. As mentioned above, ER stress is a key pathology in ALS, and mutations in TBK-1 did not result in elevated ER-stress based on markers analysed. This may be explained by the limitations of immunoblotting method used in this study. Furthermore, time points used in the study may have not been ideal for ER stress detection. In the future studies, initial time-course experiments should determine the best time-points for such experiments. In addition, in the current study, it was only possible to examine p-PERK, PERK and CHOP markers of the UPR due to time constraints. Ideally, a much more extensive analysis of the UPR should be performed, involving multiple markers. In particular, the PERK pathway should be examined in more depth.

It is important to mention several caveats of the current study. Firstly, *in vitro* cell cultures were used throughout. Whilst there are several advantages to this approach, including allowing us to perform several experimental repeats, and using identical conditions between repeats, it is also a very artificial environment, compared to *in vivo* as it lacks the presence and the interaction with adjacent tissue, that normally is present *in-vivo*. Furthermore, supplementing cells with 10% FBS in Dulbecco's modified Eagle's medium (DMEM), containing 4.5g/L D-glucose, represents diabetic levels of glucose supplementation, and hence does not mimic physiological conditions, despite being standard conditions for culturing cells *in vitro*. In addition, any conclusions reached from experiments using HEK293 cells

must be made with caution in relation to ALS pathology, because these cells do not bear neuronal/MN characteristics. Another caveat that should be mentioned is that because of time limitations, it was possible to perform some experiments only twice. Ideally, additional repetitions are necessary to further support our preliminary observations. Another limitation is that whilst LC3 is the most widely used marker of autophagosomes, and in this study we followed the internationally agreed Klionsky guidelines to detect LC3 levels, ideally additional markers and approaches should be analysed. Finally, as mentioned above, in this study it was only possible to examine three UPR markers, much more extensive analyses would ideally be performed.

Future directions

As well as the future studies already proposed above, a number of additional future experiments follow on logically from the findings obtained in this study.

To investigate in more detail whether optineurin recruits TBK-1 to autophagosomes, depletion of optineurin expression using small interfering RNA (siRNA) or CRISPR/Cas9 approaches could be used, examining the recruitment of TBK-1 to autophagosomes. Future studies should examine in more detail how the inhibition of recruitment of TBK-1 to autophagosomes perturbs autophagy. It would also be worthwhile to examine whether the ALS-associated TBK-1 mutants interact with wildtype optineurin, and also whether this also perturbs autophagy.

In the future, the effect of TBK-1 mutations in autophagy and ER-stress should be investigated in more depth. For this purpose, stable NSC-34 cell lines overexpressing the TBK-1 mutants could be used, or ideally, primary neurons from either mouse or human, as used by others in our group¹⁶¹, which could be transduced using lentiviral approaches²⁰⁹. Furthermore, because only low levels of TBK-1 expression were achieved in cell lines used in this study, the TBK-1 mutants should be expressed in a vector with a different backbone. Alternatively, another approach that could be used rather than protein overexpression and its associated issues, are CRISPR/Cas9 techniques²¹⁰. The kinase activity of TBK-1 wildtype and mutants should be analysed more specifically using kinase assays, or monitoring phosphorylation of TBK-1 substrates, such as IRF3, optineurin or p62.

As stated above, additional markers of autophagy other than LC3 could enable determination of which step of autophagy is influenced by ALS-mutant TBK-1, and what the long term consequences of this dysfunction are. Future experiments could examine the formation of the omegasome, the precursor of the autophagosome which is derived from the ER, or alternatively autophagy events downstream of autophagosome formation, including fusion to the lysosome. Furthermore, another interesting possibility is to investigate how mutant-TBK-1 proteins affects optineurin mediated phase of autophagy.

Concluding remarks

ALS and FTD are both fatal neurodegenerative diseases, with no effective treatment or cure. Cytoplasmic protein aggregates are the pathological hallmark of ALS and several genes responsible for maintaining proteostasis are mutated in both ALS and FTD. One recently discovered gene linked to fALS, sALS and FTD, *TBK-1*, has major roles in the control of innate immunity and autophagy. Furthermore well-balanced autophagy is a crucial component of proteostasis. To date, no study has examined the role of TBK-1 in ALS pathology. Here we provide preliminary evidence to show that ALS-mutant TBK-1 proteins dysregulate autophagy in HEK293 cells. Moreover, expression of the kinase deficient TBK-1 mutants led to decreased expression of CHOP, although the mechanism for this remains unclear. It still remains unknown how the ALS-mutant TBK-1 may perturb autophagy and ER stress, but these preliminary results imply that these pathways are relevant to TBK-1-associated ALS/FTD, and these possibilities should be investigated in the future.

REFERENCES

- 1 Kiernan, M. C. *et al.* Amyotrophic lateral sclerosis. *Lancet (London, England)* **377**, 942-955, (2011).
- 2 Purves, A., Fitzpatrick, H. & LaMantia, M. Williams (2004). *Neuroscience, third edition. Sinauer Associates.*
- 3 Stifani, N. Motor neurons and the generation of spinal motor neuron diversity. *Frontiers in cellular neuroscience* **8** (2014).
- 4 Brooks, B. R. El Escorial World Federation of Neurology criteria for the diagnosis of amyotrophic lateral sclerosis. *Journal of the neurological sciences* **124**, 96-107 (1994).
- 5 Brooks, B. R., Miller, R. G., Swash, M. & Munsat, T. L. El Escorial revisited: revised criteria for the diagnosis of amyotrophic lateral sclerosis. *Amyotrophic Lateral Sclerosis and Other Motor Neuron Disorders* **1**, 293-299 (2000).
- 6 Swinnen, B. & Robberecht, W. The phenotypic variability of amyotrophic lateral sclerosis. *Nature reviews. Neurology* **10**, 661-670, (2014).
- 7 Gorelick, P. *Handbook of neuroepidemiology*. Vol. 29 (Marcel Dekker, 1994).
- 8 Chiò, A., Calvo, A., Moglia, C., Mazzini, L. & Mora, G. Phenotypic heterogeneity of amyotrophic lateral sclerosis: a population based study. *Journal of Neurology, Neurosurgery & Psychiatry* **82**, 740-746 (2011).
- 9 Shoesmith, C. L., Findlater, K., Rowe, A. & Strong, M. J. Prognosis of amyotrophic lateral sclerosis with respiratory onset. *Journal of Neurology, Neurosurgery, and Psychiatry* **78**, 629-631, (2007).
- 10 Rowland, L. P. & Shneider, N. A. Amyotrophic lateral sclerosis. *The New England journal of medicine* **344**, 1688-1700, (2001).
- 11 Sabatelli, M. *et al.* Natural history of young-adult amyotrophic lateral sclerosis. *Neurology* **71**, 876-881 (2008).
- 12 Pupillo, E., Messina, P., Logroscino, G. & Beghi, E. Long - term survival in amyotrophic lateral sclerosis: A population - based study. *Annals of neurology* **75**, 287-297 (2014).
- 13 Andersen, P. M. & Al-Chalabi, A. Clinical genetics of amyotrophic lateral sclerosis: what do we really know? *Nature Reviews Neurology* **7**, 603-615 (2011).
- 14 Zoccollella, S. *et al.* Analysis of survival and prognostic factors in amyotrophic lateral sclerosis: a population based study. *Journal of Neurology, Neurosurgery & Psychiatry* **79**, 33-37 (2008).
- 15 Lambrechts, D. *et al.* VEGF is a modifier of amyotrophic lateral sclerosis in mice and humans and protects motoneurons against ischemic death. *Nature genetics* **34**, 383-394 (2003).
- 16 Saeed, M. *et al.* Age and founder effect of SOD1 A4V mutation causing ALS. *Neurology* **72**, 1634-1639, (2009).
- 17 Williams, K. L. *et al.* CCFN mutations in amyotrophic lateral sclerosis and frontotemporal dementia. *Nat Commun* **7**, 11253, (2016).
- 18 Boylan, K. Familial Amyotrophic Lateral Sclerosis. *Neurologic clinics* **33**, 807-830, (2015).
- 19 Hadano, S. *et al.* A gene encoding a putative GTPase regulator is mutated in familial amyotrophic lateral sclerosis 2. *Nature genetics* **29**, 166-173 (2001).
- 20 Greenway, M. J. *et al.* ANG mutations segregate with familial and 'sporadic' amyotrophic lateral sclerosis. *Nature genetics* **38**, 411-413 (2006).
- 21 van Es, M. A. *et al.* Angiogenin variants in Parkinson disease and amyotrophic lateral sclerosis. *Annals of neurology* **70**, 964-973 (2011).
- 22 Daoud, H. *et al.* Association of long ATXN2 CAG repeat sizes with increased risk of amyotrophic lateral sclerosis. *Archives of neurology* **68**, 739-742 (2011).
- 23 Elden, A. C. *et al.* Ataxin-2 intermediate-length polyglutamine expansions are associated with increased risk for ALS. *Nature* **466**, 1069-1075 (2010).
- 24 Bannwarth, S. *et al.* A mitochondrial origin for frontotemporal dementia and amyotrophic lateral sclerosis through CHCHD10 involvement. *Brain : a journal of neurology*, 2329-2345 (2014).
- 25 Johnson, J. O. *et al.* Mutations in the CHCHD10 gene are a common cause of familial amyotrophic lateral sclerosis. *Brain : a journal of neurology* **137**, e311-e311 (2014).

- 26 Parkinson, N. *et al.* ALS phenotypes with mutations in CHMP2B (charged multivesicular body protein 2B). *Neurology* **67**, 1074-1077 (2006).
- 27 DeJesus-Hernandez, M. *et al.* Expanded GGGGCC hexanucleotide repeat in noncoding region of C9ORF72 causes chromosome 9p-linked FTD and ALS. *Neuron* **72**, 245-256 (2011).
- 28 Renton, A. E. *et al.* A hexanucleotide repeat expansion in C9ORF72 is the cause of chromosome 9p21-linked ALS-FTD. *Neuron* **72**, 257-268 (2011).
- 29 Snowden, J. S. *et al.* Distinct clinical and pathological characteristics of frontotemporal dementia associated with C9ORF72 mutations. *Brain : a journal of neurology* **135**, 693-708 (2012).
- 30 Lesage, S. *et al.* C9orf72 repeat expansions are a rare genetic cause of parkinsonism. *Brain : a journal of neurology* **136**, 385-391 (2013).
- 31 Mitchell, J. *et al.* Familial amyotrophic lateral sclerosis is associated with a mutation in D-amino acid oxidase. *Proceedings of the National Academy of Sciences* **107**, 7556-7561 (2010).
- 32 Münch, C. *et al.* Heterozygous R1101K mutation of the DCTN1 gene in a family with ALS and FTD. *Annals of neurology* **58**, 777-780 (2005).
- 33 Vilariño-Güell, C. *et al.* Characterization of DCTN1 genetic variability in neurodegeneration. *Neurology* **72**, 2024-2028 (2009).
- 34 Münch, C. *et al.* Point mutations of the p150 subunit of dynactin (DCTN1) gene in ALS. *Neurology* **63**, 724-726 (2004).
- 35 Chow, C. Y. *et al.* Deleterious variants of FIG4, a phosphoinositide phosphatase, in patients with ALS. *The American Journal of Human Genetics* **84**, 85-88 (2009).
- 36 Vance, C. *et al.* Mutations in FUS, an RNA processing protein, cause familial amyotrophic lateral sclerosis type 6. *Science* **323**, 1208-1211 (2009).
- 37 Kwiatkowski, T. J. *et al.* Mutations in the FUS/TLS gene on chromosome 16 cause familial amyotrophic lateral sclerosis. *Science* **323**, 1205-1208 (2009).
- 38 Kim, H. J. *et al.* Mutations in prion-like domains in hnRNPA2B1 and hnRNPA1 cause multisystem proteinopathy and ALS. *Nature* **495**, 467-473 (2013).
- 39 Johnson, J. O. *et al.* Mutations in the Matrin 3 gene cause familial amyotrophic lateral sclerosis. *Nature neuroscience* **17**, 664-666 (2014).
- 40 Maruyama, H. *et al.* Mutations of optineurin in amyotrophic lateral sclerosis. *Nature* **465**, 223-226 (2010).
- 41 Gonzalez-Perez, P. *et al.* Identification of rare protein disulfide isomerase gene variants in amyotrophic lateral sclerosis patients. *Gene* **566**, 158-165, (2015).
- 42 Wu, C.-H. *et al.* Mutations in the profilin 1 gene cause familial amyotrophic lateral sclerosis. *Nature* **488**, 499-503 (2012).
- 43 Chen, Y.-Z. *et al.* DNA/RNA helicase gene mutations in a form of juvenile amyotrophic lateral sclerosis (ALS4). *The American Journal of Human Genetics* **74**, 1128-1135 (2004).
- 44 Belzil, V. V. *et al.* Genetic analysis of SIGMAR1 as a cause of familial ALS with dementia. *European Journal of Human Genetics* **21**, 237-239 (2013).
- 45 Al - Saif, A., Al - Mohanna, F. & Bohlega, S. A mutation in sigma - 1 receptor causes juvenile amyotrophic lateral sclerosis. *Annals of neurology* **70**, 913-919 (2011).
- 46 Fukunaga, K., Shinoda, Y. & Tagashira, H. The role of SIGMAR1 gene mutation and mitochondrial dysfunction in amyotrophic lateral sclerosis. *Journal of pharmacological sciences* **127**, 36-41 (2015).
- 47 Rosen, D. R. *et al.* Mutations in Cu/Zn superoxide dismutase gene are associated with familial amyotrophic lateral sclerosis. *Nature* **362**, 59-62 (1993).
- 48 Daoud, H. *et al.* Exome sequencing reveals SPG11 mutations causing juvenile ALS. *Neurobiology of aging* **33**, 839. e835-839. e839 (2012).
- 49 Fecto, F. *et al.* SQSTM1 mutations in familial and sporadic amyotrophic lateral sclerosis. *Archives of neurology* **68**, 1440-1446 (2011).
- 50 Neumann, M. *et al.* Ubiquitinated TDP-43 in frontotemporal lobar degeneration and amyotrophic lateral sclerosis. *Science* **314**, 130-133 (2006).
- 51 Cirulli, E. T. *et al.* Exome sequencing in amyotrophic lateral sclerosis identifies risk genes and pathways. *Science* **347**, 1436-1441, (2015).
- 52 Smith, B. N. *et al.* Exome-wide rare variant analysis identifies TUBA4A mutations associated with familial ALS. *Neuron* **84**, 324-331 (2014).

- 53 Deng, H.-X. *et al.* Mutations in UBQLN2 cause dominant X-linked juvenile and adult-onset ALS and ALS/dementia. *Nature* **477**, 211-215 (2011).
- 54 Nishimura, A. L. *et al.* A mutation in the vesicle-trafficking protein VAPB causes late-onset spinal muscular atrophy and amyotrophic lateral sclerosis. *The American Journal of Human Genetics* **75**, 822-831 (2004).
- 55 Johnson, J. O. *et al.* Exome sequencing reveals VCP mutations as a cause of familial ALS. *Neuron* **68**, 857-864 (2010).
- 56 Ling, S. C., Polymenidou, M. & Cleveland, D. W. Converging mechanisms in ALS and FTD: disrupted RNA and protein homeostasis. *Neuron* **79**, 416-438, (2013).
- 57 Ringholz, G. *et al.* Prevalence and patterns of cognitive impairment in sporadic ALS. *Neurology* **65**, 586-590 (2005).
- 58 Wheaton, M. *et al.* Cognitive impairment in familial ALS. *Neurology* **69**, 1411-1417 (2007).
- 59 Arai, T. *et al.* TDP-43 is a component of ubiquitin-positive tau-negative inclusions in frontotemporal lobar degeneration and amyotrophic lateral sclerosis. *Biochemical and biophysical research communications* **351**, 602-611 (2006).
- 60 Kaur, S. J., McKeown, S. R. & Rashid, S. Mutant SOD1 mediated pathogenesis of Amyotrophic Lateral Sclerosis. *Gene* **577**, (2016).
- 61 Elchuri, S. *et al.* CuZnSOD deficiency leads to persistent and widespread oxidative damage and hepatocarcinogenesis later in life. *Oncogene* **24**, 367-380 (2005).
- 62 Robberecht, W. Genetics of amyotrophic lateral sclerosis. *Journal of neurology* **247**, VI2-VI6 (2000).
- 63 Sau, D. *et al.* Mutation of SOD1 in ALS: a gain of a loss of function. *Human molecular genetics* **16**, (2007).
- 64 Reaume, A. G. *et al.* Motor neurons in Cu/Zn superoxide dismutase-deficient mice develop normally but exhibit enhanced cell death after axonal injury. *Nature genetics* **13**, 43-47, (1996).
- 65 Rutherford, N. J. *et al.* Novel Mutations in TARDBP (TDP-43) in Patients with Familial Amyotrophic Lateral Sclerosis. *PLoS Genetics* **4**, e1000193, (2008).
- 66 Sreedharan, J. *et al.* TDP-43 mutations in familial and sporadic amyotrophic lateral sclerosis. *Science* **319**, 1668-1672, (2008).
- 67 Sreedharan, J. *et al.* TDP-43 mutations in familial and sporadic amyotrophic lateral sclerosis. *Science* **319**, 1668-1672 (2008).
- 68 Buratti, E. & Baralle, F. E. TDP-43: gumming up neurons through protein-protein and protein-RNA interactions. *Trends in biochemical sciences* **37**, 237-247 (2012).
- 69 Lagier-Tourenne, C., Polymenidou, M. & Cleveland, D. W. TDP-43 and FUS/TLS: emerging roles in RNA processing and neurodegeneration. *Human molecular genetics* **19**, R46-R64 (2010).
- 70 Polymenidou, M. & Cleveland, D. W. Prion-like spread of protein aggregates in neurodegeneration. *The Journal of experimental medicine* **209**, 889-893 (2012).
- 71 Ayala, Y. M. *et al.* Structural determinants of the cellular localization and shuttling of TDP-43. *Journal of cell science* **121**, 3778-3785 (2008).
- 72 Winton, M. J. *et al.* Disturbance of nuclear and cytoplasmic TAR DNA-binding protein (TDP-43) induces disease-like redistribution, sequestration, and aggregate formation. *Journal of Biological Chemistry* **283**, 13302-13309 (2008).
- 73 Barmada, S. J. *et al.* Cytoplasmic mislocalization of TDP-43 is toxic to neurons and enhanced by a mutation associated with familial amyotrophic lateral sclerosis. *The Journal of neuroscience : the official journal of the Society for Neuroscience* **30**, 639-649, (2010).
- 74 Vanden Broeck, L., Callaerts, P. & Dermaut, B. TDP-43-mediated neurodegeneration: towards a loss-of-function hypothesis? *Trends in molecular medicine* **20**, 66-71, (2014).
- 75 Wegorzewska, I., Bell, S., Cairns, N. J., Miller, T. M. & Baloh, R. H. TDP-43 mutant transgenic mice develop features of ALS and frontotemporal lobar degeneration. *Proceedings of the National Academy of Sciences* **106**, 18809-18814 (2009).
- 76 Wils, H. *et al.* TDP-43 transgenic mice develop spastic paralysis and neuronal inclusions characteristic of ALS and frontotemporal lobar degeneration. *Proceedings of the National Academy of Sciences* **107**, 3858-3863 (2010).
- 77 Igaz, L. M. *et al.* Dysregulation of the ALS-associated gene TDP-43 leads to neuronal death and degeneration in mice. *The Journal of clinical investigation* **121**, 726-738 (2011).

- 78 Arnold, E. S. *et al.* ALS-linked TDP-43 mutations produce aberrant RNA splicing and adult-onset motor neuron disease without aggregation or loss of nuclear TDP-43. *Proceedings of the National Academy of Sciences* **110**, E736-E745 (2013).
- 79 Zhou, Y., Liu, S., Öztürk, A. & Hicks, G. G. FUS-regulated RNA metabolism and DNA damage repair: Implications for amyotrophic lateral sclerosis and frontotemporal dementia pathogenesis. *Rare Diseases* **2**, e29515, (2014).
- 80 Daigle, J. G. *et al.* RNA-binding ability of FUS regulates neurodegeneration, cytoplasmic mislocalization and incorporation into stress granules associated with FUS carrying ALS-linked mutations. *Human molecular genetics* **22**, 1193-1205, (2013).
- 81 Vance, C. *et al.* ALS mutant FUS disrupts nuclear localization and sequesters wild-type FUS within cytoplasmic stress granules. *Human molecular genetics* **22**, 2676-2688, (2013).
- 82 Lanson, N. A. & Pandey, U. B. FUS-related proteinopathies: lessons from animal models. *Brain research* **1462**, 44-60 (2012).
- 83 Boeve, B. F. *et al.* Characterization of frontotemporal dementia and/or amyotrophic lateral sclerosis associated with the GGGGCC repeat expansion in C9ORF72. *Brain : a journal of neurology* **135**, 765-783, (2012).
- 84 Chio, A. *et al.* Clinical characteristics of patients with familial amyotrophic lateral sclerosis carrying the pathogenic GGGGCC hexanucleotide repeat expansion of C9ORF72. *Brain : a journal of neurology* **135**, 784-793, (2012).
- 85 Cooper-Knock, J. *et al.* Clinico-pathological features in amyotrophic lateral sclerosis with expansions in C9ORF72. *Brain : a journal of neurology* **135**, 751-764, (2012).
- 86 Hsiung, G. Y. *et al.* Clinical and pathological features of familial frontotemporal dementia caused by C9ORF72 mutation on chromosome 9p. *Brain : a journal of neurology* **135**, 709-722, (2012).
- 87 Mahoney, C. J. *et al.* Frontotemporal dementia with the C9ORF72 hexanucleotide repeat expansion: clinical, neuroanatomical and neuropathological features. *Brain : a journal of neurology* **135**, 736-750, (2012).
- 88 Simon-Sanchez, J. *et al.* The clinical and pathological phenotype of C9ORF72 hexanucleotide repeat expansions. *Brain : a journal of neurology* **135**, 723-735, (2012).
- 89 Snowden, J. S. *et al.* Distinct clinical and pathological characteristics of frontotemporal dementia associated with C9ORF72 mutations. *Brain : a journal of neurology* **135**, 693-708, (2012).
- 90 Farg, M. A. *et al.* C9ORF72, implicated in amyotrophic lateral sclerosis and frontotemporal dementia, regulates endosomal trafficking. *Human molecular genetics* **23**, 3579-3595, (2014).
- 91 Byrne, S. *et al.* Cognitive and clinical characteristics of patients with amyotrophic lateral sclerosis carrying a C9orf72 repeat expansion: a population-based cohort study. *The Lancet. Neurology* **11**, 232-240, (2012).
- 92 Millecamps, S. *et al.* Phenotype difference between ALS patients with expanded repeats in C9ORF72 and patients with mutations in other ALS-related genes. *Journal of medical genetics* **49**, 258-263 (2012).
- 93 Stewart, H. *et al.* Clinical and pathological features of amyotrophic lateral sclerosis caused by mutation in the C9ORF72 gene on chromosome 9p. *Acta neuropathologica* **123**, 409-417 (2012).
- 94 Brundin, P., Melki, R. & Kopito, R. Prion-like transmission of protein aggregates in neurodegenerative diseases. *Nature Reviews Molecular Cell Biology* **11**, 301-307 (2010).
- 95 Holzbaur, E. L. Motor neurons rely on motor proteins. *Trends in cell biology* **14**, 233-240 (2004).
- 96 Goldberg, J. L. How does an axon grow? *Genes & development* **17**, 941-958 (2003).
- 97 Chao, M. V. Retrograde transport redux. *Neuron* **39**, 1-2 (2003).
- 98 Hollenbeck, P. J. & Saxton, W. M. The axonal transport of mitochondria. *Journal of cell science* **118**, 5411-5419 (2005).
- 99 Hollenbeck, P. J. The pattern and mechanism of mitochondrial transport in axons. *Front Biosci* **1**, d91-d102 (1996).
- 100 Sasaki, S. & Iwata, M. Impairment of fast axonal transport in the proximal axons of anterior horn neurons in amyotrophic lateral sclerosis. *Neurology* **47**, 535-540 (1996).

- 101 Sasaki, S. & Iwata, M. Mitochondrial alterations in the spinal cord of patients with sporadic amyotrophic lateral sclerosis. *Journal of Neuropathology & Experimental Neurology* **66**, 10-16 (2007).
- 102 Sasaki, S. Autophagy in spinal cord motor neurons in sporadic amyotrophic lateral sclerosis. *Journal of Neuropathology & Experimental Neurology* **70**, 349-359 (2011).
- 103 Sasaki, S., Warita, H., Abe, K. & Iwata, M. Impairment of axonal transport in the axon hillock and the initial segment of anterior horn neurons in transgenic mice with a G93A mutant SOD1 gene. *Acta neuropathologica* **110**, 48-56 (2005).
- 104 Alami, N. H. *et al.* Axonal transport of TDP-43 mRNA granules is impaired by ALS-causing mutations. *Neuron* **81**, 536-543, (2014).
- 105 Collard, J.-F., Côté, F. & Julien, J.-P. Defective axonal transport in a transgenic mouse model of amyotrophic lateral sclerosis. *Nature* **375**, 61-64 (1995).
- 106 De Vos, K. J. *et al.* Familial amyotrophic lateral sclerosis-linked SOD1 mutants perturb fast axonal transport to reduce axonal mitochondria content. *Human molecular genetics* **16**, 2720-2728 (2007).
- 107 Afifi, A. K., Aleu, F. P., Goodgold, J. & MacKay, B. Ultrastructure of atrophic muscle in amyotrophic lateral sclerosis. *Neurology* **16**, 475-481 (1966).
- 108 Higgins, C. M., Jung, C. & Xu, Z. ALS-associated mutant SOD1G93A causes mitochondrial vacuolation by expansion of the intermembrane space and by involvement of SOD1 aggregation and peroxisomes. *BMC neuroscience* **4**, 16 (2003).
- 109 Kong, J. & Xu, Z. Massive mitochondrial degeneration in motor neurons triggers the onset of amyotrophic lateral sclerosis in mice expressing a mutant SOD1. *The Journal of neuroscience* **18**, 3241-3250 (1998).
- 110 Wong, P. C. *et al.* An adverse property of a familial ALS-linked SOD1 mutation causes motor neuron disease characterized by vacuolar degeneration of mitochondria. *Neuron* **14**, 1105-1116 (1995).
- 111 Kawamata, H. & Manfredi, G. Mitochondrial dysfunction and intracellular calcium dysregulation in ALS. *Mechanisms of ageing and development* **131**, 517-526 (2010).
- 112 Lino, M. M., Schneider, C. & Caroni, P. Accumulation of SOD1 mutants in postnatal motoneurons does not cause motoneuron pathology or motoneuron disease. *The Journal of neuroscience : the official journal of the Society for Neuroscience* **22**, 4825-4832 (2002).
- 113 Lee, Y. *et al.* Oligodendroglia metabolically support axons and contribute to neurodegeneration. *Nature* **487**, 443-448 (2012).
- 114 Kang, S. H. *et al.* Degeneration and impaired regeneration of gray matter oligodendrocytes in amyotrophic lateral sclerosis. *Nature neuroscience* **16**, 571-579 (2013).
- 115 Philips, T. *et al.* Oligodendrocyte dysfunction in the pathogenesis of amyotrophic lateral sclerosis. *Brain : a journal of neurology*, 471-482 (2013).
- 116 Lobsiger, C. S. & Cleveland, D. W. Glial cells as intrinsic components of non-cell-autonomous neurodegenerative disease. *Nature neuroscience* **10**, 1355-1360 (2007).
- 117 Di Giorgio, F. P., Carrasco, M. A., Siao, M. C., Maniatis, T. & Eggan, K. Non-cell autonomous effect of glia on motor neurons in an embryonic stem cell-based ALS model. *Nature neuroscience* **10**, 608-614 (2007).
- 118 Haidet-Phillips, A. M. *et al.* Astrocytes from familial and sporadic ALS patients are toxic to motor neurons. *Nature biotechnology* **29**, 824-828 (2011).
- 119 Turner, M. *et al.* Evidence of widespread cerebral microglial activation in amyotrophic lateral sclerosis: an [¹¹C](R)-PK11195 positron emission tomography study. *Neurobiology of disease* **15**, 601-609 (2004).
- 120 Beers, D. R., Henkel, J. S., Zhao, W., Wang, J. & Appel, S. H. CD4+ T cells support glial neuroprotection, slow disease progression, and modify glial morphology in an animal model of inherited ALS. *Proceedings of the National Academy of Sciences* **105**, 15558-15563 (2008).
- 121 Kigerl, K. A. *et al.* Identification of two distinct macrophage subsets with divergent effects causing either neurotoxicity or regeneration in the injured mouse spinal cord. *The Journal of Neuroscience* **29**, 13435-13444 (2009).
- 122 Beers, D. R. *et al.* Endogenous regulatory T lymphocytes ameliorate amyotrophic lateral sclerosis in mice and correlate with disease progression in patients with amyotrophic lateral sclerosis. *Brain : a journal of neurology* **134**, 1293-1314 (2011).

- 123 Liao, B., Zhao, W., Beers, D. R., Henkel, J. S. & Appel, S. H. Transformation from a
neuroprotective to a neurotoxic microglial phenotype in a mouse model of ALS. *Experimental*
124 *neurology* **237**, 147-152 (2012).
- 125 Boillée, S. *et al.* Onset and progression in inherited ALS determined by motor neurons and
microglia. *Science* **312**, 1389-1392 (2006).
- 126 Yamanaka, K. *et al.* Astrocytes as determinants of disease progression in inherited
amyotrophic lateral sclerosis. *Nature neuroscience* **11**, 251-253 (2008).
- 127 Perri, E. R., Thomas, C. J., Parakh, S., Spencer, D. M. & Atkin, J. D. The Unfolded Protein
Response and the Role of Protein Disulfide Isomerase in Neurodegeneration. *Frontiers in cell*
128 *and developmental biology* **3**, 80, (2015).
- 129 Walter, P. & Ron, D. The unfolded protein response: from stress pathway to homeostatic
regulation. *Science* **334**, 1081-1086 (2011).
- 130 Hetz, C. The unfolded protein response: controlling cell fate decisions under ER stress and
beyond. *Nature reviews Molecular cell biology* **13**, 89-102 (2012).
- 131 Soo, K. *et al.* Rab1-dependent ER-Golgi transport dysfunction is a common pathogenic
mechanism in SOD1, TDP-43 and FUS-associated ALS. *Acta neuropathologica*, 1-19, (2015).
- 132 Atkin, J. D. *et al.* Mutant SOD1 inhibits ER-Golgi transport in amyotrophic lateral sclerosis. *J*
Neurochem **129**, 190-204, (2014).
- 133 Walker, A. K. & Atkin, J. D. Stress signaling from the endoplasmic reticulum: A central player
in the pathogenesis of amyotrophic lateral sclerosis. *IUBMB life* **63**, 754-763, (2011).
- 134 Nishitoh, H. *et al.* ALS-linked mutant SOD1 induces ER stress- and ASK1-dependent motor
neuron death by targeting Derlin-1. *Genes & development* **22**, 1451-1464, (2008).
- 135 Sundaramoorthy, V. *et al.* Extracellular wildtype and mutant SOD1 induces ER-Golgi
pathology characteristic of amyotrophic lateral sclerosis in neuronal cells. *Cellular and*
molecular life sciences : CMLS **70**, 4181-4195, (2013).
- 136 Walker, A. K. *et al.* ALS-associated TDP-43 induces endoplasmic reticulum stress, which
drives cytoplasmic TDP-43 accumulation and stress granule formation. *PLoS One* **8**, e81170,
(2013).
- 137 Farg, M. A. *et al.* Mutant FUS induces endoplasmic reticulum stress in amyotrophic lateral
sclerosis and interacts with protein disulfide-isomerase. *Neurobiology of aging* **33**, 2855-
2868, (2012).
- 138 Saxena, S., Cabuy, E. & Caroni, P. A role for motoneuron subtype-selective ER stress in
disease manifestations of FALS mice. *Nature neuroscience* **12**, 627-636 (2009).
- 139 Ahlberg, J., Marzella, L. & Glaumann, H. Uptake and degradation of proteins by isolated rat
liver lysosomes. Suggestion of a microautophagic pathway of proteolysis. *Laboratory*
investigation; a journal of technical methods and pathology **47**, 523-532 (1982).
- 140 Dice, J. F. Peptide sequences that target cytosolic proteins for lysosomal proteolysis. *Trends*
in biochemical sciences **15**, 305-309 (1990).
- 141 Feng, Y., He, D., Yao, Z. & Klionsky, D. J. The machinery of macroautophagy. *Cell research* **24**,
24-41 (2014).
- 142 Cai, Y. *et al.* Interplay of endoplasmic reticulum stress and autophagy in neurodegenerative
disorders. *Autophagy* **12**, 225-244, (2016).
- 143 Chan, S. N. & Tang, B. L. Location and membrane sources for autophagosome formation -
from ER-mitochondria contact sites to Golgi-endosome-derived carriers. *Molecular*
membrane biology **30**, 394-402, (2013).
- 144 Soubannier, V. *et al.* A vesicular transport pathway shuttles cargo from mitochondria to
lysosomes. *Current biology : CB* **22**, 135-141, (2012).
- 145 Cebollero, E., Reggiori, F. & Kraft, C. Reticulophagy and ribophagy: regulated degradation of
protein production factories. *International journal of cell biology* **2012** (2012).
- 146 Knodler, L. A. & Celli, J. Eating the strangers within: host control of intracellular bacteria via
xenophagy. *Cellular microbiology* **13**, 1319-1327,
- 147 Lamark, T. & Johansen, T. Aggrephagy: selective disposal of protein aggregates by
macroautophagy. *International journal of cell biology* **2012** (2012).
- 148 Cheung, Z. H. & Ip, N. Y. Autophagy deregulation in neurodegenerative diseases—recent
advances and future perspectives. *Journal of neurochemistry* **118**, 317-325 (2011).
- 149 Levine, B. & Kroemer, G. Autophagy in the pathogenesis of disease. *Cell* **132**, 27-42 (2008).

- 148 Zhang, X. *et al.* Rapamycin treatment augments motor neuron degeneration in SOD1(G93A)
149 mouse model of amyotrophic lateral sclerosis. *Autophagy* **7**, 412-425 (2011).
- 149 B'Chir, W. *et al.* The eIF2alpha/ATF4 pathway is essential for stress-induced autophagy gene
150 expression. *Nucleic acids research* **41**, 7683-7699, (2013).
- 150 Ogata, M. *et al.* Autophagy is activated for cell survival after endoplasmic reticulum stress.
151 *Molecular and cellular biology* **26**, 9220-9231 (2006).
- 151 Høyer-Hansen, M. & Jäättelä, M. Connecting endoplasmic reticulum stress to autophagy by
152 unfolded protein response and calcium. *Cell Death & Differentiation* **14**, 1576-1582 (2007).
- 152 Gade, P. *et al.* Regulation of the death-associated protein kinase 1 expression and autophagy
153 via ATF6 requires apoptosis signal-regulating kinase 1. *Molecular and cellular biology* **34**,
4033-4048 (2014).
- 153 Kalvakolanu, D. V. & Gade, P. IFNG and autophagy: a critical role for the ER-stress mediator
154 ATF6 in controlling bacterial infections. *Autophagy* **8**, 1673-1674 (2012).
- 154 Zalckvar, E. *et al.* DAP - kinase - mediated phosphorylation on the BH3 domain of beclin 1
155 promotes dissociation of beclin 1 from Bcl - XL and induction of autophagy. *EMBO reports*
10, 285-292 (2009).
- 155 Tooze, S. A. & Yoshimori, T. The origin of the autophagosomal membrane. *Nat Cell Biol* **12**,
831-835, (2010).
- 156 Maruyama, H. *et al.* Mutations of optineurin in amyotrophic lateral sclerosis. *Nature* **465**,
223-226, (2010).
- 157 Li, Y., Kang, J. & Horwitz, M. S. Interaction of an adenovirus E3 14.7-kilodalton protein with
158 a novel tumor necrosis factor alpha-inducible cellular protein containing leucine zipper
domains. *Molecular and cellular biology* **18**, 1601-1610 (1998).
- 158 Li, C. *et al.* Optineurin mutations in patients with sporadic amyotrophic lateral sclerosis in
159 China. *Amyotrophic lateral sclerosis & frontotemporal degeneration* **16**, 485-489, (2015).
- 159 Rezaie, T. *et al.* Adult-onset primary open-angle glaucoma caused by mutations in
160 optineurin. *Science* **295**, 1077-1079, (2002).
- 160 Pottier, C. *et al.* Whole-genome sequencing reveals important role for TBK1 and OPTN
161 mutations in frontotemporal lobar degeneration without motor neuron disease. *Acta*
neuropathologica **130**, 77-92, (2015).
- 161 Sundaramoorthy, V. *et al.* Defects in optineurin- and myosin VI-mediated cellular trafficking
162 in amyotrophic lateral sclerosis. *Human molecular genetics* **24**, 3830-3846, (2015).
- 162 Osawa, T. *et al.* Optineurin in neurodegenerative diseases. *Neuropathology* **31**, 569-574,
(2011).
- 163 Wild, P. *et al.* Phosphorylation of the autophagy receptor optineurin restricts Salmonella
164 growth. *Science* **333**, 228-233, (2011).
- 164 Sirohi, K. & Swarup, G. Defects in autophagy caused by glaucoma-associated mutations in
165 optineurin. *Experimental eye research* **144**, 54-63, (2016).
- 165 Morton, S., Hesson, L., Pegg, M. & Cohen, P. Enhanced binding of TBK1 by an optineurin
166 mutant that causes a familial form of primary open angle glaucoma. *FEBS letters* **582**, 997-
1002, (2008).
- 166 Ying, H. & Yue, B. Y. Cellular and molecular biology of optineurin. *International review of cell*
and molecular biology **294**, 223-258, (2012).
- 167 Freischmidt, A. *et al.* Haploinsufficiency of TBK1 causes familial ALS and fronto-temporal
168 dementia. *Nature neuroscience* **18**, 631-636, (2015).
- 168 Pomerantz, J. L. & Baltimore, D. NF-kappaB activation by a signaling complex containing
169 TRAF2, TANK and TBK1, a novel IKK-related kinase. *The EMBO Journal* **18**, 6694-6704,
(1999).
- 169 Fitzgerald, K. A. *et al.* IKKepsilon and TBK1 are essential components of the IRF3 signaling
170 pathway. *Nature immunology* **4**, 491-496, (2003).
- 170 Panne, D., McWhirter, S. M., Maniatis, T. & Harrison, S. C. Interferon regulatory factor 3 is
171 regulated by a dual phosphorylation-dependent switch. *Journal of Biological Chemistry* **282**,
22816-22822 (2007).
- 171 Ma, X. *et al.* Molecular basis of Tank-binding kinase 1 activation by
transautophosphorylation. *Proceedings of the National Academy of Sciences* **109**, 9378-9383
(2012).

- 172 Ikeda, F. *et al.* Involvement of the ubiquitin - like domain of TBK1/IKK - i kinases in
regulation of IFN - inducible genes. *The EMBO journal* **26**, 3451-3462 (2007).
- 173 Goncalves, A. *et al.* Functional dissection of the TBK1 molecular network. *PLoS One* **6**, e23971
(2011).
- 174 Gijssels, I. *et al.* Loss of TBK1 is a frequent cause of frontotemporal dementia in a Belgian
cohort. *Neurology* **85**, 2116-2125, (2015).
- 175 Le Ber, I. *et al.* TBK1 mutation frequencies in French frontotemporal dementia and
amyotrophic lateral sclerosis cohorts. *Neurobiology of aging* **36**, 3116.e3115-3118, (2015).
- 176 Kishore, N. *et al.* IKK-i and TBK-1 are Enzymatically Distinct from the Homologous Enzyme
IKK-2 COMPARATIVE ANALYSIS OF RECOMBINANT HUMAN IKK-i, TBK-1, AND IKK-2.
Journal of Biological Chemistry **277**, 13840-13847 (2002).
- 177 Hou, F. *et al.* MAVS forms functional prion-like aggregates to activate and propagate antiviral
innate immune response. *Cell* **146**, 448-461 (2011).
- 178 Clark, K. *et al.* Novel cross-talk within the IKK family controls innate immunity. *Biochem. J*
434, 93-104 (2011).
- 179 Cashman, N. R. *et al.* Neuroblastoma spinal cord (NSC) hybrid cell lines resemble developing
motor neurons. *Developmental dynamics* **194**, 209-221 (1992).
- 180 Ishikawa, H., Ma, Z. & Barber, G. N. STING regulates intracellular DNA-mediated, type I
interferon-dependent innate immunity. *Nature* **461**, 788-792, (2009).
- 181 Jung, C. H., Ro, S. H., Cao, J., Otto, N. M. & Kim, D. H. mTOR regulation of autophagy. *FEBS
letters* **584**, 1287-1295, (2010).
- 182 Klionsky, D. J. *et al.* Guidelines for the use and interpretation of assays for monitoring
autophagy (3rd edition). *Autophagy* **12**, 1-222, (2016).
- 183 Cai, Y. *et al.* Interplay of endoplasmic reticulum stress and autophagy in neurodegenerative
disorders. *Autophagy* **12**, 225-244 (2016).
- 184 Herman, M. *et al.* Heterozygous TBK1 mutations impair TLR3 immunity and underlie herpes
simplex encephalitis of childhood. *The Journal of experimental medicine* **209**, 1567-1582,
(2012).
- 185 Kingston, R. E., Chen, C. A. & Rose, J. K. Calcium phosphate transfection. *Current protocols in
molecular biology / edited by Frederick M. Ausubel ... [et al.] Chapter 9*, Unit 9.1, (2003).
- 186 Dalby, B. *et al.* Advanced transfection with Lipofectamine 2000 reagent: primary neurons,
siRNA, and high-throughput applications. *Methods (San Diego, Calif.)* **33**, 95-103, (2004).
- 187 Thompson, C. D., Frazier-Jessen, M. R., Rawat, R., Nordan, R. P. & Brown, R. T. Evaluation of
methods for transient transfection of a murine macrophage cell line, RAW 264.7.
BioTechniques **27**, 824-826, 828-830, 832 (1999).
- 188 Graham, F. L., Smiley, J., Russell, W. C. & Nairn, R. Characteristics of a human cell line
transformed by DNA from human adenovirus type 5. *The Journal of general virology* **36**, 59-
74, (1977).
- 189 Shaw, G., Morse, S., Ararat, M. & Graham, F. L. Preferential transformation of human neuronal
cells by human adenoviruses and the origin of HEK 293 cells. *FASEB journal : official
publication of the Federation of American Societies for Experimental Biology* **16**, 869-871,
(2002).
- 190 Saul, V. V., Niedenthal, R., Pich, A., Weber, F. & Schmitz, M. L. SUMO modification of TBK1 at
the adaptor-binding C-terminal coiled-coil domain contributes to its antiviral activity.
Biochimica et biophysica acta **1853**, 136-143, (2015).
- 191 Ye, J. S. *et al.* Lysine 63-linked TANK-binding kinase 1 ubiquitination by mindbomb E3
ubiquitin protein ligase 2 is mediated by the mitochondrial antiviral signaling protein.
Journal of virology **88**, 12765-12776, (2014).
- 192 Pilli, M. *et al.* TBK-1 promotes autophagy-mediated antimicrobial defense by controlling
autophagosome maturation. *Immunity* **37**, 223-234, (2012).
- 193 Tanida, I., Minematsu-Ikeguchi, N., Ueno, T. & Kominami, E. Lysosomal turnover, but not a
cellular level, of endogenous LC3 is a marker for autophagy. *Autophagy* **1**, 84-91 (2005).
- 194 Korac, J. *et al.* Ubiquitin-independent function of optineurin in autophagic clearance of
protein aggregates. *Journal of cell science* **126**, 580-592, (2013).
- 195 Newman, A. C. *et al.* TBK1 kinase addiction in lung cancer cells is mediated via autophagy of
Tax1bp1/Ndp52 and non-canonical NF-kappaB signalling. *PLoS One* **7**, e50672, (2012).

- 196 Szegezdi, E., Logue, S. E., Gorman, A. M. & Samali, A. Mediators of endoplasmic reticulum stress-induced apoptosis. *EMBO Rep* **7**, 880-885, (2006).
- 197 Liu, Y.-P. *et al.* Endoplasmic reticulum stress regulates the innate immunity critical transcription factor IRF3. *The Journal of Immunology* **189**, 4630-4639 (2012).
- 198 Woo, C. W. *et al.* Adaptive suppression of the ATF4-CHOP branch of the unfolded protein response by toll-like receptor signalling. *Nature cell biology* **11**, 1473-1480 (2009).
- 199 Matsumoto, G., Shimogori, T., Hattori, N. & Nukina, N. TBK1 controls autophagosomal engulfment of polyubiquitinated mitochondria through p62/SQSTM1 phosphorylation. *Human molecular genetics* **24**, 4429-4442, (2015).
- 200 Gleason, C. E., Ordureau, A., Gourlay, R., Arthur, J. S. & Cohen, P. Polyubiquitin binding to optineurin is required for optimal activation of TANK-binding kinase 1 and production of interferon beta. *The Journal of biological chemistry* **286**, 35663-35674, (2011).
- 201 Richter, B. *et al.* Phosphorylation of OPTN by TBK1 enhances its binding to Ub chains and promotes selective autophagy of damaged mitochondria. *Proceedings of the National Academy of Sciences*, 201523926 (2016).
- 202 Williams, K. L. *et al.* Novel TBK1 truncating mutation in a familial amyotrophic lateral sclerosis patient of Chinese origin. *Neurobiology of aging*, (2015).
- 203 Tsai, P. C. *et al.* Mutational analysis of TBK1 in Taiwanese patients with amyotrophic lateral sclerosis. *Neurobiology of aging* **40**, 191.e111-196, (2016).
- 204 Thomas, P. & Smart, T. G. HEK293 cell line: a vehicle for the expression of recombinant proteins. *Journal of pharmacological and toxicological methods* **51**, 187-200, (2005).
- 205 Thurston, T. L., Ryzhakov, G., Bloor, S., von Muhlinen, N. & Randow, F. The TBK1 adaptor and autophagy receptor NDP52 restricts the proliferation of ubiquitin-coated bacteria. *Nature immunology* **10**, 1215-1221, (2009).
- 206 Atkin, J. D. *et al.* Endoplasmic reticulum stress and induction of the unfolded protein response in human sporadic amyotrophic lateral sclerosis. *Neurobiology of disease* **30**, 400-407 (2008).
- 207 Liu, Y. P. *et al.* Endoplasmic reticulum stress regulates the innate immunity critical transcription factor IRF3. *Journal of immunology (Baltimore, Md. : 1950)* **189**, 4630-4639, (2012).
- 208 Walker, A. K. *et al.* Protein disulphide isomerase protects against protein aggregation and is S-nitrosylated in amyotrophic lateral sclerosis. *Brain : a journal of neurology* **133**, 105-116, (2010).
- 209 Wollebo, H. S., Woldemichaele, B. & White, M. K. Lentiviral transduction of neuronal cells. *Methods in molecular biology (Clifton, N.J.)* **1078**, 141-146, (2013).
- 210 Cong, L. *et al.* Multiplex genome engineering using CRISPR/Cas systems. *Science* **339**, 819-823, (2013).